NOTE TO USERS

Wind Loading on Rainscreen Walls: A Wind Tunnel Investigation

Sudeesh Kalavenkataraman

A Thesis

In

The Department

of

Building, Civil and Environmental Engineering

Presented in Partial Fulfillment of the Requirements
for the Degree of Master of Applied Science (Building Engineering) at
Concordia University
Montreal, Quebec, Canada

April 2005

Your file Votre référence
ISBN: 0-494-10220-9
Our file Notre référence
ISBN: 0-494-10220-9

ABSTRACT

Wind Loading on Rainscreen Walls: A Wind Tunnel Investigation

Sudeesh Kalavenkataraman

Wind loading is important but difficult to evaluate in the design of rainscreen walls. Full-scale measurements concerning pressure equalization of rainscreen facades have been carried out at the Technical University of Eindhoven (TUE) in the Netherlands. The measurements of the exterior and the cavity pressures for limited leakage-area and venting-area configurations have been taken over a period of more than a year on a central panel of the main TUE building and the field data has been analyzed in both time and frequency domains. The present wind tunnel study attempts to simulate these full-scale measurements in order to establish the techniques and parameters required for a detailed investigation of the rainscreen wall behaviour under the influence of the wind. The study presents the results of the wind tunnel experiments, compares them with the full-scale data and discusses their similarity after introducing appropriate corrections. Both mean and fluctuating pressures are evaluated for central and edge rainscreen wall panels exposed to a variety of wind directions. The study quantifies the parameters involved in the design of Pressure-Equalized Rainscreen (PER) walls and attempts to establish specific design guidelines for wind standards and codes of practice. The inadequacy of the currently available limited code and standard provisions for the design of rainscreen walls is fully demonstrated through comparisons with both field and wind tunnel data.

Acknowledgements

The author wishes to express his sincere gratitude to Dr. T. Stathopoulos and Dr. S. Kumar for their keen interest, inspiration and excellent guidance throughout the course of this study, in particular, for their helpful suggestions in writing.

The author is most grateful to Dr. P.J. Saathoff for his timely assistance in experiments. Sincere thanks are due to Mr. Joe, Mr. Robert and Mr. Joseph for their help in model making and instrumentation.

The author is also indebted to Concordia University for the award of Partial Tuition Fee Waiver for International Students.

My special thanks are due to Mr. Amit Gupta for his help and fruitful discussions during the work. Further, I express my sincere thanks to all my friends for their excellent company and cooperation at the Department of Building, Civil and Environmental Engineering.

I wish to express a special note of thanks to my family for their love and constant encouragement throughout my research.

Table of Contents

LIST OF FIGURES

LIST OF TABLES

NOMENCLATURE

Aw	panel area
C_c	coefficient of contraction
C_d	discharge coefficient
C_{eq}	pressure-equalization factor
C	flow coefficient
Cab	flow coefficient of air barrier
C_p	pressure coefficient
$\overline{C}_p$	mean pressure coefficient
$\hat{C}_p$	peak pressure coefficient
$\hat{C}_{p\text{-corrected}}$	corrected peak pressure coefficient
$Cp, rms_{corrected}$	corrected root-mean-square pressure coefficient
g	dimensionless peak factor
k	Weibull constant
n	flow exponent
P	pressure difference

Pe	external pressure
Pi	internal pressure
Pc	cavity pressure
Pe-Pi	pressure acting across panel
Pe-Pc	pressure acting on rainscreen
p_o	free-stream pressure
Q	flow rate
U	mean wind speed at reference height
V	mean velocity at height Z
Vg	mean velocity at gradient height Zg
Z	height
Zg	gradient height

Greek symbols

α	profile exponent
ε	irregularity factor
Θ	wind direction

ρ	density of air

Abbreviations

MPEC	mean pressure-equalization constant
MaxPEC	maximum pressure-equalization constant
PEI	pressure-equalization index
PEP	pressure-equalization percentage
PER	pressure-equalized rainscreen
rms	root-mean-square
SPEC	standard deviation pressure-equalization constant
T.I	turbulence intensity

CHAPTER 1

INTRODUCTION

1.1 *Overview*

The concept of Pressure-Equalized Rainscreen Wall system has evolved since way back in 1960's. Prior to this approach various other techniques had been employed to prevent rainwater from entering into the façade. First came the mass wall system, which required immense labor and material in construction. Then the researchers proposed the face-sealed approach to prevent rainwater penetration by sealing the joints of the panels. This approach had the problem of poor workmanship, where in, the joints could not be sealed to perfection. Thus, understanding the difficulty of the problem, the researchers proposed a new approach that involved placing a screen in front of the wall to drive away most of the rain water and a good drainage system to drain away the water that did penetrate. This led to the advent of the modern screened walled systems. There are essentially two types of screened wall designs: (1) drained and back ventilated design, and (2) pressure-equalized rainscreen design. The former allows water to penetrate the joints into the cavity where it runs down the back of the rainscreen and is subsequently drained. On the other hand, the pressure-equalized approach aims to prevent any water from penetrating the rainscreen. However, cavity and weep-holes are also a part of this approach as secondary defense to water penetration.

1.2 *Pressure-Equalized Rainscreen Approach*

Pressure-Equalized rainscreen approach is considered to be the state-of-the-art in preventing rainwater penetration. The amount of wind-driven rain entering into the building façade depends on various parameters like gravity, surface tension, capillary action and the air pressure differential across the wall. Air pressure differential could be induced by stack effect, mechanical systems and wind. This approach takes into consideration the pressure differential caused by wind, as this is the strongest force that stimulates rainwater penetration. The rainscreen system could be considered as having three parts: (1) an outer rainscreen, (2) an inner leaf called the air barrier and (3) an air space or cavity in between. Figure 1.1 shows a typical pressure-equalized rainscreen.

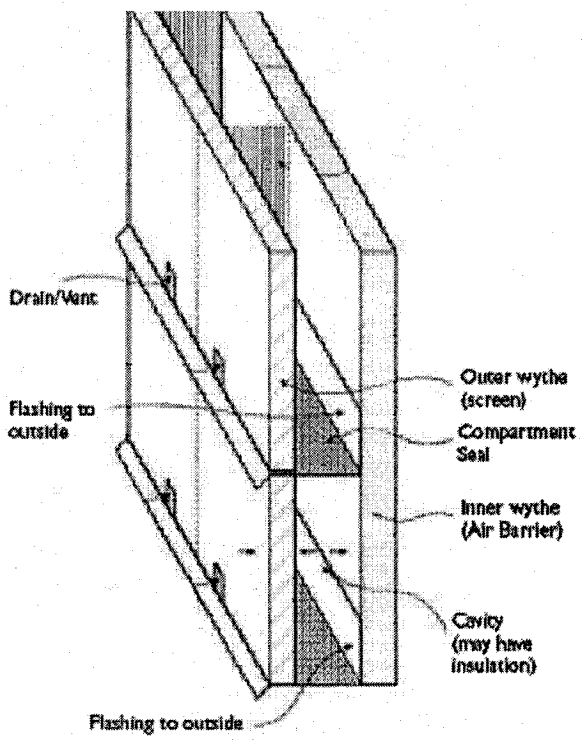

Figure 1.1: A typical pressure-equalized rainscreen wall

The primary function of the outer rainscreen, also called the outer blade, is to prevent any rainwater from penetrating into the façade. Deliberate vents are provided in the rainscreen in order to establish equalization of cavity pressure with the external pressure. This tries to reduce the impetus that causes rainwater penetration. The other component of a rainscreen wall called the air barrier or inner blade is essentially the structural system resisting the wind load and preventing airflow. Figure 1.2 shows another example of a PER wall with the external, cavity and internal pressures.

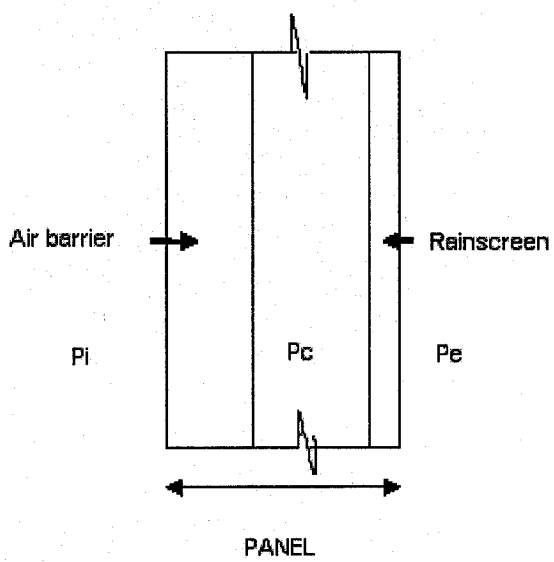

Figure 1.2: A PER Wall

Note that, Pe = External pressure, Pi = Internal pressure, Pc = Cavity pressure. Also, Pe – Pi = Pressure acting across the panel called as panel pressure and Pe – Pc = Pressure acting on rainscreen called as rainscreen pressure.

The two important design criteria of rainscreen walls are (a) rain penetration resistance and (b) transfer of wind loads onto the air barrier. The first design criterion holds good as sustained pressure difference can cause rain infiltration; thereby, with careful designs one can prevent rainwater penetration. The complexity involved in the wind loading on raincreens is primarily because the wind design criterion is still at its infancy stage. Little is known about parameters like mean pressures, temporal

pressure variations and spatial pressure variations. An ideal rainscreen wall would equalize pressure instantly, but research has shown that a time lag always exists between applied wind loads and pressure equalization in the cavity. Hence, there is no immediate and constant equalization when subjected to dynamic pressures.

Wind design is a safety and complex issue. It becomes difficult to have a specific design criterion. Hence, one designs both layers of a rainscreen for the same wind load. This is not economically healthy. A small reduction in load can save millions of dollars in construction. Hence, any design carried out should try to reduce wind loads on the outer rainscreen and transfer all loads onto the air barrier.

Several design features like total venting area of raincreen, venting location, air barrier stiffness, effective leakage area, cavity volume etc have to be taken into account while designing for pressure-equalization. A perfect design incorporates these features in the best possible way to minimize the wind loading on rainscreen. Research is furthering in the direction of achieving a proper pressure-equalized rainscreen system that accepts maximum wind load on the air barrier and also prevents rainwater penetration. Various experiments and analytical simulations are being carried out to analyze the unknown parameters and thereby to devise a method to quantify them for design.

1.3 *Objective*

Full-scale measurements concerning pressure equalization of rainscreen facades have been carried out by Kumar [1] at the Technical University of Eindhoven (TUE) in the Netherlands. The measurements of the exterior and the cavity pressures for limited leakage-area and venting-area configurations have been taken over a period of one year on one panel of the main building and the field data has been

analyzed in the frequency domain (Kumar et. al. 2003) [2]. Kumar [1] has put forth various generalized approaches for the theoretical prediction of cavity pressures and has also suggested a prediction model for this purpose. Further, frequency domain techniques have been utilized to show the influence of wind as well as façade characteristics on the pressure equalization performance.

In this study, wind tunnel experiments have been carried out at the Centre of Building Studies of Concordia University to simulate the above full-scale measurements. After drawing meaningful comparisons with the field data, the wind tunnel model can be used to carry out a multitude of experiments in order to study the effect of various design parameters on pressure equalization. Such parametric study is possible to be done in a wind tunnel within a short period of time, as opposed to full-scale, which may take years to complete. The objectives of this study are (1) to develop a wind tunnel model which draws meaningful comparison with field data, and (2) to study the effect of various design parameters and quantify them for standards and codes of practice.

1.4 *Thesis Outline*

The thesis is divided into six chapters and a list of references. A detailed literature survey is documented in Chapter 2. The experimental procedure listing out the details of full-scale measurements, selection of appropriate building model for wind tunnel tests, design of raincreen panel through static pressurization tests and the wind tunnel experimentation performed are described in Chapter 3. The results of the experiments are laid out in Chapter 4, analyzing the effect of all the design parameters on pressure equalization individually. The results in this chapter are divided into Center and Edge Configurations and meaningful comparisons with the field

measurements are drawn for the Center Configuration, thereby, paving the way to establish specific design guidelines that have been broached in Chapter 5. Contributions of this study as well as recommendations for future work are provided in Chapter 6, which is followed by the list of references.

CHAPTER 2

LITERATURE REVIEW

2.1 *A Brief Historical Perspective*

Modern rainscreen wall systems employ the equalization of pressure technique between the cavity and the exterior to prevent rainwater penetration into the building façade. A typical pressure-equalized rainscreen (PER) comprises of an outer rainscreen, inner air barrier and an air space or cavity in between. Many researchers have studied the various aspects of rainscreen systems and have put forth their findings. The concept of rainscreen design in not new to the construction industry. The early drained and back ventilated cladding designs existed for many years in Norway [3]. The technique of minimizing wind-induced pressure differential gained immense progress after the 1960's in the construction industry. For instance, Birkeland [4] in 1962 suggested that venting the air cavity with the exterior would equalize the cavity pressure with the external. In 1963, Garden at the National Research Council of Canada (NRCC) introduced the 'open rainscreen principle' that allowed the outer rainscreen wall to have vents, so that, rapid pressure equalization between the cavity and the external occurred [5]. Garden also suggested on having compartments within the cavity, in order, to improve pressure equalization. Preliminary design guidelines for compartments were also provided.

In the early 1970's, the theory and application of pressure equalization and rainscreen principle in curtain wall design was published in a book by the North American Architectural Aluminum Manufacturer's Association [6]. Almost the same material was covered by Latta [7] at the Canadian National Research Council's

Division of Building Research in 1973. The book provided a theoretical treatment of pressure equalization process by assuming the openings in the rainscreen and air barrier to be sharp-edged orifices. According to this theory, the relative pressure drops across the layers change with the square of the ratio of the relative area of the openings in both layers.

Fundamental studies have been carried out regarding the mechanical characteristics of vents, for instance, in 1976 Yamaguchi [8] examined the non-steady characteristics of orifices on the assumption that the free streamline forms an ellipse on the hodogram. The study found the coefficient of contraction of orifice, C_c, to be greater than that for steady flow during the period of acceleration and smaller during the period of deceleration. In the mean pulsating flow the mean value was found to be slightly smaller than the steady flow value. The opposite was true for the coefficient of discharge, C_d, defined by the instantaneous flow rate and the pressure difference.

The design principles and guidelines for rainscreen cladding are documented by Anderson and Gill [3]. The pressure equalization technique is employed in places where the air cavity is seen as a means of controlling the effects of wind action. The rain penetration caused by the air pressure differentials is attenuated by pressure equalization using vents on the outer rainscreen. Inculet and Davenport [9] carried out a theoretical and experimental study of the pressure-equalization in rainscreen walls to improve the understanding of several design parameters. The study was performed through theoretical models, wind tunnel experiments and full-scale measurements of two rainscreen designs.

Though the concept of pressure-equalization seems to be easy, the task of implementing it becomes relatively difficult. Many studies have been carried out on the rainscreen walls to analyze the unknown parameters and, interestingly, the

importance of wind-loading on such walls has increased. The difficulty involved in the wind loading on rainscreen causes one to be conservative as both layers are designed for the same wind loads. Although, PER wall systems have been in practice for almost two decades as of 1980, these walls still face the problem of wind loading. Most of the design features are qualitative and the need to quantify them has gained importance of late. In this regard, Kumar [10] reviewed the state-of-art information concerning pressure-equalization of rainscreen walls and tried to disseminate the existing knowledge for architects and building engineers. The review analyzed the experimental and theoretical investigations that had been done after the 1980's concerning pressure equalization of rainscreen walls and laid emphasis on the design guidelines and codification procedure for the Pressure Equalized Rainscreen Walls. The study found that efficient quantitative guidelines could not be suggested due to the lack of comprehensive information about the effect of these parameters on the pressure equalization process. Hence he suggested areas like the cavity pressure prediction, discharge coefficients for flow through opening, venting of rainscreen, mean and unsteady pressure gradients, water penetration of screens under external pressure variations need to be delved into before consistent design guidelines could be proposed. Thus, the need for consistent design guidelines comes in effect due to increased construction costs. In this respect, many researchers have looked into the performance of PER walls in the last two decades. The following sections summarize the research and developments in the wind loading aspect of PER walls that has happened to- date.

2.2 *Experimental Investigations*

2.2.1 Wind tunnel experiments

Irwin et al. [11] carried out a wind tunnel investigation of two rainscreen wall systems. Plexiglass models of rainscreen walls were fabricated on a 1:200 geometric scale and tested under simulated environmental conditions in the wind tunnel. One of the rainscreen walls was fabricated similar to that of the Place Air Canada building [12], in order to compare the full-scale data of the Place Air Canada building with the wind tunnel results. The major differences between the model and full-scale were (1) nonrepresentative overall building dimensions, (2) nonrepresentative tap locations, (3) distorted cavity depth (0.5 mm provided instead of 0.063 mm according to a scale of 1:200), and (4) nonrepresentative flow exponent of 1.0 for the venting. The results were reported as pressure coefficients for wall design. Further, Irwin et al. [11] carried out wind tunnel experiments on a brick veneer wall model with a continuous air space. The study suggested that a well-compartmented and vented wall could be designed for 70% of cladding loads.

Morrison and Hershfield Ltd [13] analyzed the pressure equalization performance of a wood frame wall. Wind tunnel experiments were carried out on the same rainscreen wall with and without compartmentalization. They found that compartmentalization improved the pressure equalization process and hence suggested that compartmentalization is necessary at corners of buildings and the seals should be designed to withstand 2-3 times the wind load. Inculet [14] performed a wind tunnel study to validate the pressure equalization theory. The model used was scaled at 1:12 for allowing proper flow characteristics. The scale violation was justified as the study primarily intended to validate the pressure equalization theory. Gerhardt and Janser [15] in an experimental study on wind loading of porous façade

systems, varied parameters like relative building dimensions, porosity and gap width and analyzed both the time averaged and fluctuating pressures. One aspect of the results showed the importance of the gap flow resistance. With an increasing gap width, an increasing net pressure coefficient was found. The study also found that the net pressure and the wind load acting on the rainscreen without sealing of the vertical edge was significantly larger than for the case with edge sealing.

Earlier studies have shown that compartmentalization is necessary for maximum pressure equalization. Exclusive studies have been carried out at the University of Western Ontario concerning mean pressure gradients and unsteady pressure gradients to strengthen this concept. Lin and Inculet [16] studied the mean pressure gradients for various wind angles relative to a building face. Another study by Skerlj and Surry [17] investigated the mean pressure gradients very close to the edges. In a similar study, Surry et al. [18] reported the mean and unsteady pressure gradients on buildings as a means of providing practical guidelines for compartmentalization of building envelopes.

The progress of research in the direction of achieving a proper venting scheme for pressure equalization has showed that proper venting locations and proper venting size could accordingly alter the rate of pressure equalization possible. Inculet and Surry [19] performed a study that sought to achieve a venting scheme for a partially pressurized rainscreen. The concept was to vent the rainscreen compartment at the location of its maximum mean exterior pressure, thereby creating an outward acting mean pressure across the rainscreen, which opposes water infiltration everywhere. A pressure module comprising a variable number and size of vented compartments was inserted into the face of a rectangular building at the center top and side edges, corner and center. The compartments were vented only at the edge farthest from the nearest

building edge where the mean exterior pressure is most positive. Mean exterior and cavity pressures were measured and the results were found to be most promising. The study showed the partially pressurized rainscreen to be a viable concept and found the design to work exceptionally well at the building top and side edges, which received most of the wind-driven rain. As a course of future studies, an examination of the mean exterior pressure field over a face to determine the various compartment sizes was suggested. Since the study involved only mean pressures, a future study involving unsteady pressures was also suggested as these might create the net pressures across the rainscreen to be positive. Again, Inculet et al [20] performed an experimental study of pressure distributions on a range of building models along with a focus on the design of pressure-moderated rainscreens. Both mean and unsteady pressure gradients were considered. The study concluded that the partially pressurized rainscreen to be a viable concept and a useful refinement of the pressure-equalized design.

The current thesis deals with wind tunnel experiments intended to simulate full-scale measurements and thereafter, carry out a parametric study. Note that the key advantages of wind tunnel experiments are (1) easy to carry out a parametric study and (2) short durations experiments. On the other hand, in full-scale measurements, one has to wait for years to get some meaningful measurement results.

2.2.2 Laboratory experiments

Numerous laboratory studies have been carried out under idealized conditions. For instance, Killip and Cheetam [21] showed the variation in distribution of air pressure between two plates with changes in opening sizes. The results showed that Latta's [7] approach overestimate the pressure equalization effect compared to the

present measurements. They stated the difference to be due to the viscous behaviour of airflow through cracks. The study also showed that a higher external to internal opening area is required to create the same amount of pressure equalization predicted by Latta's equation. Ganguli and Quirouette [22] studied the pressure equalization performance of the full-scale spandrel section of a metal and glass curtain wall under static and dynamic loading conditions.

Pressure fluctuations have a prominent effect on the pressure equalization process. The NRCC Institute for Research in Construction performed a laboratory testing of pressure equalized walls under spatially uniform sinusoidal pressures at different frequencies. The study noted a decrease in the pressure equalization process at high frequencies even for an air tight air barrier and high venting to leakage ratios [23]. In a similar study at the Dynamics Loading Facility of IRC/NRCC, a brick veneer rainscreen wall was investigated. The wall segment was excited by sinusoidal pressure fluctuations in the range of 0.1 to 2 Hz. The study introduced a 'Pressure Equalization Index' (PEI) to quantify the pressure equalization performance of wall systems. Another study on air pressure equalization in raincreen joints using sinusoidal air pressure showed that the equalization performance worsened for a combination of low frequency, small cavity volume and large venting area [24]. Xie et al. [25] tested full-scale curtain wall panels under sinusoidal pressure fluctuations mainly to validate the model performance. They used pressure reduction factors to quantify the pressure equalization performance of curtain wall systems. Choi and Wang [26] studied the behaviour of curtain wall systems and evaluated design parameters by using full-scale specimens. They developed a numerical model that takes into account the flexibility of the back-panel for the prediction of cavity pressures. The effect of flexibility of the back panel on pressure equalization

performance was analyzed by subjecting full-scale specimens to sinusoidal pressure fluctuations as well as random wind generated by an aero plane engine. The comparison between the model and field results were in good agreement. The study also revealed that the pressure-equalization performance of metal curtain walls could be different from that having rigid back-panels. This difference could be attributed to the material property that directly affects the back-panel stiffness. The tests were conducted at single frequencies and later a conclusion was drawn for the entire wind spectrum.

In reality, the external wind pressures are random and non-uniform over the walls. While designing the layers for cladding loads, one has to know the spatial non-uniformity, as well as the random characteristics of wind pressures. Until the actual wind environment is simulated in a laboratory, the results from such studies should be handled with caution.

2.2.3 Full-scale experiments

Ganguli and Dalgliesh [12] measured the wind pressure differences across the rainscreen and air barrier of precast open rainscreen wall panels of the Place Air Canada building model in Montreal. The pressure equalization performance of these panels was satisfactory with most of the wind load being transferred onto the air barrier. Full pressure equalization could not be achieved due to small spatial variations of pressures in the cavity. It was seen that the largest pressure difference across the entire panel never coincided with the peak pressure difference on the rainscreen. The study also suggested that significant reductions in design pressures for the rainscreen occur when venting and compartmentalization are effective. Similarly, a study by NRCC on the Lethbridge Courthouse in Alberta [27], showed the wall of

the building to be leaky and poorly compartmentalized. Under positive pressure, the wall carried as much as 64% of the instantaneous load and 55% of the load when averaged over 4 min. Under negative peak gusts, up to 90% of the pressure was carried by the rainscreen.

Some of the critical data from Place Air Canada as well as Lethbridge Courthouse were analyzed by Inculet [14] in the frequency domain. In the case of Lethbridge Courthouse, the poor pressure equalization performance was due to its high leakage and venting ratio, where as the efficiency of the Place Air Canada model was attributed to its large venting to volume ratio, its small compartment size and its air tight air barrier. Later, the University of Waterloo, Canada, tested a variety of full-scale rainscreen wall systems to evaluate their pressure equalization performance [28, 29]. The testing showed a relatively high degree of pressure equalization over long time periods in comparison to the poor equalization performance for short-term wind gusts. The pressure equalization performance was poor due to the spatial variability of wind pressures.

Most of the full-scale studies are carried out on rainscreens that already exist on buildings. The nature of such studies is limited and specific. Thus, the need to analyze the unknown parameters in further detail has motivated researchers to come up with a systematic investigation of such rainscreen designs. For instance, The Faculty of Architecture, Building and Planning, Technical University of Eindhoven (TUE), The Netherlands, has performed an investigation on the pressure equalization performance of rainscreen walls. Exterior and cavity pressure time histories were measured at several tap locations of a panel located on the west side of the façade of the main building. Provisions were made for parameters like cavity volume, leakage area and venting area to vary [30, 31]. An overview of the field experiments is given

in Refs. [1, 2, 32]. This research studies the impact of various design parameters on the rainscreen wind loading. Also, the current status of the available codes and standards regarding the wind loads on rainscreen walls are presented and the full-scale results are compared with some of the available provisions.

2.3 *Theoretical Investigations*

2.3.1 Models based on the Helmholtz resonator theory

Holmes [33] introduced a damped Helmholtz resonator model to predict internal building pressure variations subjected to time varying external pressures. The Helmholtz resonator theory was first used by Irwin et al. [11] to calculate the undamped natural frequency of the wall system. Later, Baskaran and Brown [24] calculated the time lag of the cavity response using this theory. Using the same theory, Inculet [14] developed a model to predict cavity pressures under sinusoidal and random exterior pressure fluctuations with or without leakage through the air barrier. They discussed the primary factors which control the pressure-equalization like the leakage of the air barrier, the aerodynamic damping introduced by the venting in the rainscreen and the spatial non-uniformity of the steady and fluctuating exterior pressures. It was found that an increase in venting area for constant volume or a decrease in volume for constant venting area results in both a higher natural frequency and a higher critical damping frequency. Without the air barrier leakage, the cavity pressure is a spatial average of exterior pressures over the vents for frequencies below the critical damping frequency. But the linearized theory employed overestimated the low frequency fluctuations of pressure across the rainscreen and under estimated higher frequency fluctuations. This approach is numerical and uses frequency response to describe the cavity pressures and the pressure drops across the rainscreen.

The values predicted by the models are matched with the measurements after modifying the discharge coefficient, (C_d). As compared to steady flow, the values of discharge coefficient are found to be significantly lower for fluctuating flow and unidirectional oscillating flow conditions [9]. In 1992, Vickery and Bloxham [34] studied the dynamics of internal pressure due to a sudden formation of a windward opening in an otherwise sealed building. Based on the study they developed some simple predictable methods for both steady state and transient behaviour, which were confirmed by the experimental study. The paper described the behaviour following a sudden failure and an equation to compute the variance of the internal pressure after failure. The results validated the effect of the background leakage to be of minor consequence if the leakage area was less than about 10% of the main opening. The theory had its own limitations as it was confined to single openings and openings on the windward side.

On the basis on Helmholtz theory, Choi and Wang [26] developed a numerical model for the prediction of cavity pressure that takes into account the flexibility of the back panel. The damping of the cavity pressure increases as the frequency increases, especially in the case of flexible back-panel. Irrespective of whether the back-panel is flexible or rigid, the importance of vent factor is clear. A higher vent factor achieved good pressure equalization, at least at low frequencies. Kumar and van Schijndel [35] developed an analytical model for the prediction of cavity pressure for a rigid rainscreen wall, based on Helmholtz principle. This model includes air flow through the air barrier in its formulation. The model uses an exponent of 0.5 for both the rainscreen and the air barrier. In most real conditions, the air barrier has small cracks that make the exponent to deviate from 0.5. In these circumstances, this model cannot be applied. Further, the authors showed that mostly the undamped natural frequency

of the wall system is much higher than the frequencies of major external pressures. Any resonance arising from the inertial term of this model lies in the high frequency tail of the external pressure spectrum and hence, is unlikely to be excited to any significant amplitude. This shows that the inertial term can be avoided in the formulation of this model and without this inertial term, the model is similar to any model based on the first principles with a flow exponent of 0.5 for both the rainscreen and the air barrier. In the same light, Kumar and van Schijndel [36] presented two theoretical models to improve the understanding of the design parameters involved in the pressure equalization process. One model was based on mass balance and the other on the Helmholtz resonator theory for the prediction of cavity pressures in rigid rainscreen walls. The study showed the mass balance model to accurately estimate the cavity pressure variations. The model performance was further validated using full-scale data and the results were found to be in good agreement.

2.3.2 Models based on first principles

Models derived on the basis of standard gas law equation, mass continuity equation and equation of air flow through walls are listed in this category. Latta [7] derived a simple relationship of load sharing between the rainscreen and air barrier that is independent of the absolute total pressure drop. However, the equation is valid only for steady wind loading under the assumption of the orifice flow equation. Killip and Cheetam [21] assumed the leakage paths through the air barrier and came up with a new equation that opposed the earlier theory. They used Kimura's equation [37] and showed that the pressure drop across the rainscreen could be expressed as the square of the pressure drop across the air barrier. Fazio and Kontopidis [38] formulated a relationship to correlate the cavity pressure, exterior wind pressure and the size and

distribution of openings in the two layers based on the steady-state incompressible flow assumption. Later, Inculet [14] came up with a relationship between mean pressure differences across rainscreen and air barrier based on the assumption that the flow is incompressible and steady. They used an exponent of 0.5 for the rainscreen and 0.65 for the air barrier. The equation developed showed a dependence of rainscreen load sharing on the total pressure drop. The difference is attributed not only to the difference in the exponents of rainscreen and air barrier employed but also on the ratio of venting to leakage characteristics.

Baskaran and Brown [24] came up with a model to simulate the PER wall performance. The study assumed the steady state incompressible flow conditions to dominate the pressure equalization process. The unknown cavity pressure was solved iteratively. Computed results matched the measurements in most of the cases. The results showed that an increase in the leakage ratio decreases the pressure equalization of the wall system. Also, the cavity pressure amplitudes are overestimated and the phase shift of the cavity pressure is underestimated by the model. While the discrepancy in phase shift is attributed to the estimation of time lag constant which is independent of the leakage area and loading rate, the discrepancy in cavity pressure amplitudes is attributed to the use of 0.5 as the flow exponent for air barrier. A similar study by Tamura et al. [39] has shown the flow exponent through the building envelope cracks to vary from 0.5 to 1.0, converging on 0.65 for buildings with HVAC systems. This increase in flow exponent of air barrier can reduce cavity pressure amplitudes.

Xie et al. [25] developed a numerical model for the prediction of net pressure on pressure equalized cavities. The model is based on isothermal process and the pressure over the panel is spatially uniform. Further, the flexibility of the panel in the

form of deflection at the center of panel is analyzed. Simulated exterior pressure fluctuations such as sinusoidal as well as random were used for computation. The results showed good agreement between measured and the predicted pressure difference across the exterior cladding. The mean pressure is found to significantly affect the stiffness of the back panel with higher mean pressures improving its stiffness. Kontopidis et al. [40] developed a mathematical model to reduce rain penetration problems in buildings with rainscreen walls. They validated the model results with laboratory experiments as well as full-scale measurements. Though, the concept of rain penetration was addressed, the authors failed to give attention to the increment in design load for most of the walls.

Burgress [41] developed a process to forecast the cladding joint variation, which affect rainscreen joint weather tightness in buildings. He presented a numerical model to solve the governing equation of air flow within the cavity of a rainscreen joint when subjected to a sinusoidal air pressure variation. The governing equations were based on the assumptions that air is incompressible and the air flow through the air barrier is laminar. The model developed was validated with measurements. In this study, a Pressure Equalization Percentage (PEP) to measure the degree to which the internal joint cavity air pressure can equalize with the external air pressure at specific frequencies is introduced. The results indicated that geometric alterations of the joint opening area and the joint cavity volume affected the degree to which air pressures can equalize across the joint opening areas of pressure equalized rainscreen joints. The frequency of sinusoidal air pressure fluctuations has also been shown to affect the pressure equalization of a jointing system.

Van Schijndel and Schols [31] modeled pressure equalization in cavities through a first order one zone model. A test setup was developed that consisted of a

cavity with perforated blades. The porosity of the blades could be altered to vary the cavity volume. The results of the model showed good agreement with the experimental data. The study found that at lower frequencies (<0.1Hz) the simulated pressure across the outer blade equaled the measured pressure and also the fast fluctuations (>0.1 Hz) were more damped in the case of the simulated pressure. In 2000, Chaplin et al. [42] studied the turbulent ventilation of a single opening enclosure by carrying out experiments to examine the ventilation flow through the opening. They described the mechanisms of ventilation by non-linear oscillator equations, which contained two ill-defined parameters- the inertia and loss coefficients. The results predicted that the theoretical and experimental gain factors obtained with standard values of loss coefficients were in good agreement. The experimentally determined values of the inertia coefficients suggested that for small opening diameters the fundamental equation used in the theoretical derivation was not adequate and it required extra terms to describe the centripetal accelerations. The experimentally determined values of the loss coefficients were similar to the steady flow values. They further stated that the inconsistencies predicted between ventilation rates calculated through their approach and the one found out through experiments may not be due to inadequacies in the theory of pulsation flow, instead might be due the eddy penetration mechanisms.

Kumar and van Schijndel [36] suggested a suitable model for the theoretical prediction of cavity pressures. The time varying cavity pressure is simulated using the derived models based on first principles as well as the Helmholtz resonator theory. The results clearly show that the model based on first principles is more practical and simple compared to the other, and sufficient to predict the cavity pressure dynamics. Also, methods to quantify pressure equalization performance are provided.

2.3.3 *Models based on Computational Fluid Dynamics (CFD)*

Evaluation of pressure equalization through Computational Fluid Dynamics techniques was carried out by Baskaran [43] by developing a numerical model. The model developed is three dimensional and time dependent. The study involved two types of wall assemblies, one with an air tight air barrier and the other with a leaky air barrier. The efficiency of the numerical prediction was shown only for sinusoidal external pressure variations. Later in 1995, Brown and Ullett [44] carried out a study on the performance of pressure-equalized rainscreen walls. He found that the pressure-equalization response worsened as the leakage through the air barrier increased for a decrease in the venting area and an increase in the frequency of the applied pressure. He also found that the dynamic pressure equalization response was directly related to the cavity volume to vent ratio and the governing criteria for acceptable air barrier leakage with respect to rainwater penetration, appeared to be that required for static pressure equalization than that required for the dynamic part.

Van Mook [45] presented the results of full-scale measurements and computational fluid dynamic simulations of driving rain on building facades. The wind was simulated by a standard k-ε model and the results were compared both quantitatively and qualitatively with the measurements. It was found that the simulated wind speed at the façade was within the standard deviations of the measurements. Though, the simulated mean pressure coefficient at the windward façade agreed with measurements of previous studies done on the same building, the mean pressure coefficient at the edges was overestimated. The study simulated driving rain using raindrop spectra from literature and the results showed the simulated driving rain ratios to be outside the standard deviations of the measured driving-rain ratio, especially at low wind speeds. This difference was attributed either

to the errors in the calculation of the wind velocity field, the drop trajectories or the raindrop spectra chosen.

Clearly, not many concrete studies have been carried out in the past to quantify the unknown parameters involved. Research needs to be progressed towards codification. Variety of configurations needs to be tested to provide realistic and consistent design guidelines. With proper design guidelines one look forward towards economical designs.

2.4 *Design Guidelines and Codification*

2.4.1 Design guidelines

The section tries to compile the existing qualitative and quantitative design guidelines for PER walls.

General qualitative criteria for PER wall design

- Provide large venting area. This can maximize the rate of air flow necessary to equalize the cavity pressure with the external pressure. Determine venting area based on deliberate venting area to unintentional leakage area of the air barrier.
- Provide vents that offer little resistance to air flow. This can maximize the air flow required for pressure equalization.
- Vent holes should be distributed over the panel face. This reduces the average wind loading acting on rainscreen; however, this may increase the damping of higher frequency fluctuations.
- Provide smaller cavity volume. This can minimize the change in air volume required for pressure equalization.

- Determine cavity depth based on venting area and total panel area.
- Provide large venting area to account for larger cavity volume. Increase in venting for constant volume, or a decrease in volume for constant venting area, can improve pressure equalization.
- Provide airtight and continuous air barrier. This can minimize the change in air volume necessary for pressure equalization.
- Compartment the air cavity. This can minimize the change in air volume necessary for pressure equalization. This is also required to limit the spatial differences across the panel face causing the lateral flow of air within the cavity and poor pressure equalization performance.
- Provide airtight compartment seals or separators. This can minimize the change in air volume necessary for pressure equalization.
- Provide compartment seals at wall corners. This will restrict the cross flow across the panel.
- Design compartment seals at corners for higher wind loads.
- Provide stiff compartment separators. This can minimize the change in air volume necessary for pressure equalization.
- Provide stiff rainscreen and air barrier claddings. This can minimize the change in air volume necessary for pressure equalization.
- Orient the vented critical wall elements with respect to wind driven rain direction properly. This influences pressure equalization and rain penetration.
- Design the rainscreen for reduced wind load, if some pressure equalization occurs.
- Provide adequate number of ties to transfer the lateral loads from the rainscreen to the air barrier.

Limitations of the existing design guidelines

It is evident that the recommendations put forward for the design of PER walls are considerably low in comparison to the number of studies carried in pressure equalization. Further, the existing guidelines have the following limitations:

- Existing design guidelines are not comprehensive.
- Existing design guidelines are not consistent.
- Most of the design guidelines are qualitative.
- Some of the design guidelines lack proper scientific background.
- Some design parameters are not taken into account.
- The design guidelines are mainly focused towards rain penetration, not structural design.

2.4.2 Codification

There are few codes and standards that address the design of PER walls. The British Standards 8200 [46] is the only code specifically for the design of non-loading bearing vertical walls. For compartmentalization, this code specifies the following dimensions: a vertical closure spacing of 1.2 – 1.5 m from the corner for a distance of 25% of the lesser plan dimension of the building, 5m for the spacing of vertical closures in the middle region, and 10m spacing for horizontal closures. The Dutch standards [47] for loadings and deformations included a pressure equalization factor (C_{eq}) for the estimation of wind pressure on building envelope consisting of two layers with an air column in between. This standard did not provide any specific C_{eq} values, instead, suggested to use a value of one until pertinent information becomes available. On the other hand, the Dutch code for fixing of roof coverings [48] put forth a set of values for C_{eq} based on roof angles and roof zones for the estimation of

wind loads on roofs of two layers with an air space in between. Australian Standards for wind loads recommended reduction factors for the estimation of design wind loads on porous cladding [49]. These factors depend on the cladding porosity and the horizontal distance away from windward building edge. The Eurocode ENV 1991 – 2 – 3 [50] proposed internal pressure coefficients in the inside air layer of wall or a roof with respect to porosity of outer and inner wall layers, stiffness of the wall layers, the thickness of the air layer and any other entrances of air.

The lack of ready to use design guidelines for PER walls in codes and standards, prompts the need for more research to be carried out. The importance of the unknown parameters involved in design needs to be analyzed, in order, to come up with effective and economical design.

CHAPTER 3

EXPERIMENTAL PROCEDURE

3.1 *Details of Full-Scale Measurements at Eindhoven*

Field measurements concerning pressure equalization of rainscreen facades were carried out at the Technical University of Eindhoven (TUE) in the Netherlands. The field facility including the details of test panel, instrumentation and data collection are discussed under this section.

3.1.1 Test site

The experiments have been performed on the main building of TUE, Eindhoven. The dimensions of the building are length = 167m, width = 20m and height = 44.6m. This building has an exact north-south orientation with the long facades facing west and east directions. Prevailing strong wind directions are from west and southwest. The terrain condition on prevailing wind directions is suburban.

3.1.2 Meteorological tower and test panel

A SOLENT ultrasonic anemometer was mounted at the top of a 30m high mast placed on a 14m high building, 127m westward of the main building. This was used to measure the three component wind velocity. The façade of the main building is a curtain wall made of glass windows and steel parapets on steel columns with the distance between the steel columns being 1.24m center to center. For field measurements, one of the façade elements was replaced by a wooden panel of size 1m x 1.3m. The wooden panel was mounted approximately on the middle of the west

façade at a height of 39m above the ground. The field facility is shown in Figures 3.1 and 3.2.

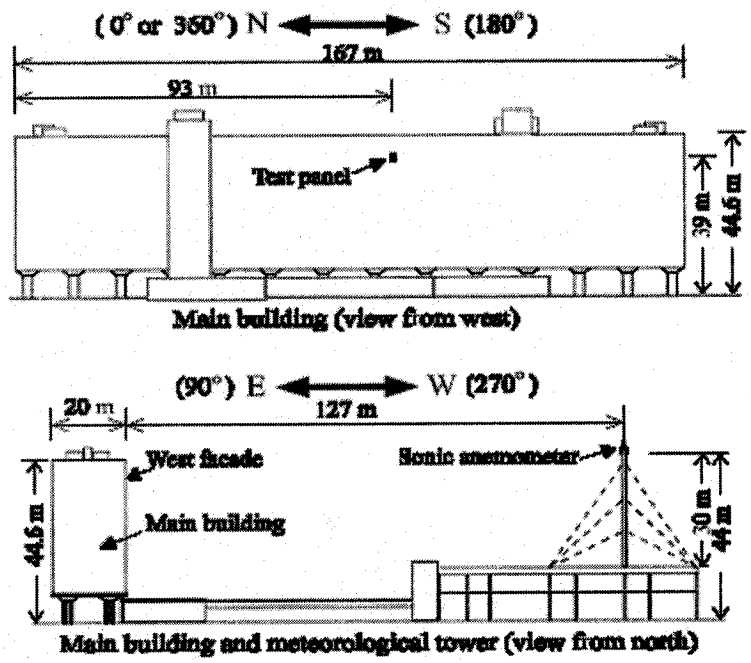

Figure 3.1: Sketch of the field facility [2]

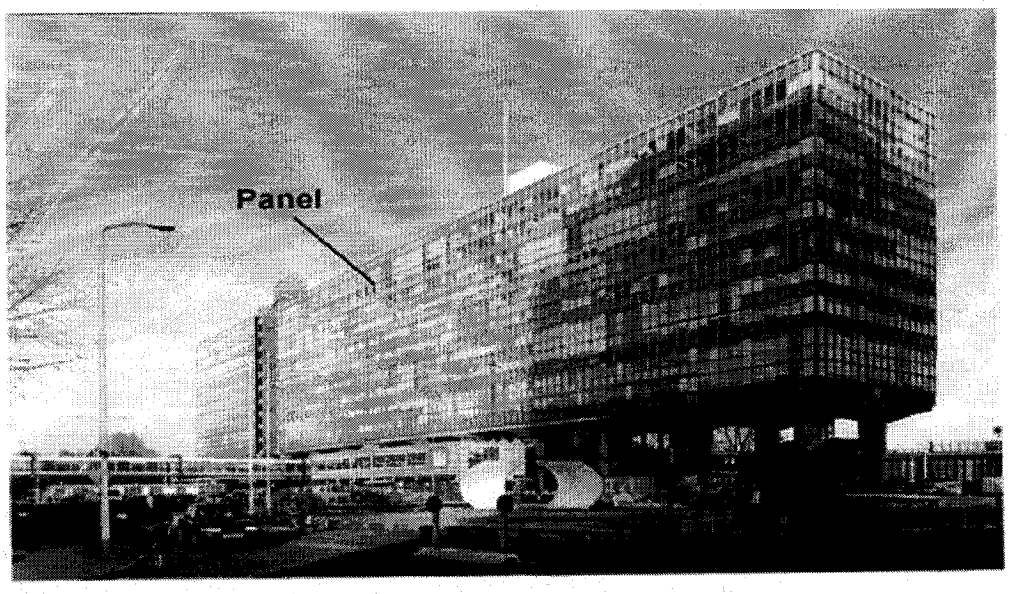

Figure 3.2: Test building view from south [2]

The test panel consists of three components: (a) rainscreen, (b) air barrier and (c) an air space or cavity between them. Here, the cavity depth could be varied. Four pressure taps each on the rainscreen and air barrier were installed for pressure measurements. Figure 3.3 shows the details of the test panel used:

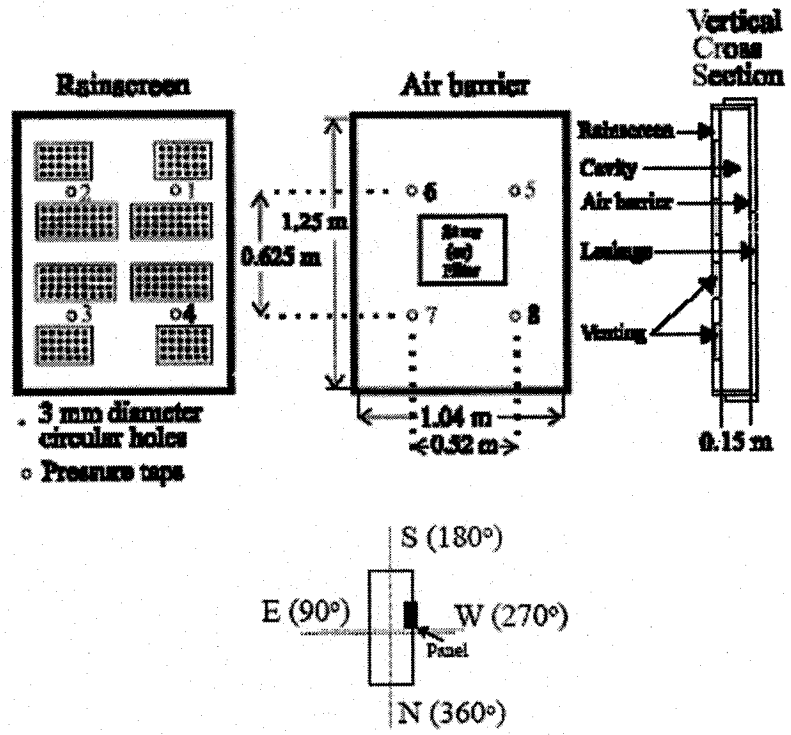

Figure 3.3: Test panel [2]

Two venting area types were used: (a) sharp-edged circular holes of 3mm diameter and 0.5 mm depth, and (b) two rectangular slits of length = 200mm, width = 11.5mm and depth = 20mm. Venting area could be altered by opening or closing the holes. Also, two air barrier leakage types were used: (a) three sets of straws, each 15cm long and 5mm in diameter, in three circular holes (dia. 2cm, 3.8cm, 2cm) at three different locations in the middle of the panel and (b) an industrial metal filter.

Pressure and velocity data were collected for six different panel configurations whose details are shown in Table 3.1. To determine the flow characteristics of venting

and air barrier leakage, simple static pressurization tests were employed. For all configurations, the cavity depth was maintained at 0.15m.

From Table 3.1, it is seen that configurations 1 and 2 differ only in venting area, with configuration 1 having approximately five times as much as venting as configuration 2. For configuration 1, its venting is six times its leakage, while for configuration 2, venting is high as its leakage. Similarly, configurations 2 and 3 have the same venting, while their leakage characteristics are quite different. Configurations 4 and 5 have airtight air barrier, but their venting geometry's are different; the venting area of configuration 5 is about 2.3 times that of configuration 4. Configuration 6 is the same as configuration 5 but with leaky air barrier.

Panel configurations used for full-scale measurements

Configuration	1	2	3	4	5	6
Venting	Circular holes $A_{vs} = 0.009613$ $C_d = 0.61$ $n1 = 0.5$	Circular holes $A_{vs} = 0.001979$ $C_d = 0.61$ $n1 = 0.5$	Circular holes $A_{vs} = 0.001979$ $C_d = 0.61$ $n1 = 0.5$	Circular holes $A_{vs} = 0.001979$ $C_d = 0.61$ $n1 = 0.5$	Rectangular slits $A_{vs} = 0.004577$ $C_d = 0.61$ $n1 = 0.5$	Rectangular slits $A_{vs} = 0.004577$ $C_d = 0.61$ $n1 = 0.5$
Air barrier leakage	Straw $C_{ab} = 0.000314$ $n2 = 0.71$	Straw $C_{ab} = 0.000314$ $n2 = 0.71$	Filter $C_{ab} = 0.000171$ $n2 = 1.0$	No leakage	No leakage	Filter $C_{ab} = 0.000171$ $n2 = 1.0$

Note: A_{vs} = venting area (m^2), C_d = discharge coefficient, $n1$ = flow exponent of air barrier, C_{ab} = flow coefficient of air barrier (mPa^{-n2}/s), $n2$ = flow exponent of air barrier.

Table 3.1: Configuration details [2]

3.1.3 Instrumentation

The differential pressures across the rainscreen and air barrier were measured using the differential pressure transducers supplied by Micro Switch. As pressure transducers tend to drift in time, special precaution was taken in the measurements to arrest such drifts using voltage regulators. These pressure transducers are connected to

pressure taps using flexible tubing, approximately of internal dia. 6mm and length 0.5m. The frequency response of this tubing system is flat at least up to 20Hz.

The study used internal building pressure as the reference pressure. In order, to avoid any abrupt internal pressure variations, tubes of dia. 4mm connected at the reference edge of the transducer were put in a thermally insulated flask placed in a protected location. For data acquisition, a Physics Data Acquisition System (PhyDAS) developed at the Faculty of Physics of the TUE was used. A PARSAM 25 (Parallel sampling A/D conversion board) was used to capture the incoming signal.

3.1.4 Data collection

For each run, the exterior and cavity pressure data were simultaneously measured at the four taps. The sampling frequency was maintained at 20Hz for duration of 10min. The velocity data were also acquired by PhyDAS at a rate of 20.83Hz. Analysis of the data was carried using UNIX workstation. The data acquisition triggered when the mean wind velocity in the last minute exceeded a preset value of 6m/s. All the pressure records collected were at turbulence intensity less than 35% and when the mean wind direction was between 180° and 360°. The measurements were carried out between May 1998 and July 1999. During this period, each of the six configurations was set for at least about two months each for measurements and in total, approximately 1500 full-scale runs were recorded.

3.2 *Scaling of Original TUE Building*

3.2.1 Overview

Wind tunnel testing tries to simulate full-scale conditions. Wind tunnel experiments are validated by appropriate field data. Following validation, further

investigations could be done in the tunnel to establish design parameters and criteria applicable to the field. Therefore, the current thesis employs such wind tunnel experiments to compare results with the original TUE building study. For this purpose, the main TUE building needs to be scaled down along with the rainscreen panel.

It is evident that scaling problems are encountered while modeling the TUE building as its width is long and the rainscreen panel area is small compared to the total façade area. To simulate the panel characteristics properly, the selection of an appropriate building size becomes critical.

3.2.2 Methodology

To choose the appropriate building model for the wind tunnel experiments, three building sizes have been chosen to examine the flow around and the pressures on their envelope, particularly at panel location. The first building (Small – Figure 3.4) is an exact 1:400 scale model of the original; blockage is negligible. The second building (Medium – Figure 3.5) is a distorted 1:200 scale model; the original building is first distorted to have a height to length ratio of 1:2 and then the resultant dimensions are modeled on a 1:200 scale. The blockage of this building is 3.1%. The third building (Large – Figure 3.6) is a 1:100 scale model with all the dimensions as per the scale except for its length, which is distorted to be equal to its height. This building model has a blockage of about 6%. Each of these three building models chosen has three pressure taps installed on its front face: one at the center where the wooden panel is located on the TUE main building; and two at the same face and height but near the two edges. This helps one to know the actual pressures acting on all the three building models at the panel location and at edges and comparisons with

each other can be made easily. As the first building model is an exact scaled replica of the original, the other two buildings are compared with this to find out the deviations in the results obtained.

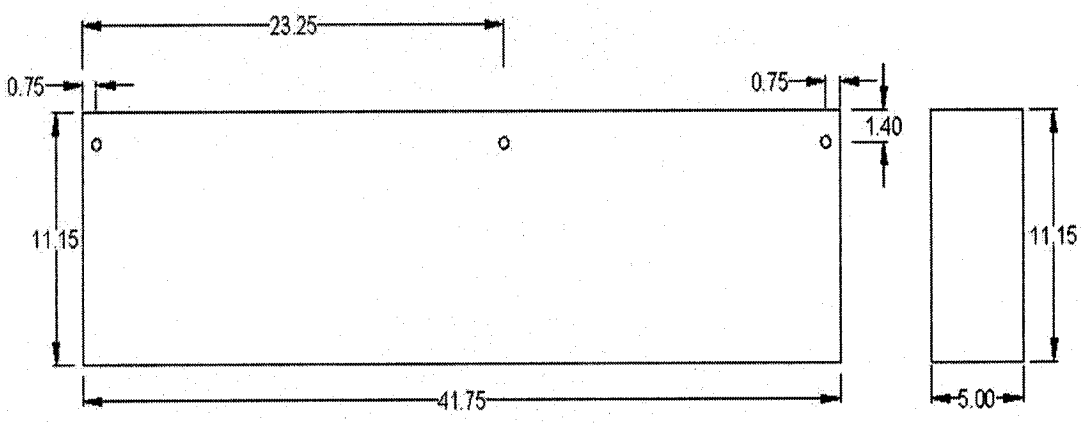

Figure 3.4: Façade of Actual 1:400 Model (Small)
(Dimensions in centimeters)

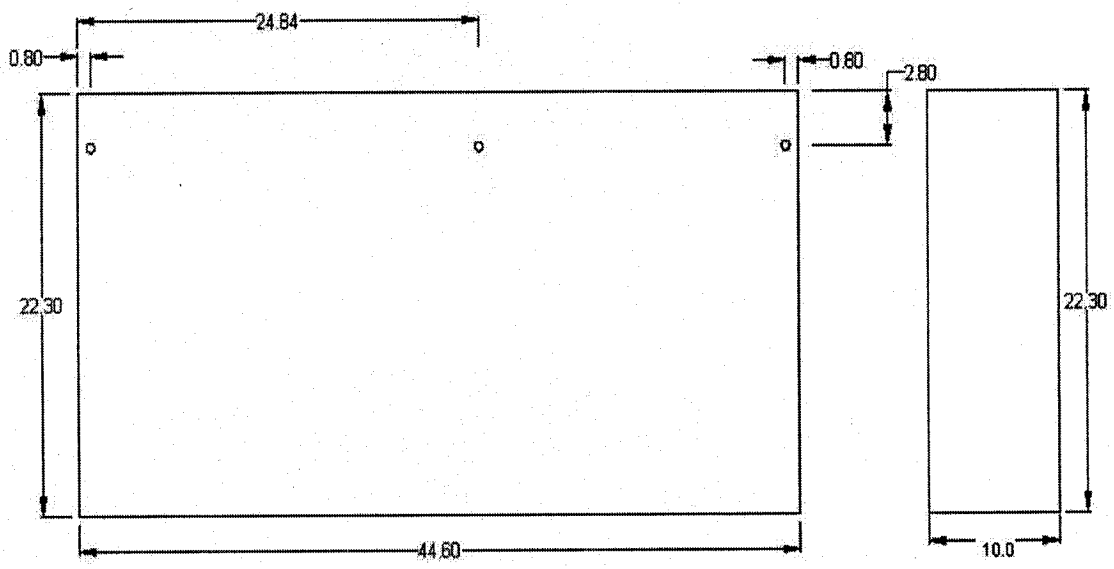

Figure 3.5: Façade of distorted 1:200 model (Medium)
(Dimensions in centimeters)

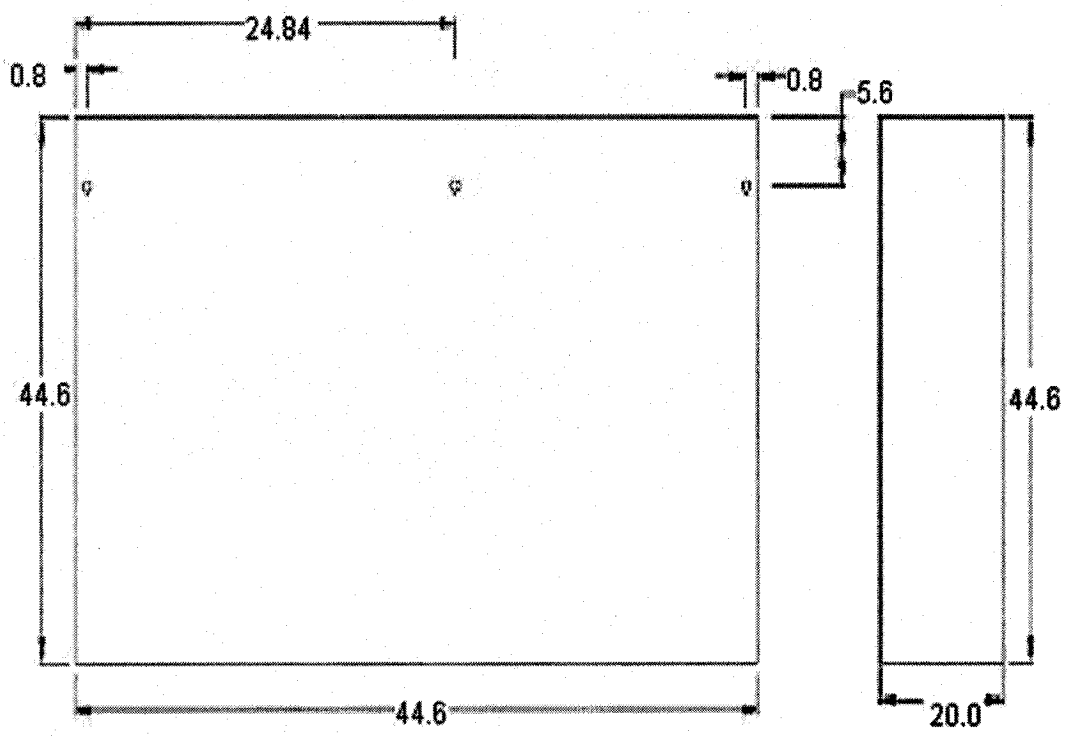

Figure 3.6: Façade of distorted 1:100 model (Large)
(Dimensions in centimeters)

3.2.3 Experimentation Results and Discussion

The pressure measurements in all three buildings are carried out under simulated urban terrain conditions. The actual terrain features of the field are not simulated here as the three buildings are just being compared for the flow around them and for the pressures at the panel location. The velocity profile for the terrain is shown in Figure 3.7 where the ratio of heights above ground is plotted against velocity ratio. The gradient velocity (Vg) is 12.5m/s obtained at a gradient height (Zg) of 600mm. The profile exponent (α) is 0.32 and the turbulence intensity obtained at panel height for the Large, Medium and Small buildings is 0.08, 0.15, and 0.23 respectively. The data is scanned using the automatic Scanivalve pressure transducer from the Scanivalve Corp USA, at a sampling rate of 200 Hz for approximately 20 seconds. The mean and maximum pressure coefficients measured on the central and

edge points for all three buildings are shown in Figures 3.8 and 3.9 respectively for a number of wind directions from West (270°) to East (90°).

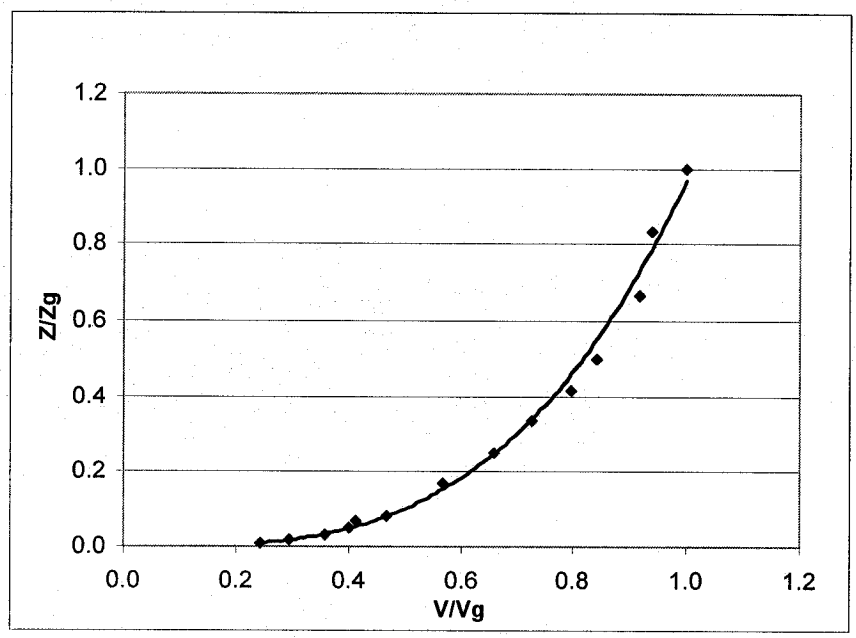

Figure 3.7: Velocity Profile

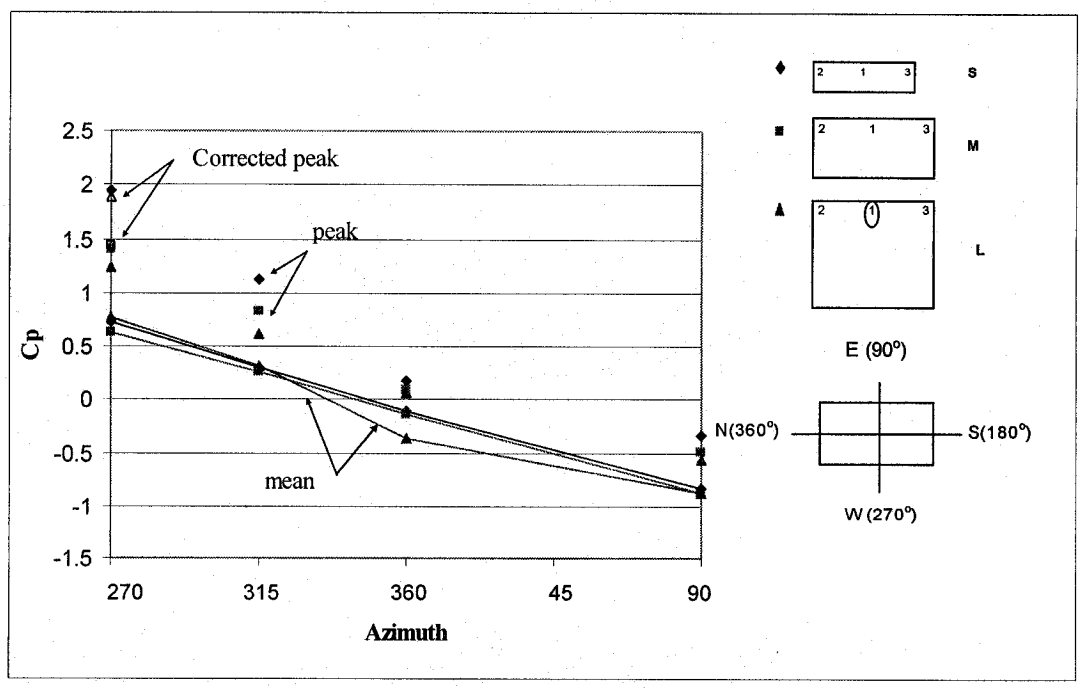

Figure 3.8: Mean and Maximum Cp for Center Tap1

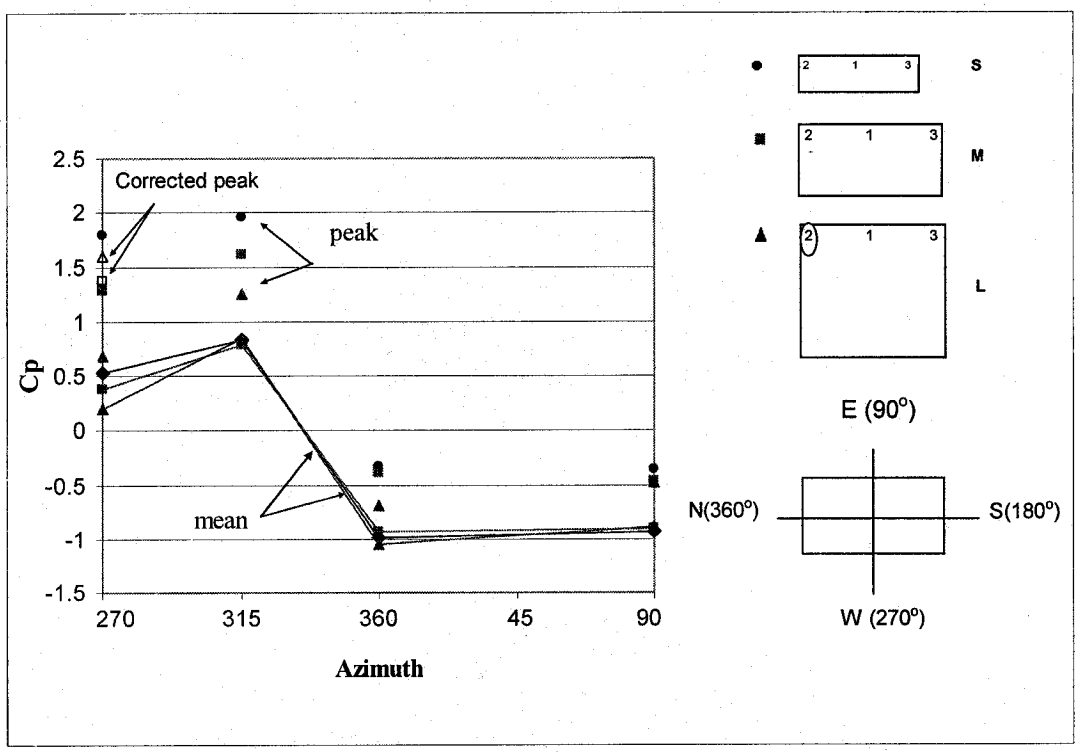

Figure 3.9: Mean and Maximum Cp for Edge Tap2

Results show that the large building model is seen as a good approximation over the small building model for both center and edge mean pressure coefficients. However, this model under-predicts the maximum Cp values due to the reduced oncoming turbulence intensity, which is only 8% in wind tunnel at panel height. Hence, the large building model could be used as a good approximation of the TUE building, only with appropriate turbulence correction based on quasi-steady theory. The corrected coefficient is determined using the following expression:

$\hat{C}_{\text{p-corrected}} = \overline{C}_{\text{p}} + 3.5(\text{T.I}_{\text{field}}/\text{T.I}_{\text{tunnel}})(C_{\text{p,rms-tunnel}})$, where T.I = Turbulence Intensity.

Note that this turbulence correction stands effective only for normal (270°) or near to normal wind directions where a Gaussian probability density function can be assumed [53]. Also, the $\text{T.I}_{\text{field}}$ is replaced by $\text{T.I}_{\text{small building}}$ as the coefficients are

compared against the small building. For example, in the wind tunnel the large building model provides a mean and maximum pressure coefficient of 0.78 and 1.23 respectively; the medium building provides a mean and maximum pressure coefficient of 0.62 and 1.40 respectively. Applying the turbulence correction for both these buildings, one gets:

$$\hat{C}_{\text{p-corrected (medium)}} = 0.62 + 3.5(0.23/0.15)(0.15) = 1.43$$

$$\hat{C}_{\text{p-corrected (large)}} = 0.78 + 3.5(0.23/0.08)(0.11) = 1.89$$

It appears that $\hat{C}_{\text{p-corrected (large)}}$ is close to the obtained maximum coefficient of the small building, which is 1.94 – see Figure 3.8. Similarly, Figure 3.9 shows the corrected C_p peak coefficients for edge taps being near the values measured for the correctly modeled small building. On this basis, the large building has been used for the experiments but turbulence corrections have been implemented in the peak and rms values of pressure coefficients obtained for azimuths ranging from 240° to 300°.

3.3 *Static Pressurization Test*

3.3.1 Scope

The venting area and leakage characteristics of the rainscreen used for the wind tunnel tests should be similar to those used in the TUE building. The rainscreen design for the wind tunnel experiments is determined through simple static pressurization tests. The objective of this test is to compare the flow coefficients and exponents of the sample rainscreen and air barrier designs with the field data and choose the one that produces results in terms of flow characteristics close to those of the field data.

3.3.2 *Methodology*

In order to carry out the wind tunnel experiments, the actual panel is modeled down on a 1:50 scale to fit the scale building. A 1:50 scale is chosen as any scale smaller than this produces a negligible vent size. The porosities of rainscreen and air barrier are also maintained in the same scale. Two rainscreen and three air barrier sections are used. The details of the sections are given in Table 3.2 followed by the sketches in Figures 3.10 and 3.11.

	Thickness (mm)	Vent diameter (mm)	No. of Vents	Porosity
Rainscreen	1	1	6	0.9 %
	1	0.7	12	0.9 %
Air barrier	10	0.33	24	0.4 %
	7	0.33	24	0.4 %
	3.5	0.33	24	0.4 %

Table 3.2: Details of rainscreen and air barrier sections

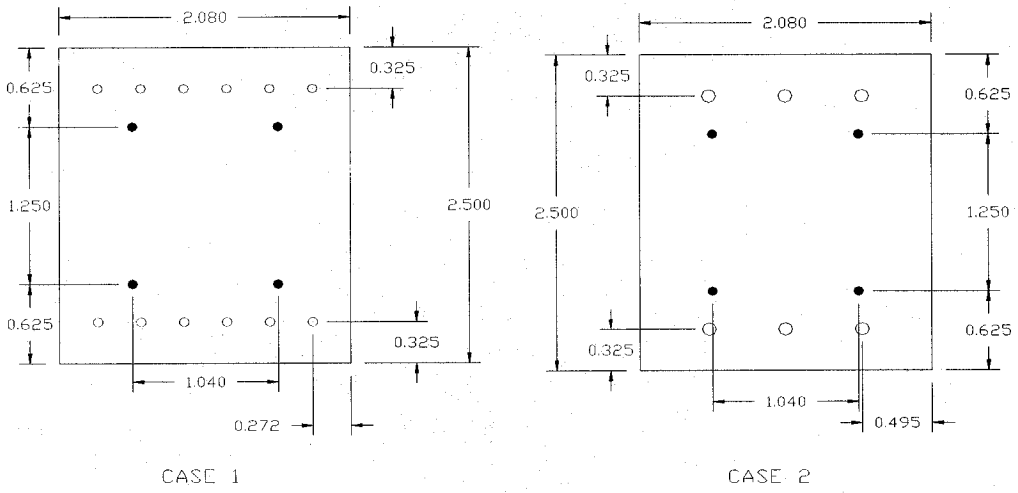

Case 1: 0.7 mm diameter vents

Case 2: 1 mm diameter vents

Figure 3.10: Rainscreen sections designed for comparison

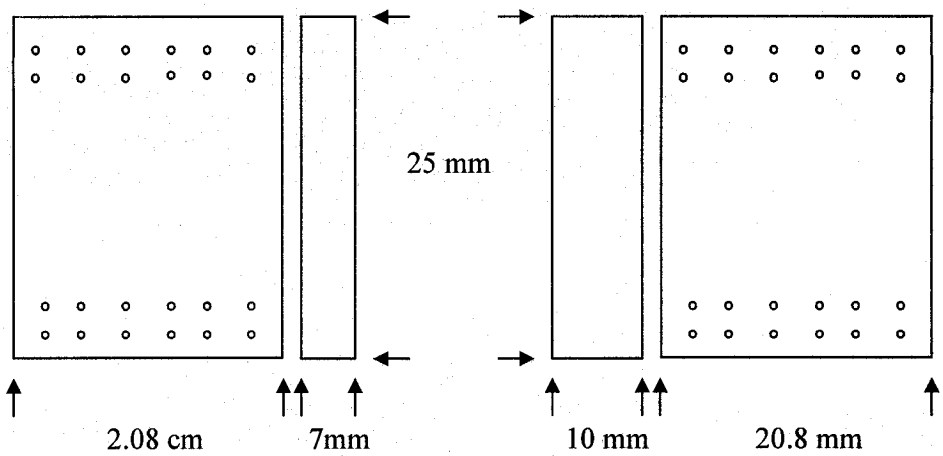

Case 1: 0.33 mm vents

Case 2: 0.33 mm vents

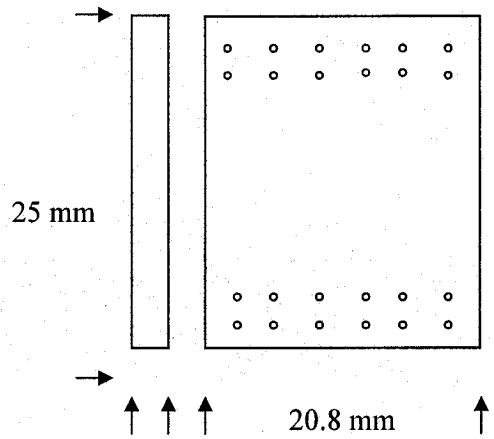

Case 3: 0.33 mm vents

Figure 3.11: Air barrier sections designed for comparison

The section that produces similar leakage and venting characteristics as that of the field will be used for further experiments.

3.3.3 Experiments

The comparison between the rainscreen and air barrier designs is carried out through static tests. A micro manometer (range of -5 to +15 inches of water) is used to note the pressure difference across the panel. Since the range is low and high air flow

rates are not needed, a flow regulator to control the air supply is used. With the flow regulator, reduced airflow rates suitable to the micro manometer are achieved. A box cavity with two halves is designed for this purpose. Each half has two provisions; one for the air supply and the other to connect to the manometer. The test section is placed in between the two halves of the box cavity and the entire structure is clamped tight to prevent air leakage. The box cavity, micro manometer and the experimental setup are shown in Figures 3.12 through 3.14.

Figure 3.12: Box cavity

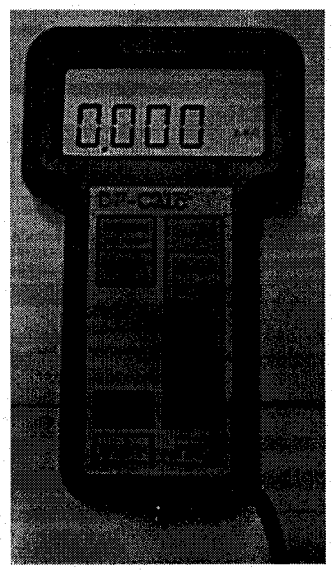

Figure 3.13: Micromanometer

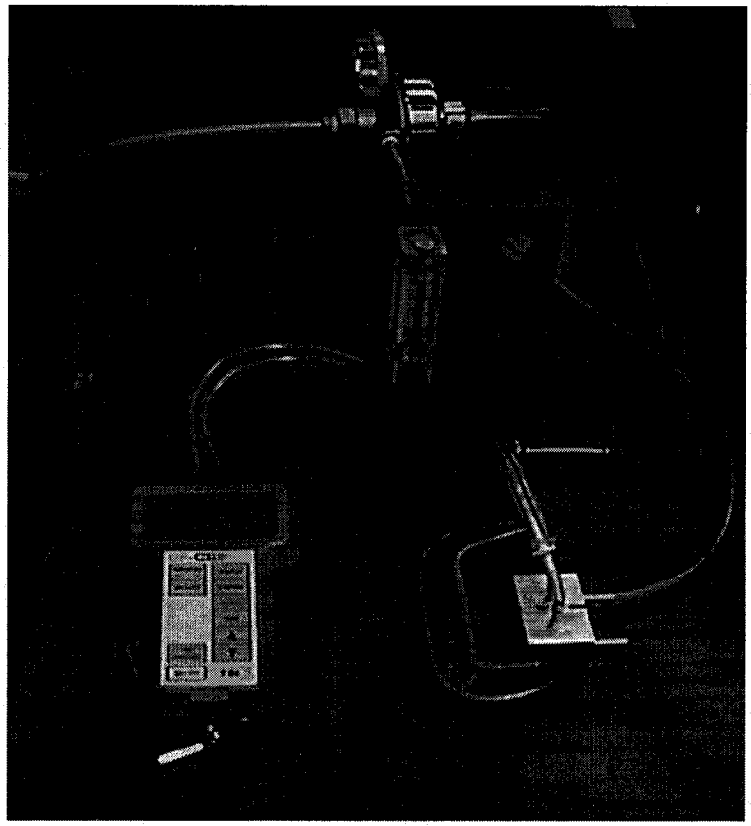

Figure 3.14: Experimental setup

The pressure difference across each section is noted for step wise increment of air flow. The air flow rate begins at 0.6 L/s and a step wise increment of 0.2 L/s is carried out.

3.3.4 Results and comparison with field data

Table 3.3 shows the field leakage characteristics of rainscreen and air barrier sections. In the wind tunnel, for each section three trial rounds were performed to check the consistency of the results. The average of all trials is shown in Figures 3.15 and 3.16 for the rainscreen and air barrier sections respectively. The logarithmic plots show the variation of flow rate (Q) as a function of pressure difference (P).

Configuration	1	2	3	4	5	6
Venting	Circular holes $A_{rs} = 0.009613$ $C_d = 0.61$ $n1 = 0.5$	Circular holes $A_{rs} = 0.001979$ $C_d = 0.61$ $n1 = 0.5$	Circular holes $A_{rs} = 0.001979$ $C_d = 0.61$ $n1 = 0.5$	Circular holes $A_{rs} = 0.001979$ $C_d = 0.61$ $n1 = 0.5$	Rectangular slits $A_{rs} = 0.004577$ $C_d = 0.61$ $n1 = 0.5$	Rectangular slits $A_{rs} = 0.004577$ $C_d = 0.61$ $n1 = 0.5$
Air barrier leakage	Straw $C_{ab} = 0.000314$ $n2 = 0.71$	Straw $C_{ab} = 0.000314$ $n2 = 0.71$	Filter $C_{ab} = 0.000171$ $n2 = 1.0$	No leakage	No leakage	Filter $C_{ab} = 0.000171$ $n2 = 1.0$

Note: A_{rs} = venting area (m^2), C_d = discharge coefficient, $n1$ = flow exponent of air barrier, C_{ab} = flow coefficient of air barrier (mPa^{-n2}/s), $n2$ = flow exponent of air barrier.

Table 3.3: Details of full-scale measurements [2]

The discharge coefficient and flow exponent of rainscreen were found to equal 0.61 and 0.5 respectively as shown in Table 3.3. For the air barrier, the flow coefficient and exponent were found to be 3.14E-04 and 0.71 respectively, for a leakage area of approximately 1.6E-03 m^2. The air barrier section has a leakage of 6.8E-07 m^2 approximately. For this leakage, the reduced field coefficient is 4.03E-07.

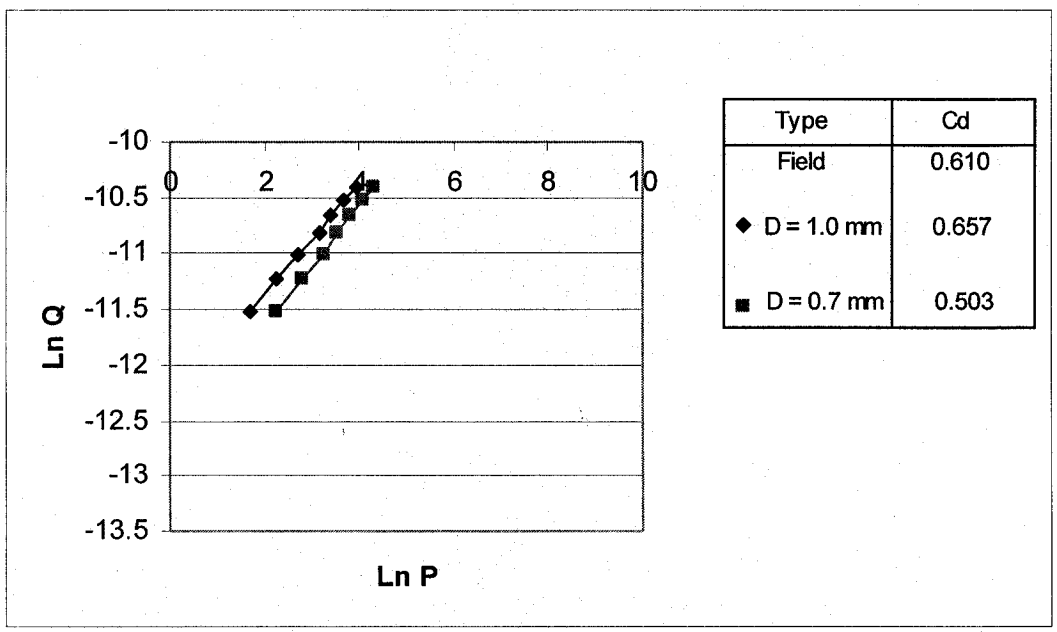

Figure 3.15: Comparison of leakage characteristics of rainscreen sections

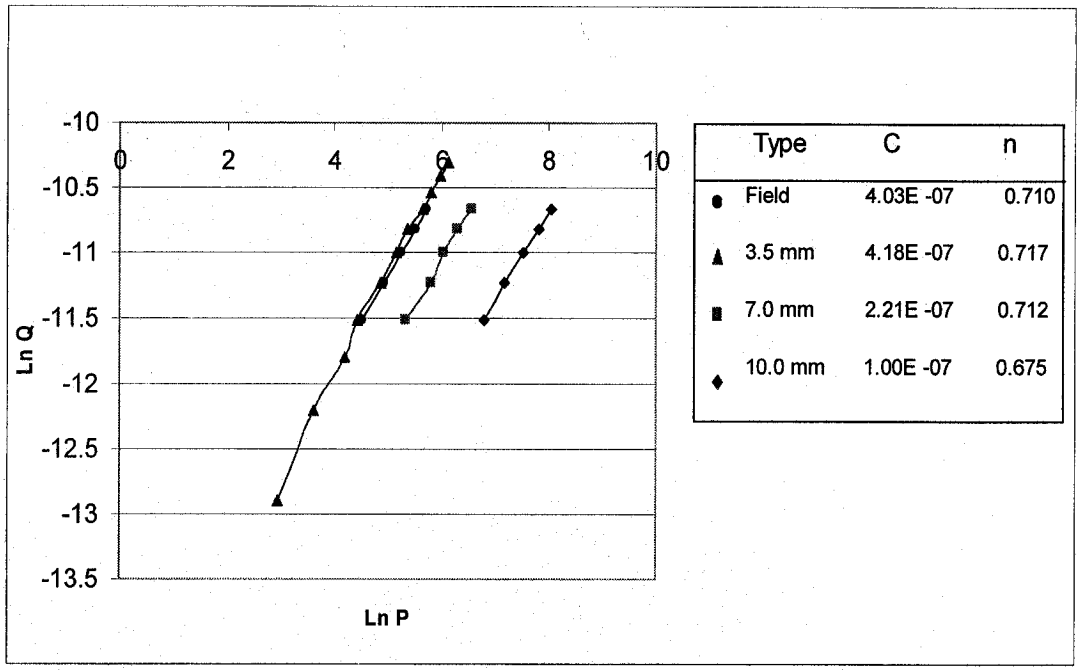

Figure 3.16: Comparison of leakage characteristics of air barrier sections

It is seen that the rainscreen with 1 mm diameter produces a discharge coefficient, C_d, of 0.657 and a flow exponent, n, of 0.49, which are close to field values. Though, the air barrier with 0.7 cm thickness produces an exponent of 0.712 that is close to field value, its flow coefficient is half that of the field value. The air barrier with 3.5 mm thickness produces a flow coefficient of 4.18E-07 and an exponent of 0.717, both of which are close to field values. In order to carry out wind tunnel experiments, the performance of these air barrier sections at low pressures is tested; it was found that the air barrier with 3.5 mm thickness is active at pressures 28 Pa and above.

3.3.5 Comparison with literature sources

The flow exponent found for the air barrier with 7 mm and 3.5 mm thickness are consistent with that provided by literature sources like ASHRAE [51] and the full-

scale results of Karava [52]. According to ASHRAE, the n value for cracks and openings in the building envelope is usually between 0.6 and 0.7. The full-scale results on the test room envelope cracks carried out by Karava in 2002 shows the flow exponent to be in the range of 0.7 to 0.73.

The Discharge Coefficient, C_d, as suggested by ASHRAE is usually considered as 0.65 if the airflow is unidirectional without mixing. It is seen that the rainscreen panel with 1 mm diameter vents produces a C_d, value close to 0.65 and an exponent close to 0.5 indicating fully turbulent flow, as the opening area is large and the opening depth is short.

3.3.6 Discussion

Two rainscreen and three air barrier sections are compared using static pressurization techniques for their leakage characteristics, in order to choose the section that provides close to full-scale values. The results are compared with field data and literature sources to decide upon the appropriate design. The rainscreen with 1 mm diameter has a C_d of 0.657 and an exponent of 0.49 while the air barrier with 3.5mm thickness has a flow coefficient of 4.18E-07 and an exponent of 0.712. For further experimentation, the air barrier with 3.5 mm thickness and rainscreen with 1 mm diameter vents will be used as the final design as they produce close to field values. The cavity depth between the rainscreen and airbarier is maintained as per the scale 1:50 but multiplied by a factor 1.24 to maintain the required gap flow resistance [15]. The final designs are shown in Figures 3.17 through 3.19:

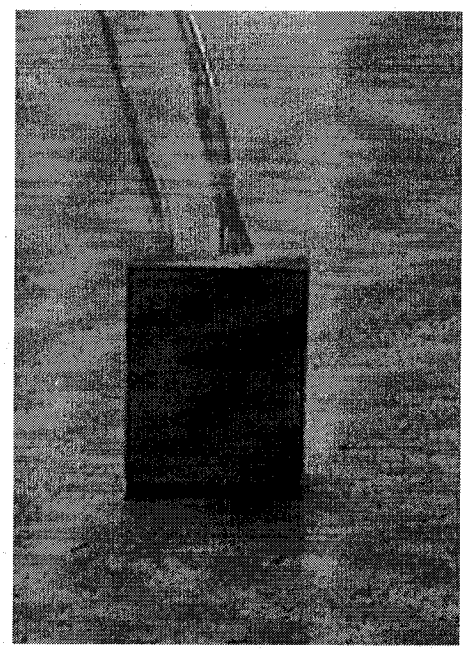

Figure 3.17: Front view of rainscreen design showing the six 1mm diameter vents and two pressure taps in the middle row

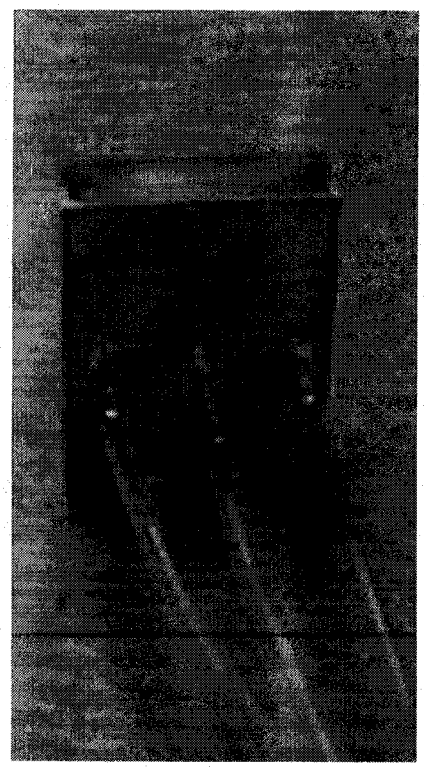

Figure 3.18: Front view of air barrier design

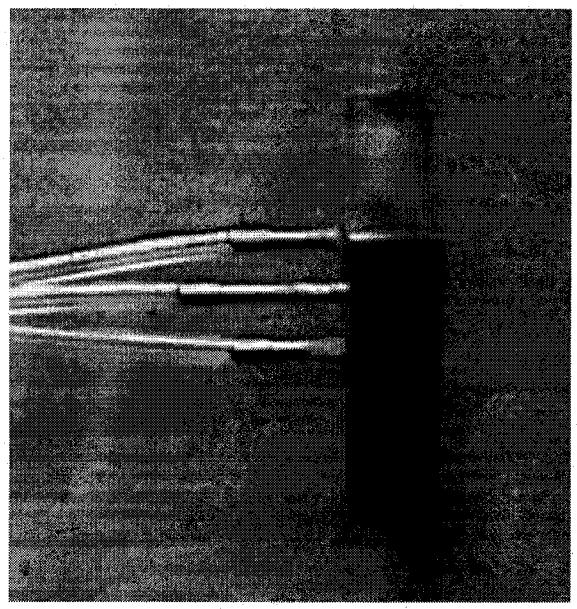

Figure 3.19: Side view showing the cavity depth

3.4 *Wind Tunnel Experimentation*

3.4.1 Building model and location

The actual set of experiments is performed on the model scale building with the rainscreen chosen through the static pressurization test. The dimensions of this building model are height = 44.6 cm, width = 44.6 cm and depth = 20 cm. Another building with dimensions, height = 14 cm, width = 40 cm and depth = 50 cm is placed in front of the main building. This building represents the mast building of the full-scale, which has approximate dimensions of 14 m x 35 m x 50 m and is shown in Figure 3.20. The long facades of the main building of TUE model are perpendicular to the mast building model as in the field. This direction represents the longitudinal axis of the wind tunnel. Figure 3.21 shows the placement of both building models together. The terrain condition is maintained suburban, i.e. similar to the actual terrain in the field, through out the experimentation.

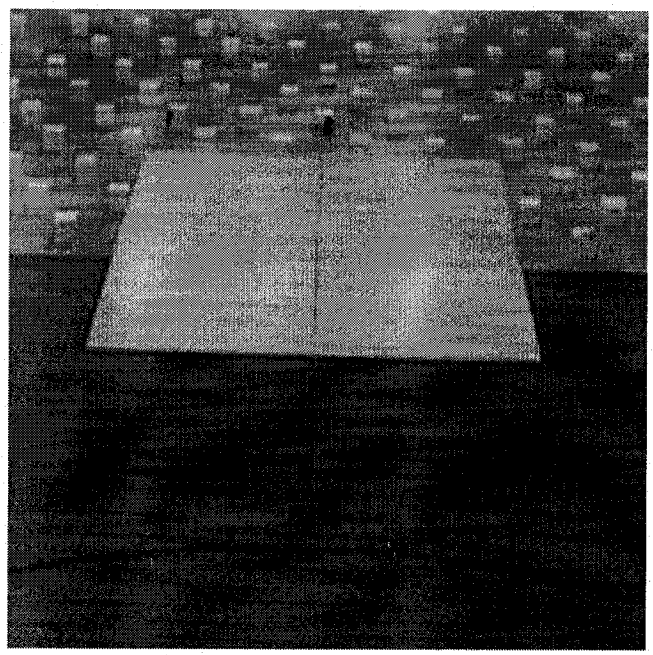

Figure 3.20: Mast building model

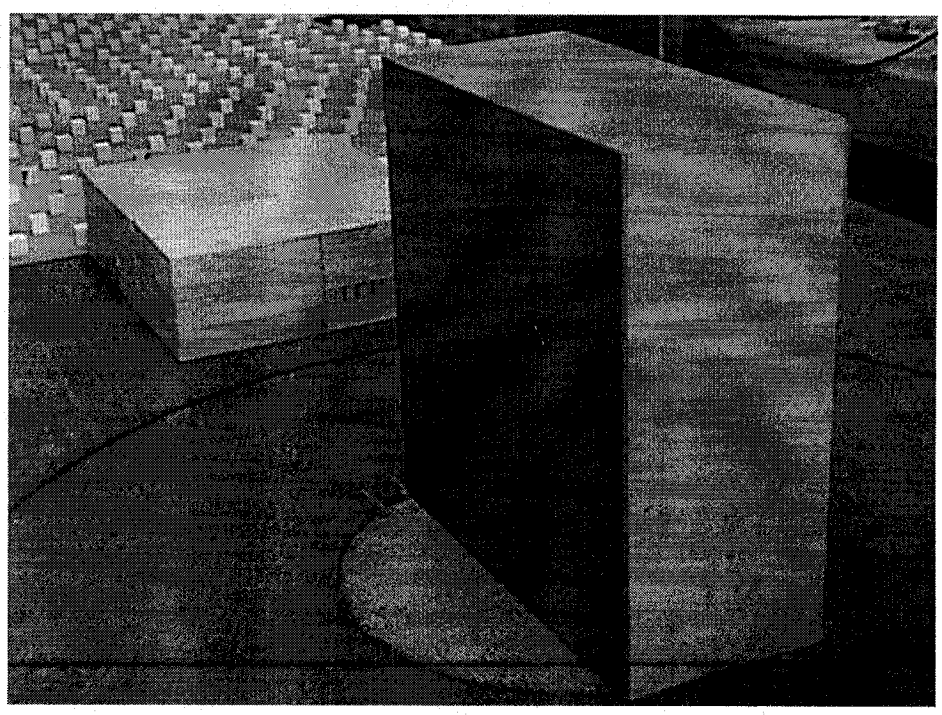

Figure 3.21: Both building models seen together

The rainscreen panel is of size 20.8 mm by 25 mm and is mounted approximately 39 cm from the base of the building. The test panel consists of three

components: (a) rainscreen, (b) air barrier and (c) air cavity in between. The cavity depth cannot be varied and is maintained at 3.27 mm. Two pressure taps are installed on the rainscreen and one on the air barrier for pressure measurements. Figure 3.22 shows the building model with the panel location.

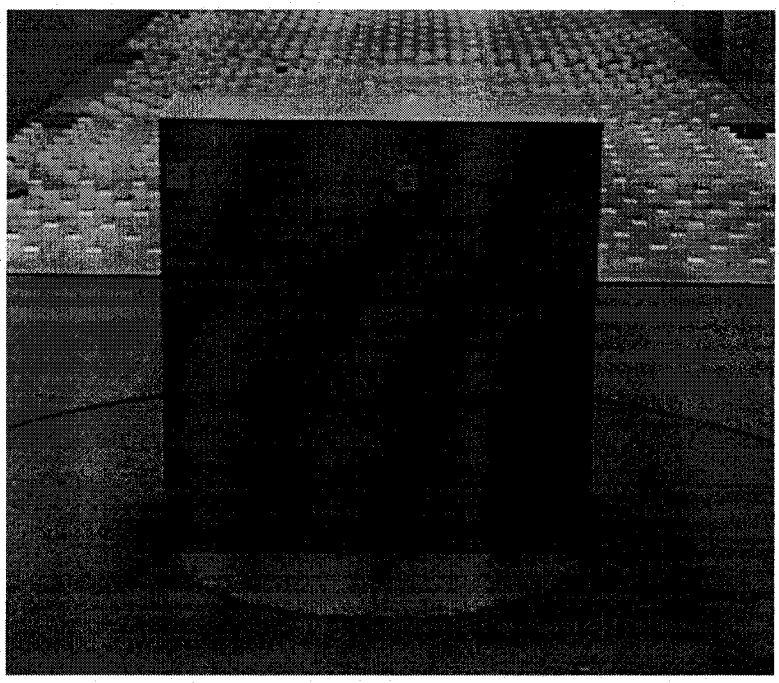

Figure 3.22: Panel location in model scale building

3.4.2 Panel configuration details

The rainscreen and air barrier designed have a maximum porosity of 0.9% and 0.4% respectively. The rainscreen has six 1-mm diameter vents while the air barrier has twenty four 0.33-mm diameter vents. The cavity depth between the rainscreen and air barrier is maintained at 3.72 mm. Venting and leakage area could be varied by opening and/or closing of vents. The actual pressures across the rainscreen and air barrier are noted for different configurations based on their venting and air barrier leakage. Only four such configurations out of the six used in the field are chosen for testing. The wind tunnel focused on a mixture of turbulent and laminar flow through

the air barrier and hence took into consideration those configurations that performed similarly. The other two configurations of the field that used filter type leakage with laminar flow characteristics alone were not used. The flow coefficient and flow exponent for these omitted field leakage types were, Cab = 0.000171 $mPa^{-n2}s^{-1}$ and n = 1.0 respectively. Details of the four configurations chosen for the wind tunnel tests are given in Table 3.4.

The configuration details are the same as in the field maintaining the same ratio of venting to leakage for each configuration. Only configuration 4 has a venting area slightly higher (approximately 0.10 % Aw) than its corresponding field values.

Configuration	**1**	**2**
Venting (μ_e)	0.75% Aw	0.15% Aw
Air barrier Leakage (μ_l)	0.13% Aw	0.13% Aw
Configuration	**3**	**4**
Venting (μ_e)	0.15% Aw	0.45% Aw
Air barrier Leakage (μ_l)	No Leakage	No leakage

Table 3.4: Porosities of rainscreen and air barrier configurations used (Aw = panel area)

Note that configurations 1 and 2 are different only in the venting area. The venting area of configuration 1 is five times larger than the venting area of configuration 2. For configuration 1, the venting area is approximately six times the leakage area. Also, the venting area of configurations 2 and 3 are the same but unlike configuration 2, there is no leakage in configuration 3. The only difference between configurations 3 and 4 is the venting area; configuration 4 has thrice the venting area as configuration 3. In all configurations, the flow coefficient, Cab, and flow exponent,

n, of air barrier are 4.18E-07 and 0.71 respectively. Similarly, the coefficient of discharge, C_d, and flow exponent, n, of rainscreen are 0.65 and 0.5 respectively.

3.4.3 Instrumentation

A differential pressure transducer has been used to measure the differential pressures across the panel and air barrier with the ambient pressure as the reference. A pictorial view of the pressure transducer used is shown in Figure 3.23. In order, to prevent any disturbance in measurement of ambient pressure, the reference pitot tube is placed far upstream of the TUE building model. The calibration curve of the pressure transducer is shown in Figure 3.24.

The pressure tapings on the panel are connected to the pressure transducer through flexible pressure tubing. Too long and narrow tubing can cause attenuation of fluctuating pressures and filter high frequencies of interest. Hence, tubes of internal diameter equal to 1.8 mm are used with connectors in between to avoid this problem. For data acquisition, LabView software is used that converts the incoming signals from all the three tapings into digital values and stores the data in text format. The data is later worked upon in Microsoft Excel to plot the graphs.

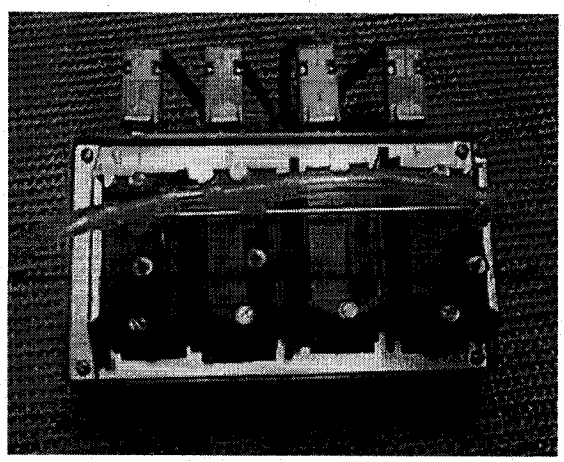

Figure 3.23: Pressure transducer

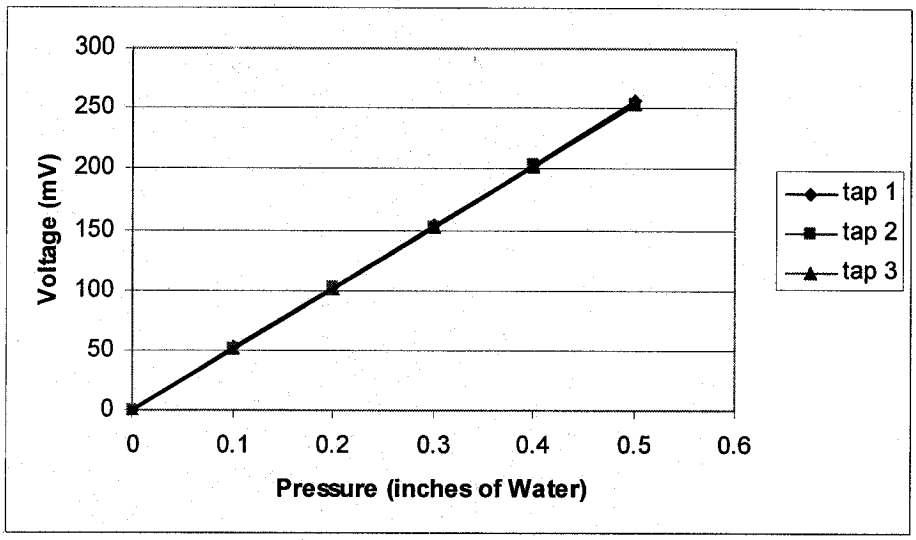

Figure 3.24: Calibration of pressure transducer

3.4.4 Data collection

For each run, the exterior and cavity pressure data in the field are collected simultaneously at a sampling rate of 20 Hz for 10 minutes. The wind tunnel data are collected at a sampling rate of 512 Hz for a 64-second scanning duration. For each configuration the data are measured from 180^{o} to 360^{o} clockwise at an increment of 30^{o}. Azimuths 180^{o} and 360^{o} indicate wind directions parallel to the building façade while azimuth 270^{o} indicates wind direction normal to façade. The terrain used is suburban with a turbulence intensity of 8% at panel height and wind velocity of 12 m/s at roof height. The field measurements had around 30% turbulence at the panel height and the effect of turbulence mis-presentation is corrected, as mentioned in section 3.2.3. Unfortunately, this turbulence correction cannot be applied for rainscreen pressures. It is noted that poor venting with considerable leakage like configuration 2 requires sufficient gusts to cause high rainscreen rms pressures. Consequently, the simulation of this particular configuration is rather difficult in comparison to other configurations.

CHAPTER 4

EXPERIMENTAL RESULTS

Pressure measurements have been performed on two panel locations on the main building of TUE model; one at the Center and the other at the Edge of the wall. The locations of the panel are shown in Figure 3.22. This chapter is divided into three sections. The first section deals with the results of the Center Configuration, while the second compares these results with the available field data. The third section presents the results of the Edge Configuration.

Please note that all pressure coefficients (C_p) are calculated based on the dynamic pressures at roof height. This non-dimensional pressure coefficient (C_p) is defined by:

$C_p = (p - p_o)/(0.5\ \rho\ U^2)$, where U = mean wind speed at reference height [53].

The maximum and minimum C_p's are selected by averaging the worst ten peaks of the time history. The definition of *MPEC*, *SPEC* and MaxPEC used in figures are as follows:

MPEC is the ratio of the absolute value of the mean pressure acting on the rainscreen to the absolute value of the mean pressure acting on the panel

SPEC is the ratio of the rms pressure acting on the rainscreen to the rms pressure acting on the panel.

MaxPEC is the ratio of the absolute value of the maximum pressure acting on the rainscreen to the absolute value of the maximum pressure acting on the panel

Maximum and minimum peak factors acting on the panel and rainscreen have been estimated for all configurations. Peak factors (g) in general are defined as follows:

g = ((peak pressure coefficient – mean pressure coefficient)/rms pressure coefficient)

4.1 *Wind Tunnel Results: Center Configuration*

4.1.1 Mean and rms pressure coefficients

- The distribution of mean and rms pressure coefficients of the panel over the azimuth is shown in Figures 4.1 and 4.2. Note that the wind directions span between $\Theta = 90^{o}$ to $\Theta = 270^{o}$, where $\Theta = 270^{o}$ indicates normal to façade. The largest mean pressure coefficients of the panel occur at $\Theta = 150^{o}$ while the largest rms pressure coefficients occur at $\Theta = 270^{o}$. The mean rainscreen pressure coefficients are independent of wind direction for configurations 3 and 4 with airtight air barrier and for configuration 1 with high venting to leakage ratio. In the case of configuration 2, the pressure coefficients depend on wind direction. For all configurations, the rms rainscreen coefficients are seen to be somewhat symmetrical about $\Theta = 180^{o}$. Also, there exists maximum difference between the mean panel and rainscreen coefficients at $\Theta = 150^{o}$ and at $\Theta = 270^{o}$ for rms panel and rainscreen coefficients indicating good pressure equalization. The amount of load shared by the rainscreen varies depending on the venting area and the air barrier leakage. In the case of configuration 2, where the venting area is reduced compared to configuration 1, the mean load is increased. Comparing configurations 3 and 4 that have airtight air barrier, it is seen that for non-normal wind directions configuration 3 with less venting carries more rainscreen load. Thus, sufficient venting area is required for better pressure equalization and consequent load reduction of mean rainscreen load.

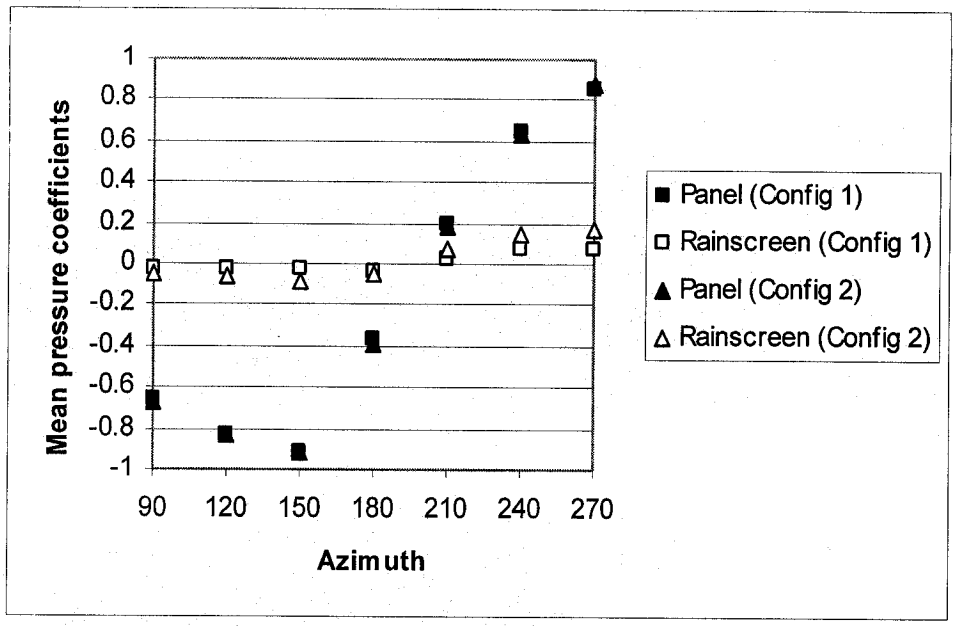

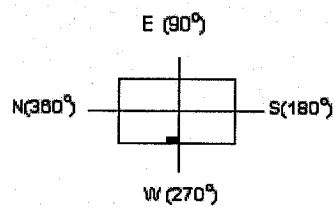

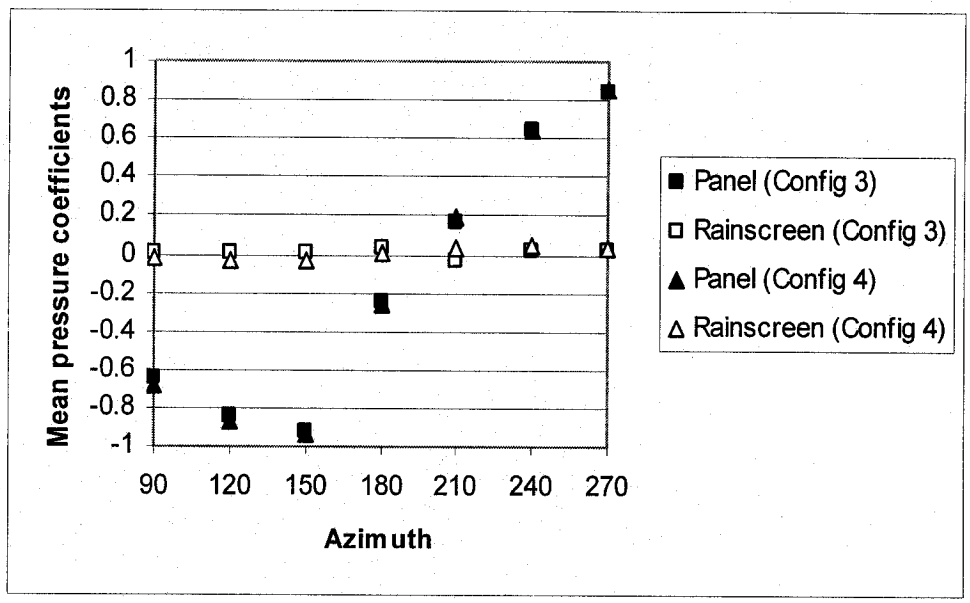

Figure 4.1: Mean pressure coefficients acting on panel and rainscreen as a function of azimuth

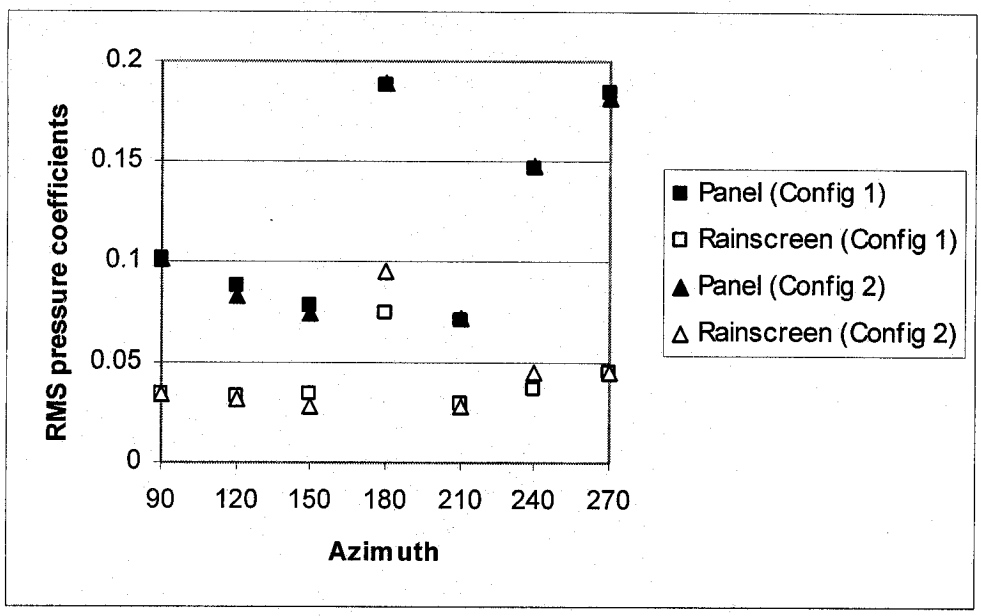

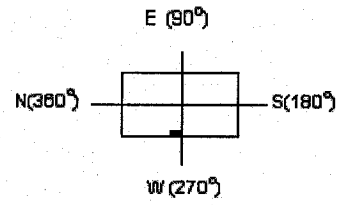

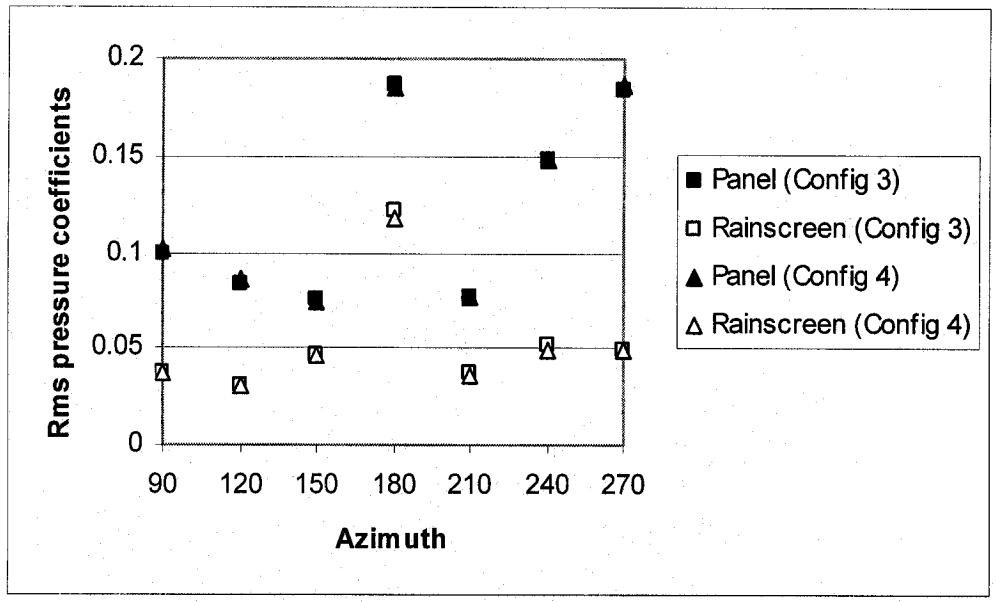

Figure 4.2: Rms pressure coefficients acting on panel and rainscreen as a function of azimuth

- The mean as well as rms pressure coefficients are compared with the corresponding mean as well as rms pressure coefficients acting on the panel and are shown in Figures 4.3 and 4.4 respectively. In all configurations, the mean as well as rms rainscreen pressure coefficients increase as the corresponding panel pressure coefficients increase.

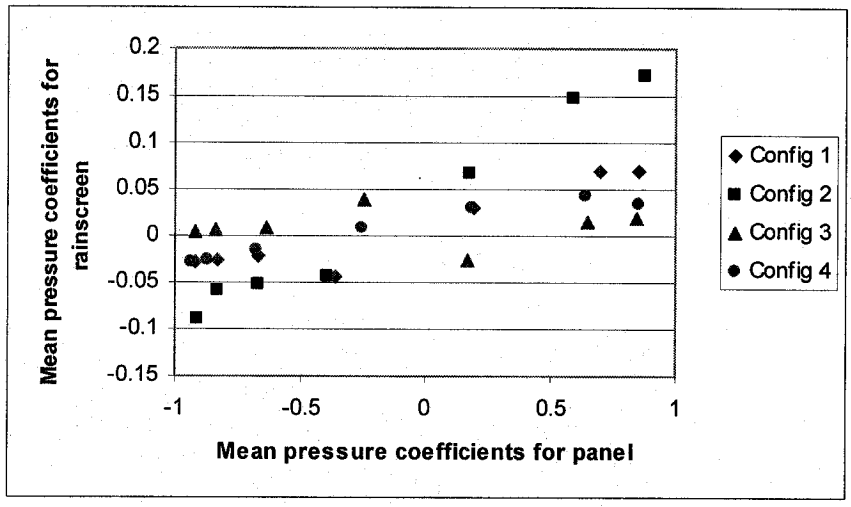

Figure 4.3: Comparison of mean pressure coefficients acting on rainscreen with mean pressure coefficients acting on panel

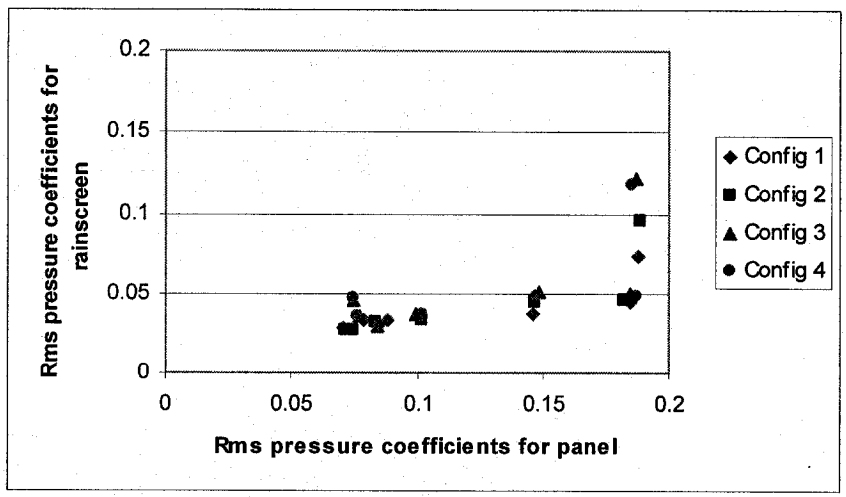

Figure 4.4: Comparison of rms pressure coefficients acting on rainscreen with rms pressure coefficients acting on panel

4.1.2 *MPEC and SPEC values*

- The variation of MPEC values with respect to wind direction and mean pressure coefficients for the panel as well as rainscreen are shown in Figures 4.5 to 4.7. MPEC values appear to depend on wind directions for all the configurations; in fact they reach a maximum at $\Theta = 210^{o}$, and thereafter their values drop down to a minimum at $\Theta = 90^{o}$. All configurations other than 2 have relatively low mean rainscreen pressure coefficient for all wind directions signifying good pressure equalization. The dependence of MPEC values on mean pressure coefficients of the panel and rainscreen are also noted. There is significant variation in the MPEC values as the mean pressure coefficient for the panel decreases from its maximum. Other than configuration 2, the MPEC values in all configurations are rather insensitive to the values of mean rainscreen pressure coefficients.

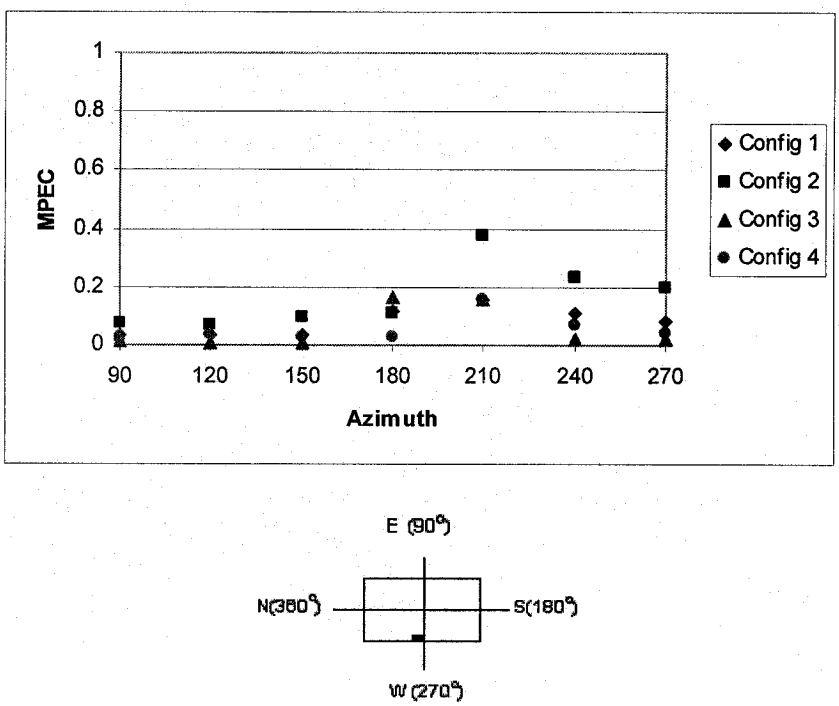

Figure 4.5: Variation of MPEC with respect to wind direction

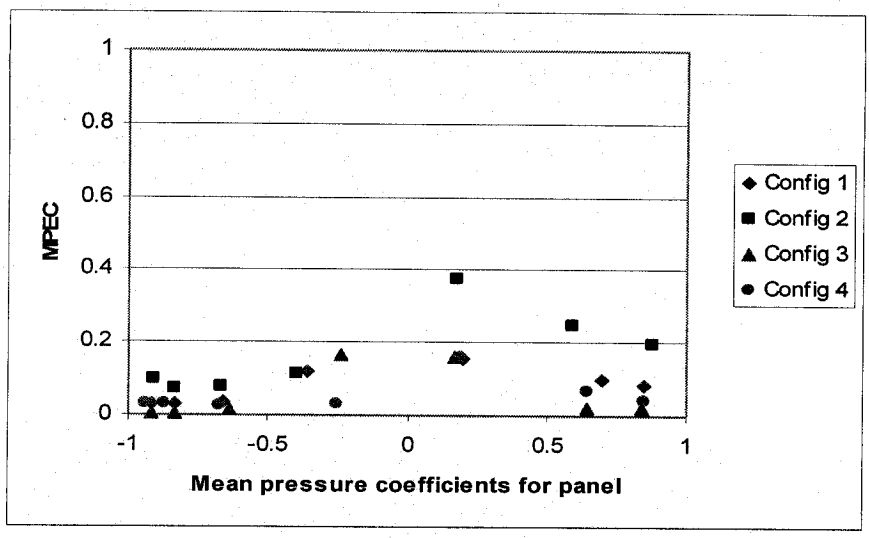

Figures 4.6: Variation of MPEC with respect to wind mean pressure coefficients acting on panel

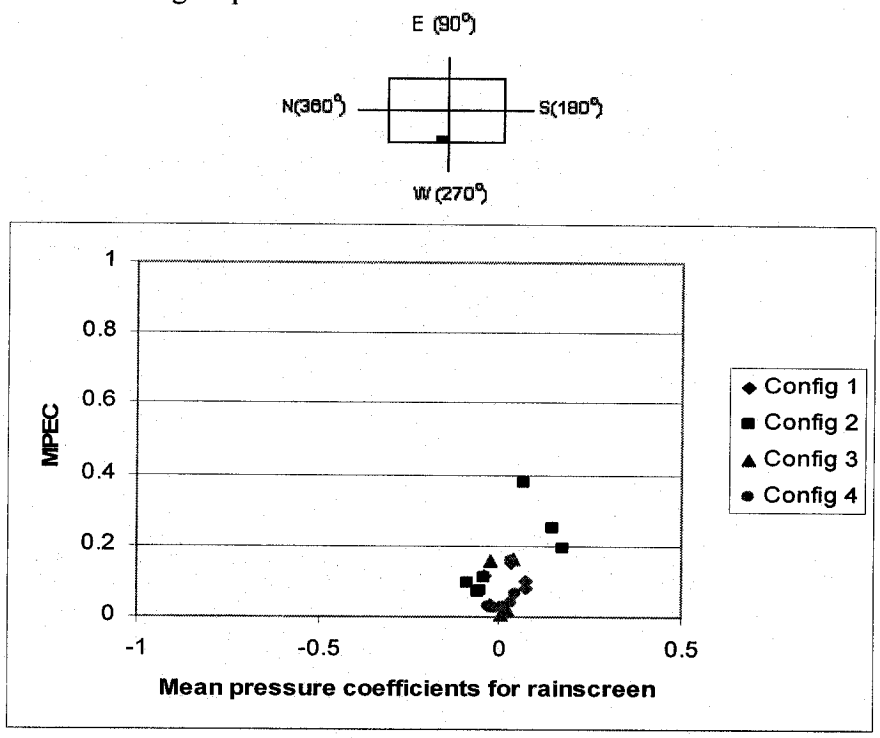

Figures 4.7: Variation of MPEC with respect to wind mean pressure coefficients acting on rainscreen

- The variation of SPEC values with respect to wind direction and rms pressure coefficients for the panel as well as rainscreen are shown in Figures 4.8 to 4.10. For all configurations, SPEC values are minimum near $\Theta = 270^{\circ}$ and

maximum near $\Theta = 180^{o}$. This indicates that there is better pressure equalization when the wind blows normal to the façade and poor pressure equalization when the wind blows parallel to the façade. Maximum SPEC values are noted when there is a decrease in the rms pressure coefficients for panel and rainscreen.

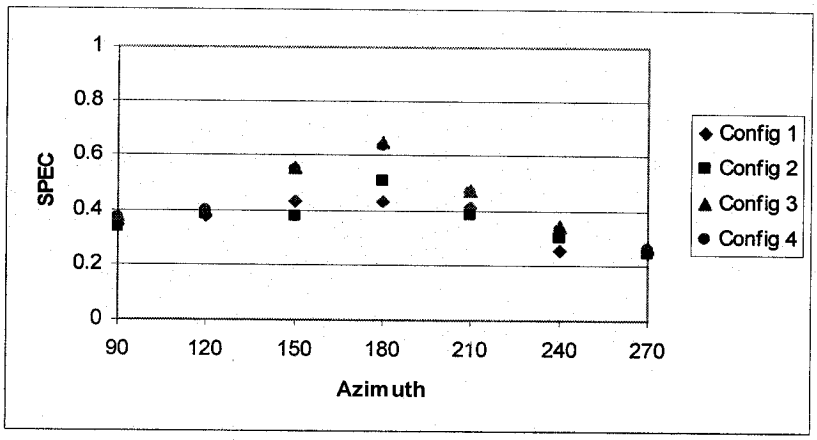

Figure 4.8: Variation of SPEC with respect to wind direction

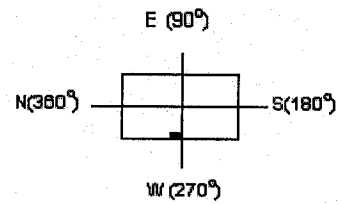

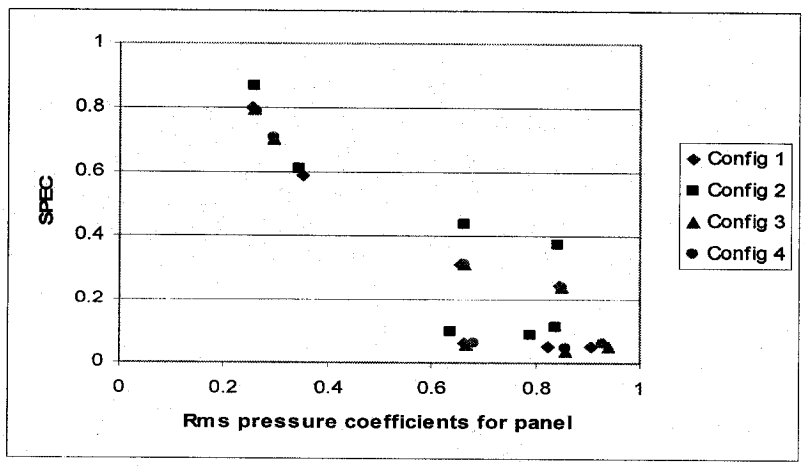

Figure 4.9: Variation of SPEC with respect to rms pressure coefficients acting on panel

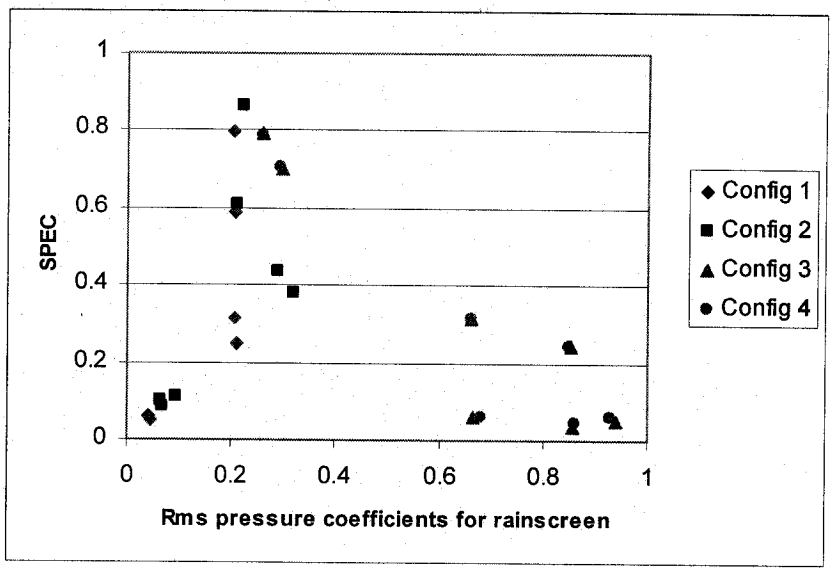

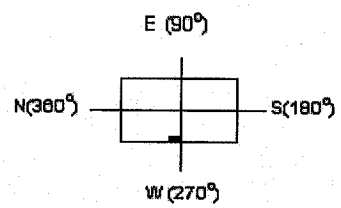

Figures 4.10: Variation of SPEC with respect to rms pressure coefficients acting on rainscreen

4.1.3 Extreme pressure coefficients and peak factors

- Maximum and minimum pressure coefficients as well as peak factors acting on the panel are shown in Figures 4.11 to 4.16. The maximum and minimum panel pressure coefficients decrease as the wind deviates away from normal to the façade (270°). The maximum peak factors are almost symmetrical about Θ = 180° with the lowest value recorded at this azimuth. This is expected due to high rms pressures at this azimuth – see Figure 4.2. The minimum peak factors are almost insensitive to wind directions. The highest maximum and minimum peak factors obtained are close to 4 and -8.6 respectively. Peak factor values depend on mean as well as rms pressures. The variation of peak panel factors against rms pressure coefficients are shown in Figures 4.15 and 4.16. In

general, low rms pressure coefficients induce higher maximum as well as minimum peak factors.

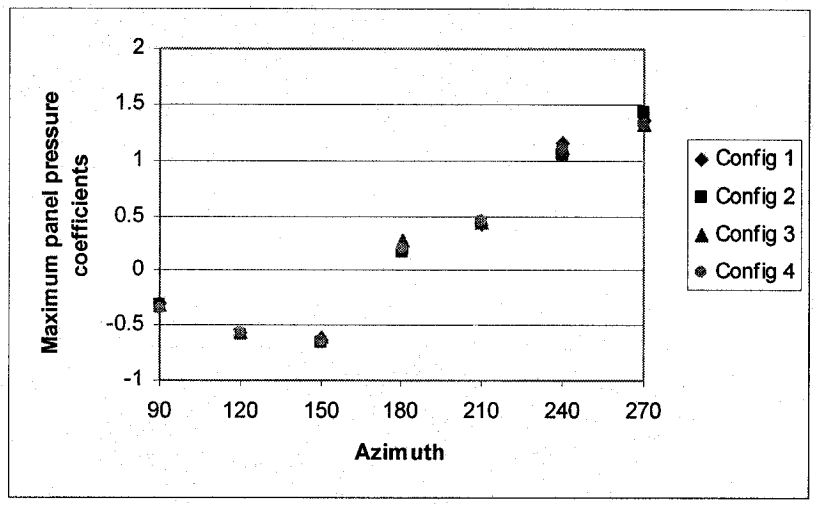

Figure 4.11: Maximum pressure coefficients acting on panel as a function of azimuth

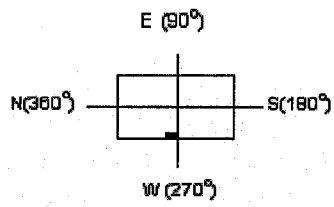

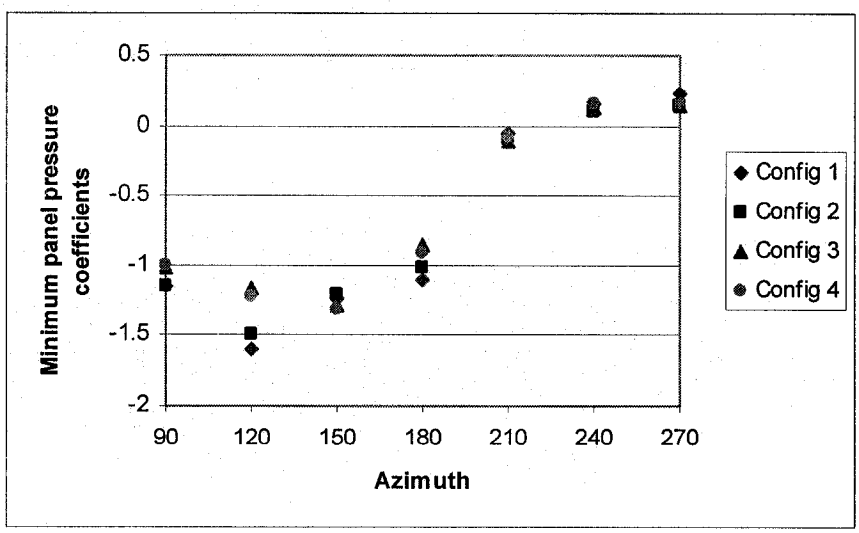

Figure 4.12: Minimum pressure coefficients acting on panel as a function of azimuth

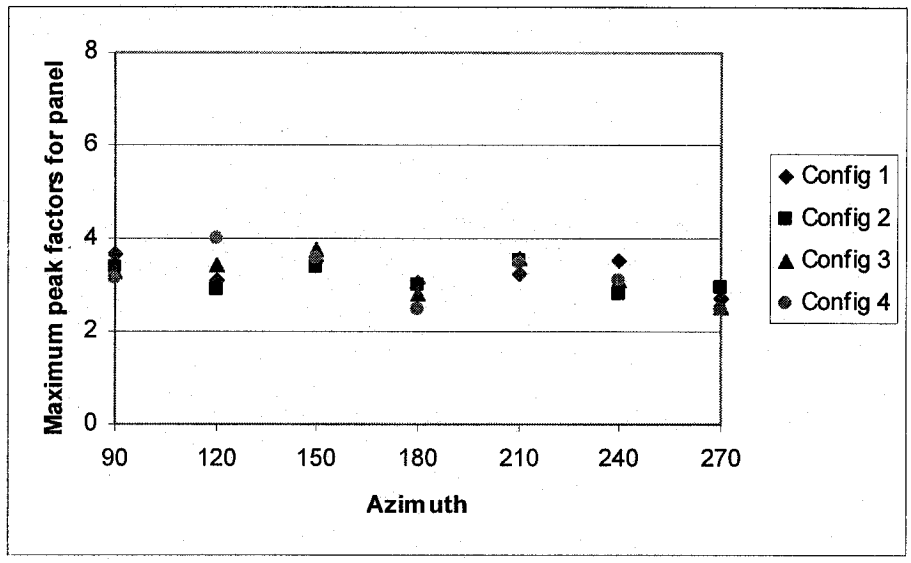

Figure 4.13: Maximum peak factors acting on panel as a function of azimuth

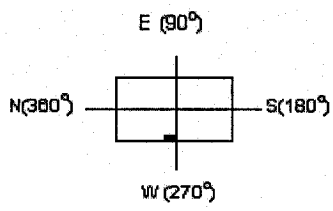

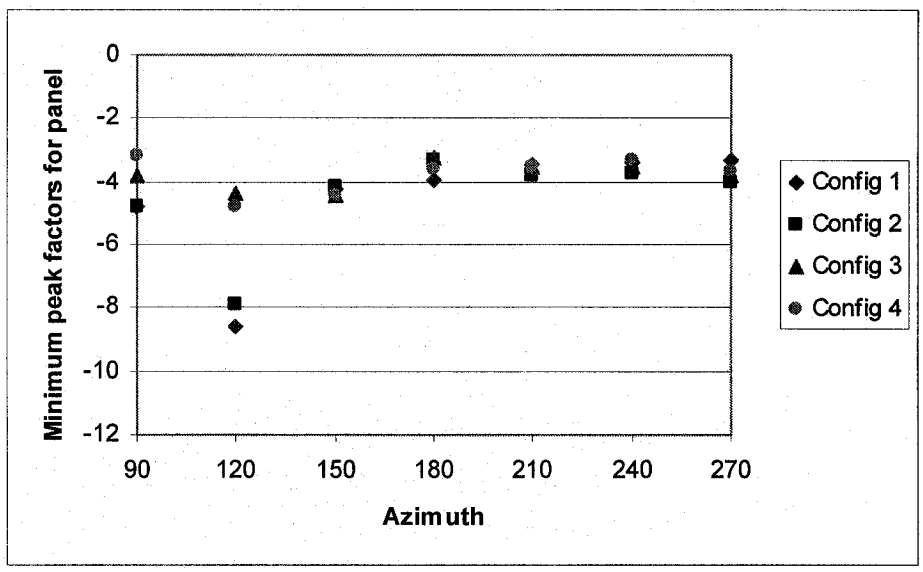

Figure 4.14: Minimum peak factors acting on panel as a function of azimuth

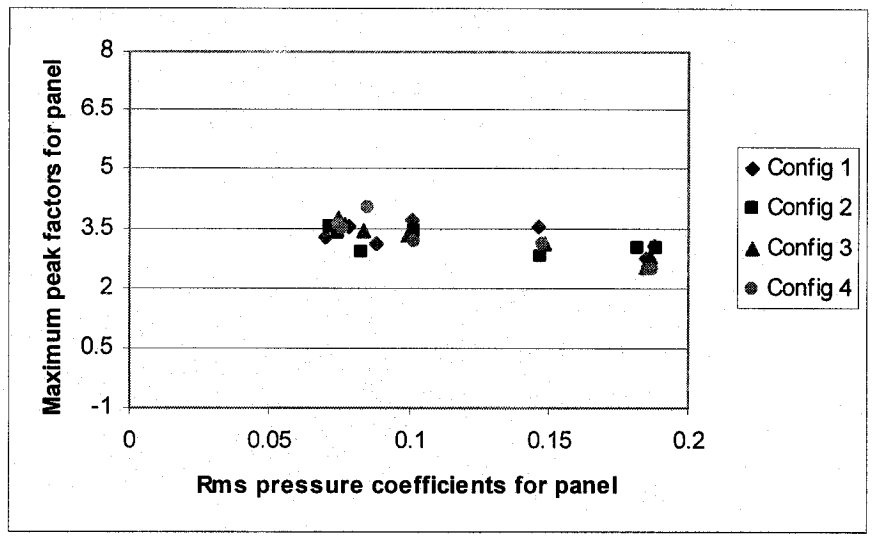

Figure 4.15: Maximum peak factors acting on panel as a function of rms pressure coefficients acting on panel

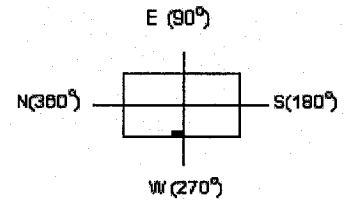

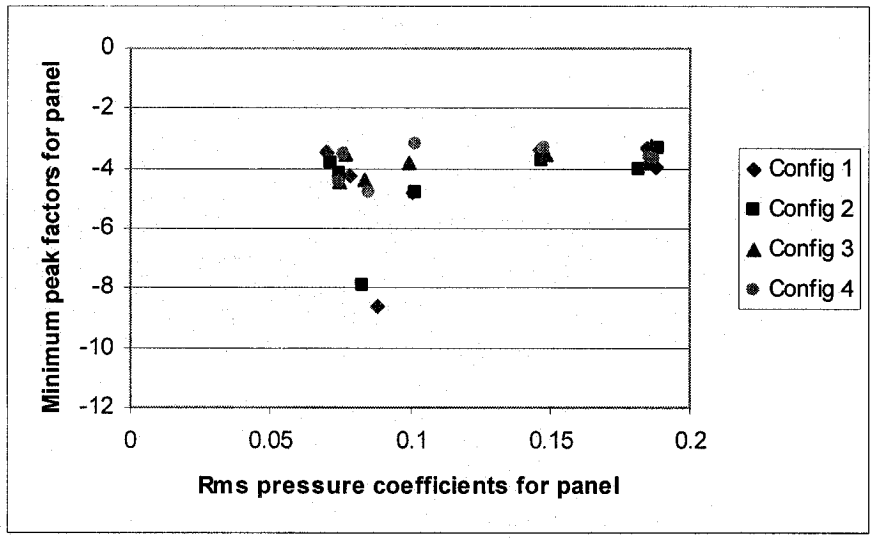

Figure 4.16: Minimum peak factors acting on panel as a function of rms pressure coefficients acting on panel

- Variation of maximum and minimum rainscreen pressure coefficients against wind direction is shown in Figures 4.17 and 4.18. The maximum and

minimum rainscreen coefficients depend on wind direction and are symmetrical about $\Theta = 180^{o}$. The magnitude of maximum and minimum rainscreen pressure coefficients depends on the venting and leakage characteristics of the respective configuration. For instance, maximum rainscreen pressure coefficients of configuration 2 are higher than those of configuration 1.

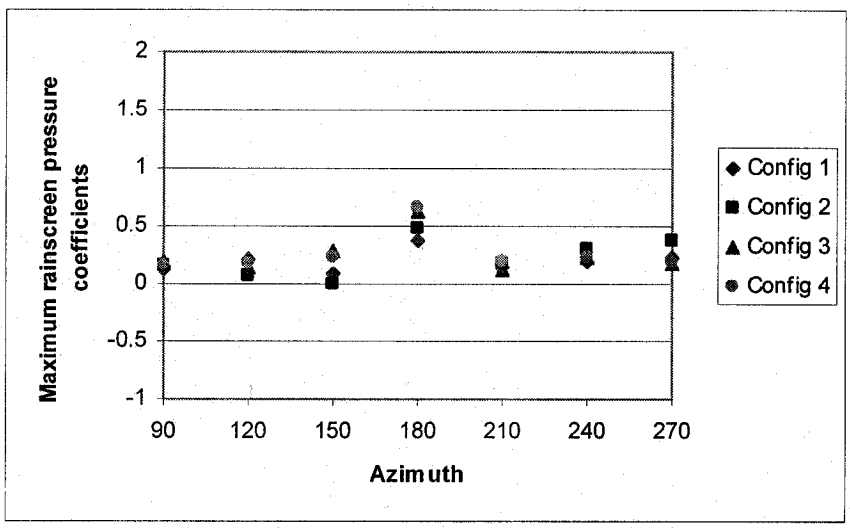

Figure 4.17: Maximum rainscreen pressure coefficients as a function of azimuth

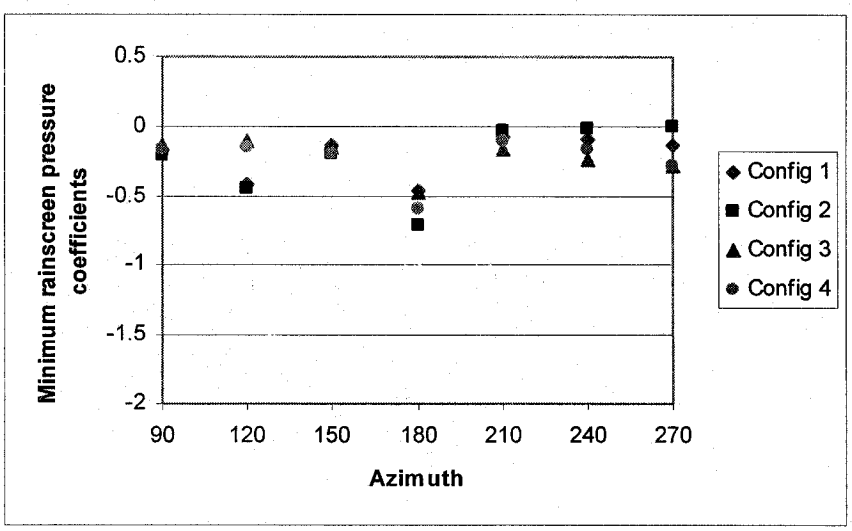

Figures 4.18: Minimum rainscreen pressure coefficients as a function of azimuth

- Variation of maximum and minimum rainscreen peak factors against wind direction and rms rainscreen pressure coefficients is shown in Figures 4.19 to 4.22. Note that the maximum rainscreen peak factors are dependent on wind directions and the minimum rainscreen peak factors are symmetrical about Θ = 180°, which is similar to the minimum rainscreen pressure coefficients – see Figure 4.18. In general, the rainscreen peak factors are much higher than panel peak factors due to the nature of the rainscreen pressures as previously mentioned. Looking at the variation of maximum and minimum rainscreen peak factors against rms pressure coefficients, it is clear that very high values of maximum as well as minimum rainscreen peak factors are associated with low rms rainscreen pressure coefficients. This wide scattering of the maximum and minimum peak factors across low rms rainscreen pressure coefficients has little physical significance.

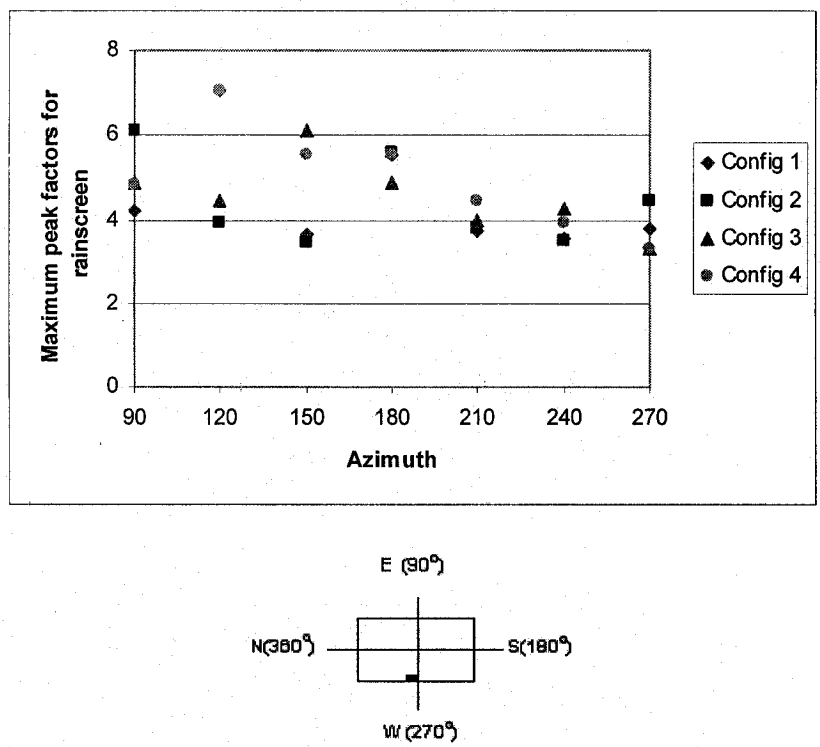

Figure 4.19: Maximum rainscreen peak factors as a function of azimuth

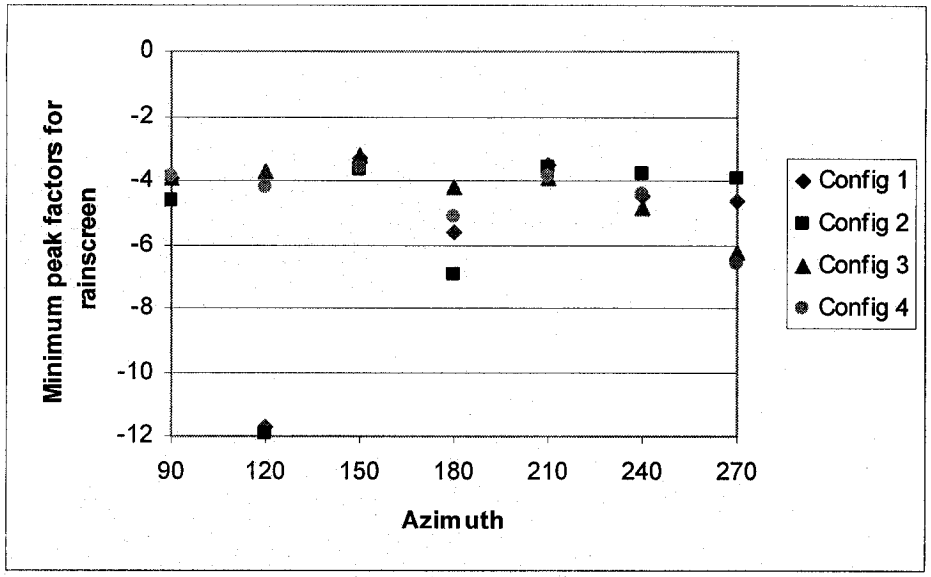

Figures 4.20 Minimum rainscreen peak factors as a function of azimuth

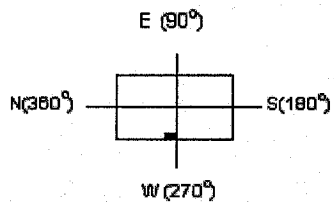

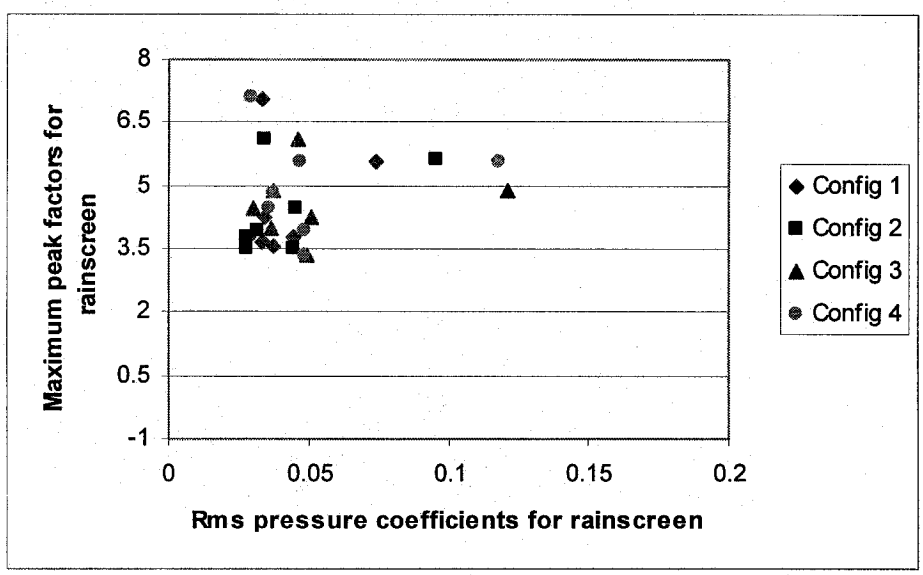

Figure 4.21: Maximum rainscreen peak factors as a function of rms rainscreen pressure coefficients

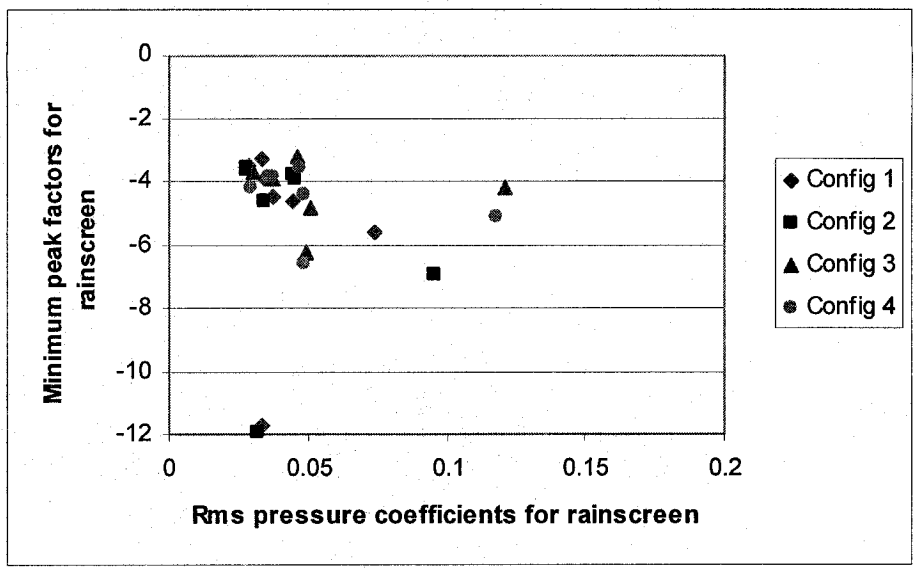

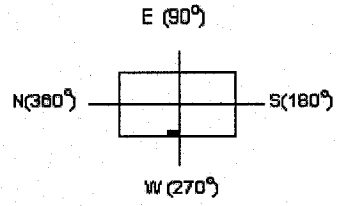

Figures 4.22: Minimum rainscreen peak factors as a function of rms rainscreen pressure coefficients

4.2 *Comparison with Full-Scale Data*

Field measurements have been carried out on the main building of TUE, Eindhoven at the Netherlands. The rainscreen panel was tested for six configurations depending on the venting and leakage characteristics; refer Table 3.1, section 3.1.2. Wind tunnel experiments are performed on the TUE building model for a rainscreen panel that has four configurations based on its venting and leakage characteristics; refer Table 3.4, section 3.4.2. Configurations 1 and 2 of the wind tunnel are similar to the field, while configurations 3 and 4 of the wind tunnel represent 4 and 5 of the field. Like in the field, the pressure coefficients for each configuration are noted for seven wind directions. In the present study, the wind direction varies between 180°

and 360°, where both 180° and 360° represent wind directions parallel to façade and 270° represents wind direction normal to façade.

4.2.1 Mean and rms pressure coefficients

- The mean and rms pressure coefficients of the panel and rainscreen are compared with the field results in Figures 4.23 to 4.26. The variation of the field data for the respective configurations is quite significant. It was thus decided to show the range of the field data and locate the measured wind tunnel results on the same graphs. Figure 4.23 shows mean pressure coefficients measured for panel and rainscreen wall sections for configurations 1 and 2, whereas Figure 4.24 shows similar data for configurations 3 and 4. The panel data measured in the wind tunnel seems to fall well within the range of field data for all cases. Rainscreen data are somewhat off with configuration 2 showing clearly that wind tunnel data underestimate the field values, the variation of which is significantly smaller than that of the panel. The rms panel and rainscreen coefficients are shown in Figures 4.25 and 4.26. The rms panel coefficients are corrected for normal and almost normal azimuths using the quasi-steady approach. The corrected values are shown in the same figures. The distribution of the rms panel pressure coefficients over the azimuth is nearly symmetrical about 270° that is normal to façade. The oncoming turbulence in the tunnel is low as compared to the field value and this is reflected in the results. After appropriate turbulence corrections, as per section 3.2.3, the revised rms panel coefficients fall in the field data range. For example, the rms panel coefficient in the tunnel is 0.18 and accordingly:

$$Cp, rms_{corrected} = (0.35/0.08) * 0.18 = 0.79.$$

Note that in case of configuration 3, full-scale data is available only from 180° to 270° for both mean and rms rainscreen pressure coefficients.

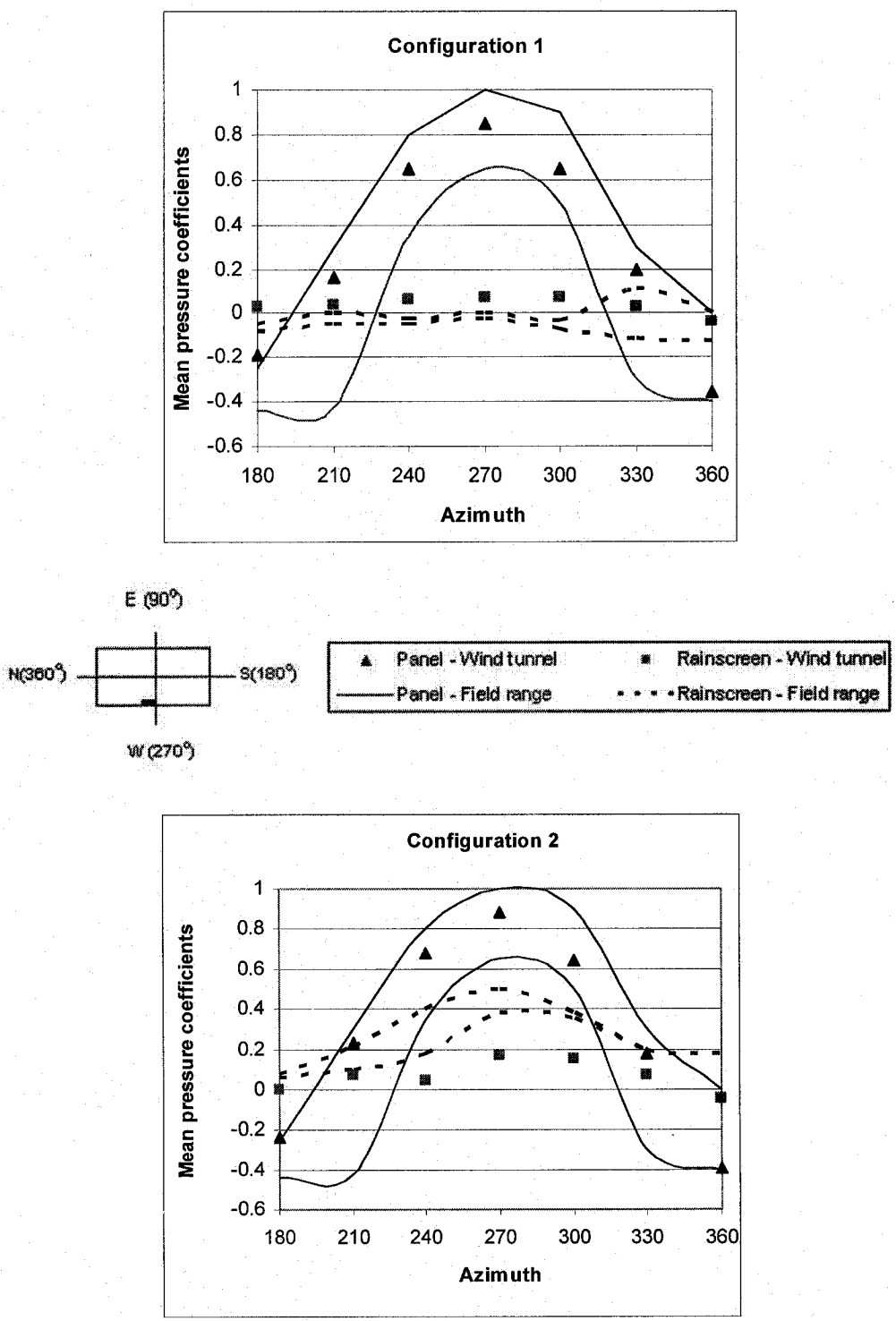

Figure 4.23: Mean pressure coefficients for panel and rainscreen: Configurations 1, 2

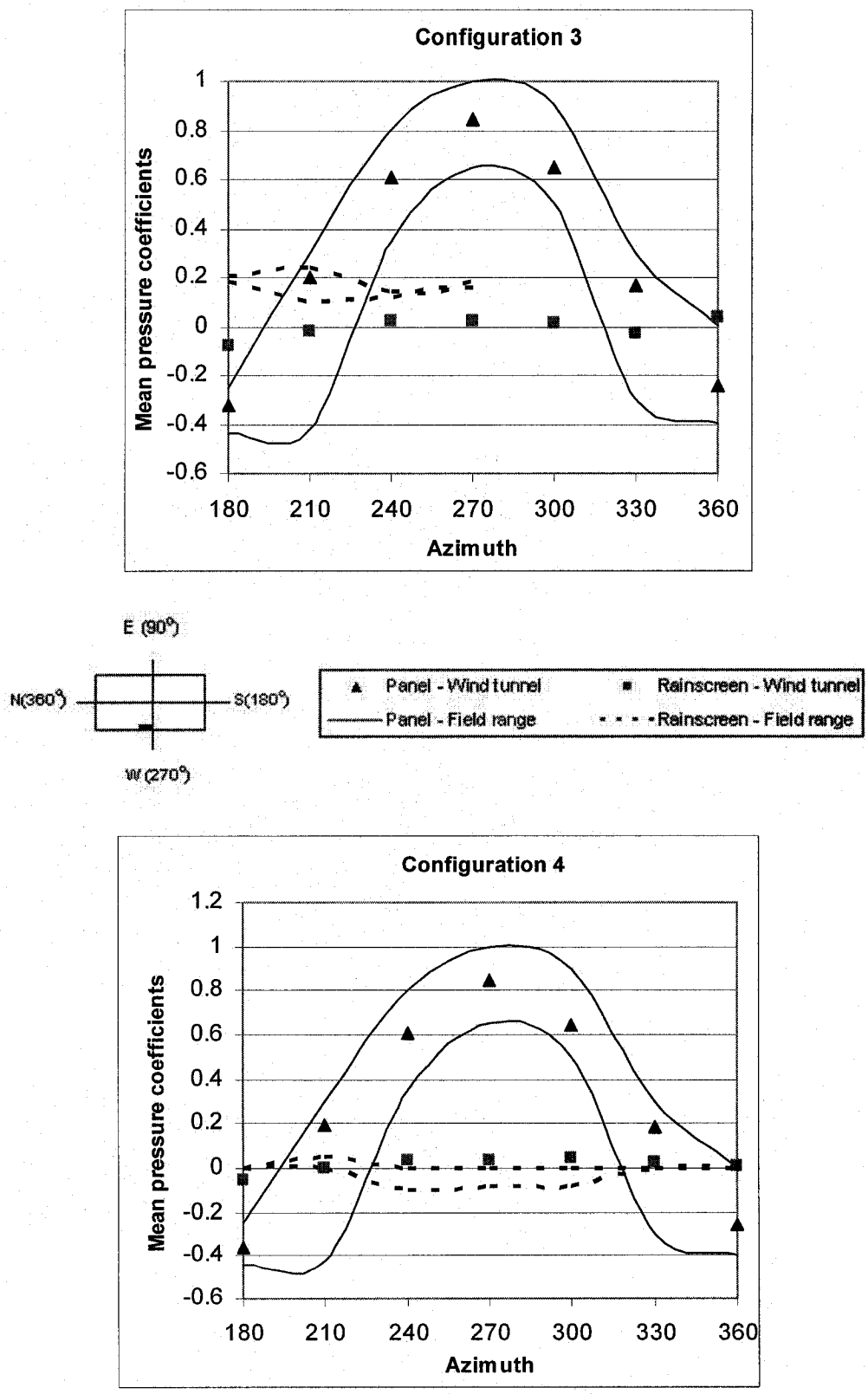

Figure 4.24: Mean pressure coefficients for panel and rainscreen: Configurations 3, 4

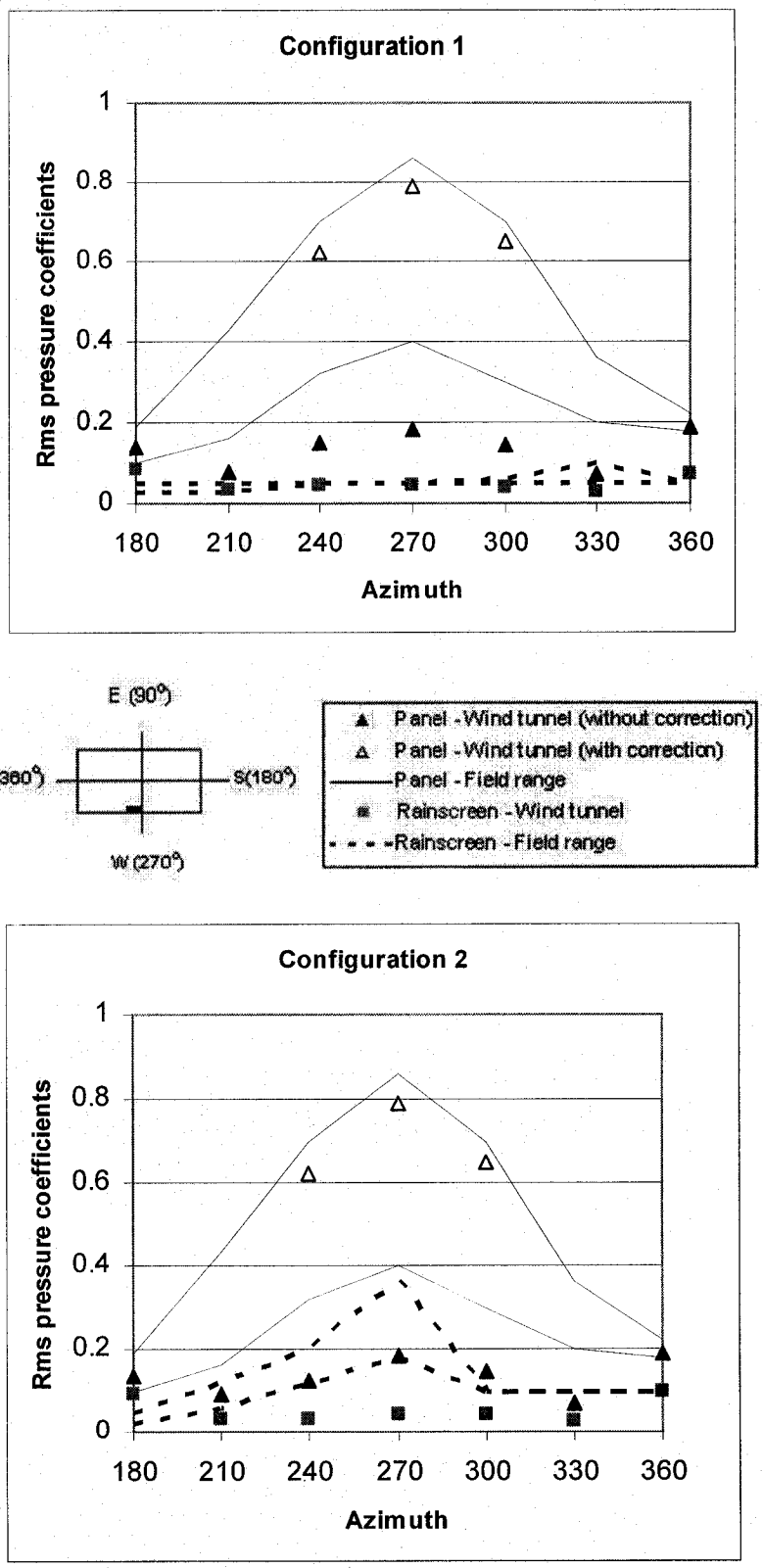

Figure 4.25: Rms pressure coefficients for panel and rainscreen: Configurations 1, 2

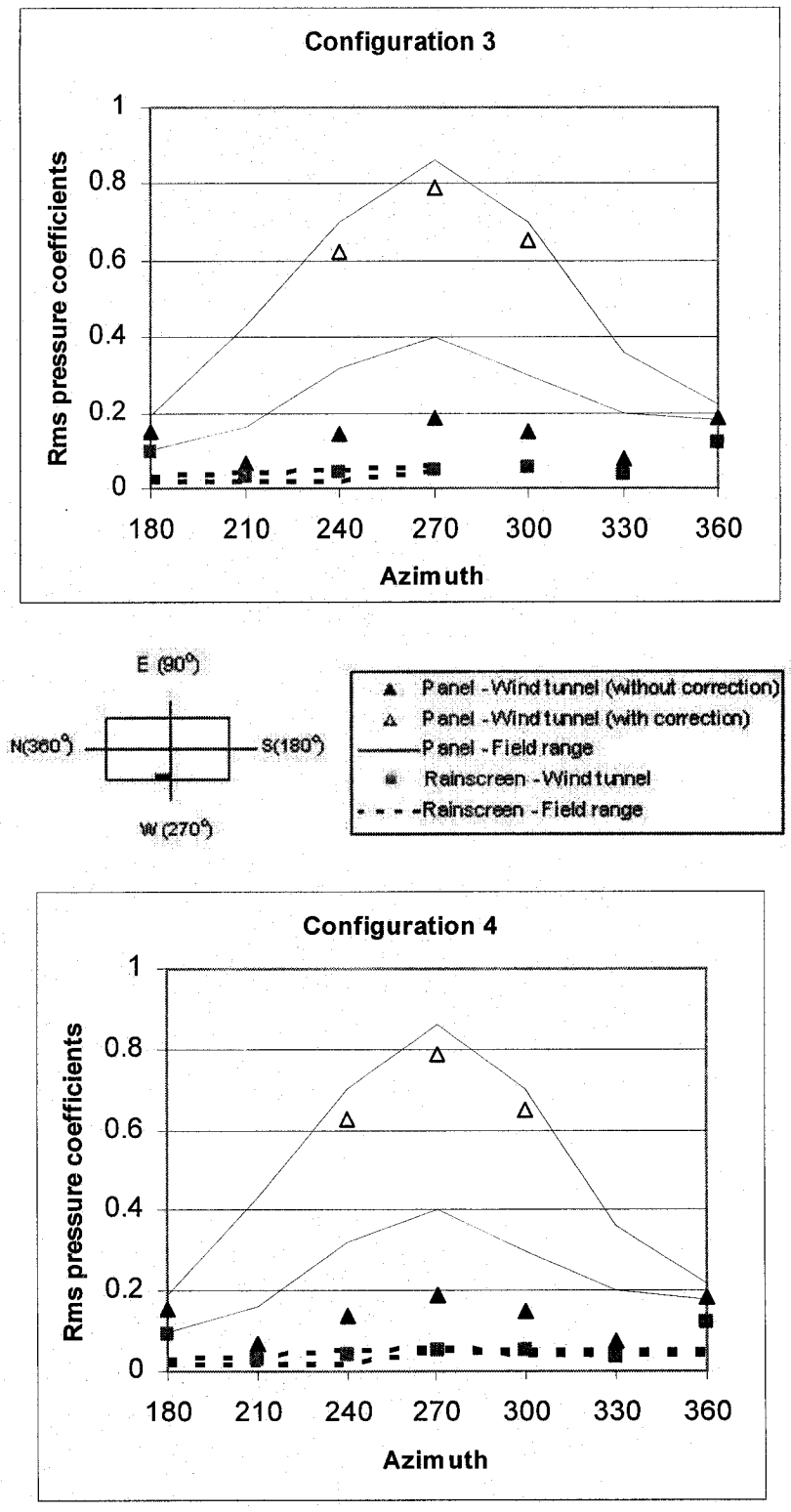

Figure 4.26: Rms pressure coefficients for panel and rainscreen: Configurations 3, 4

- Figures 4.27 and 4.28 compare the field mean as well as rms pressure coefficients with the corresponding wind tunnel mean as well as rms pressure coefficients acting on the panel. Note that in configuration 1, the upper and lower bounds of the field range are the same. Configurations 2 and 3 seem to under-predict the field values while 1 and 4 over-predict them. Furthermore, the difference between the mean rainscreen pressure coefficients obtained in wind tunnel for configurations 3 and 4 is less compared to the field. Thus, for configurations with no air barrier leakage, the wind tunnel predicts a less difference in rainscreen pressures than the field. On the other hand, the wind tunnel rms rainscreen coefficients are noticed only for low panel rms values while the field rms rainscreen coefficients are scattered throughout. This could be due to the low turbulence generated in the wind tunnel as discussed in section 4.2.1.

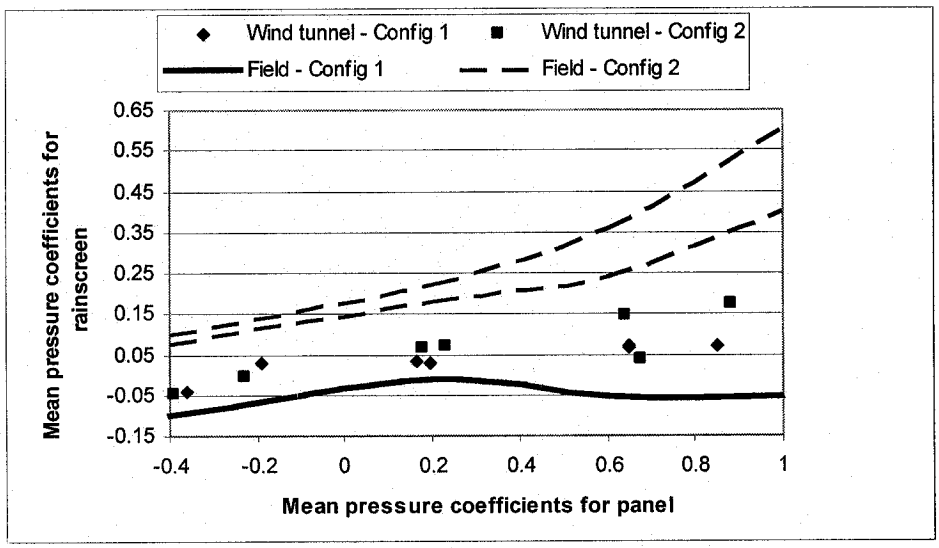

Figure 4.27a: Comparison of mean pressure coefficients acting on rainscreen with mean pressure coefficients acting on panel for field and wind tunnel

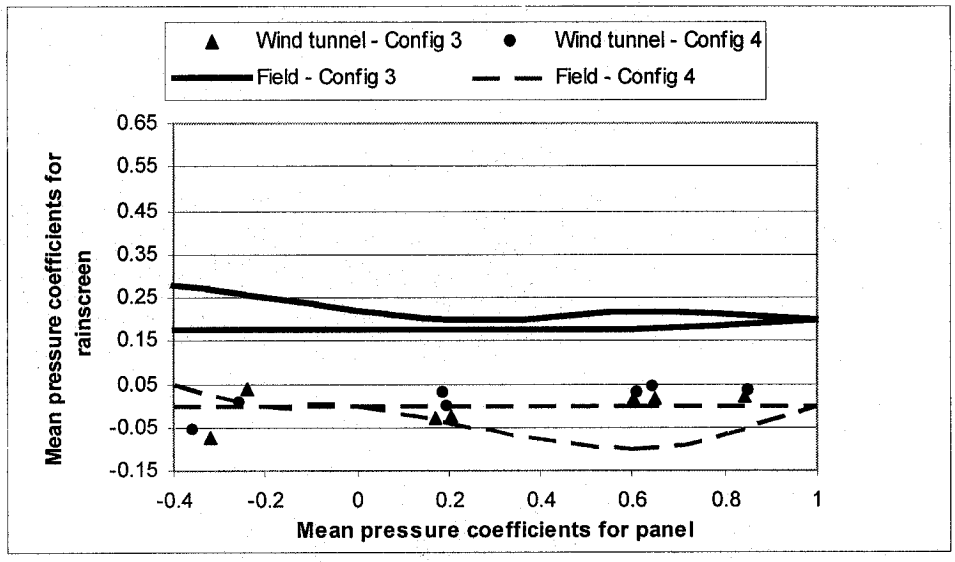

Figure 4.27b: Comparison of mean pressure coefficients acting on rainscreen with mean pressure coefficients acting on panel for both field and wind tunnel

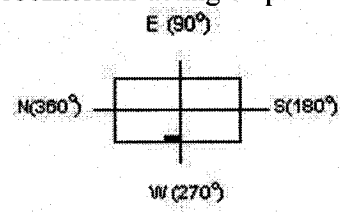

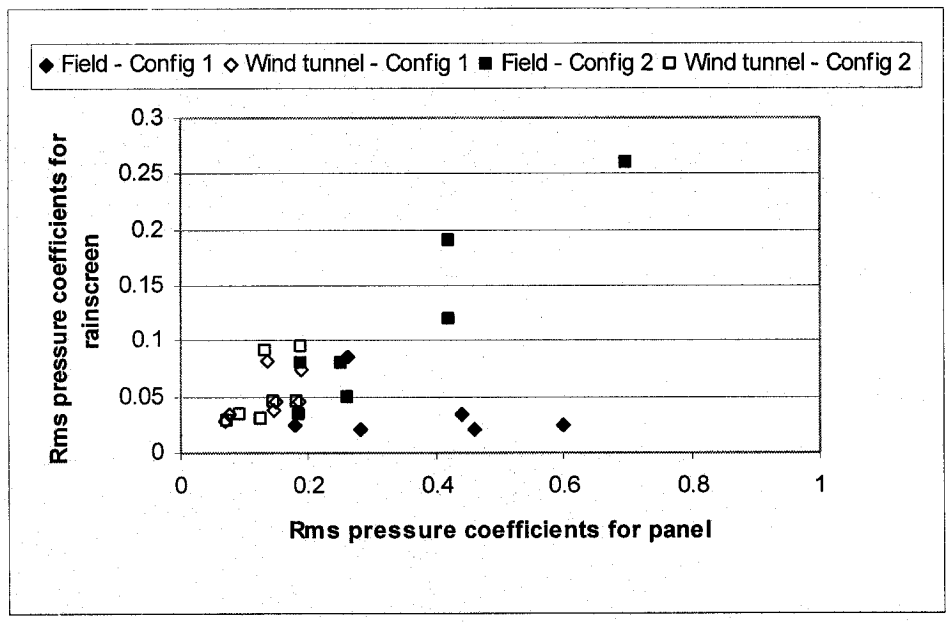

Figure 4.28a: Comparison of rms pressure coefficients acting on rainscreen with rms pressure coefficients acting on panel for both field and wind tunnel

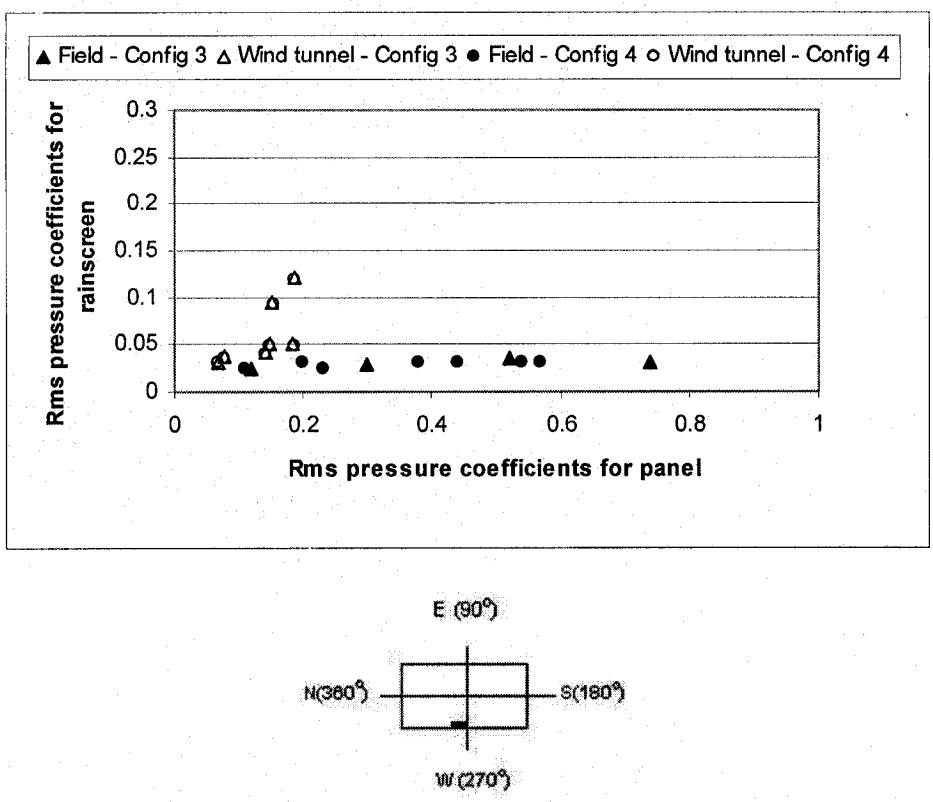

Figure 4.28b: Comparison of rms pressure coefficients acting on rainscreen with rms pressure coefficients acting on panel for both field and wind tunnel

4.2.2 Maximum pressure coefficients and peak factors

- Maximum pressure coefficients acting on the panel are plotted against wind direction for wind tunnel and field data in Figures 4.29 and 4.30. Note that in configuration 4, field data exist only up to 330°. Similarly with rms pressure coefficients, the maximum panel coefficients constantly under-predict the field values but the corrected wind tunnel values fall well into the field range. Likewise, the maximum rainscreen coefficients fall within the range of field data for all cases except, again, configuration 2, which under-predicts the field values significantly. This is attributed to the lower rms values of this configuration, as compared to the field due to the reduced turbulence, as mentioned previously. Clearly, configurations with no leakage record lower

peaks irrespective of their venting. Also, when there is sufficient leakage, there needs to be adequate venting for the rainscreen to take less wind load, unlike configuration 2 which has minimal venting. The difference between rainscreen and panel coefficients is at a maximum for normal wind directions to façade and decreases for different wind directions. This indicates good pressure equalization when wind blows normal to the façade.

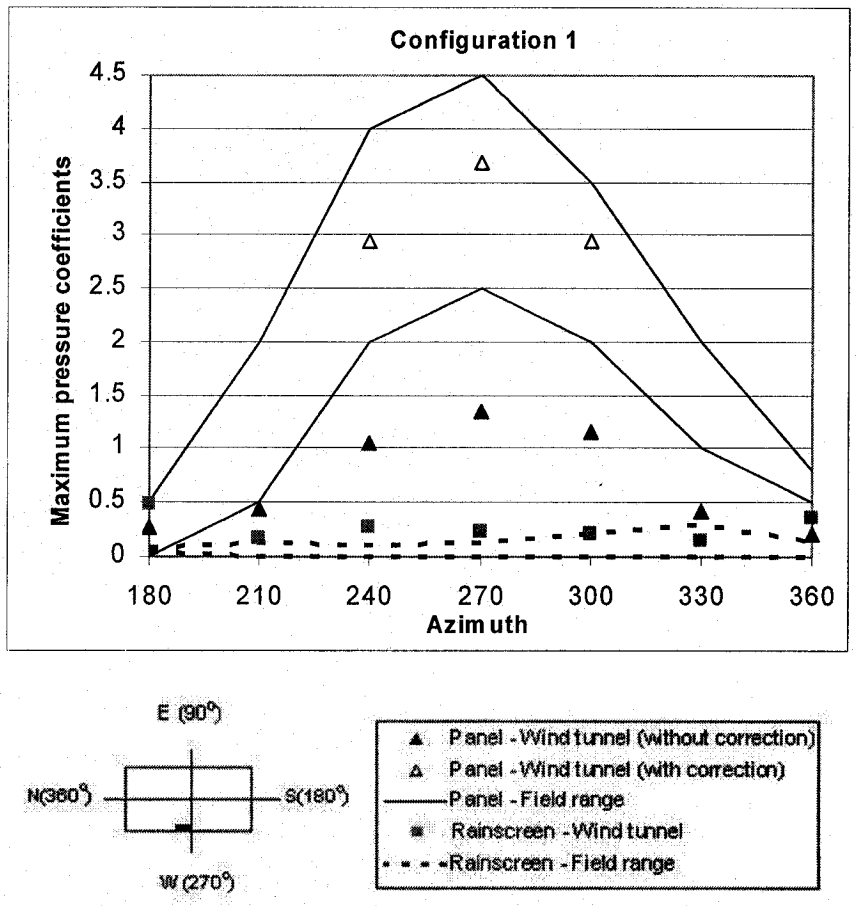

Figure 4.29a: Maximum pressure coefficients for panel and rainscreen: Configurations 1, 2

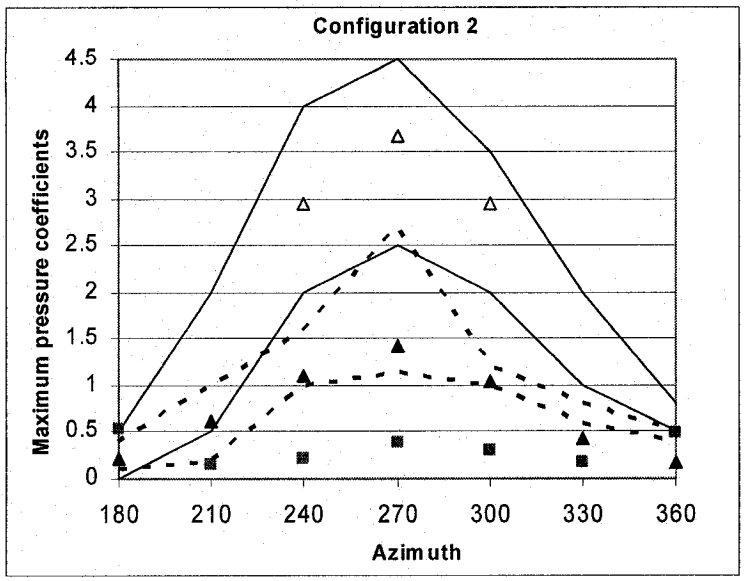

Figure 4.29b: Maximum pressure coefficients for panel and rainscreen: Configurations 1, 2

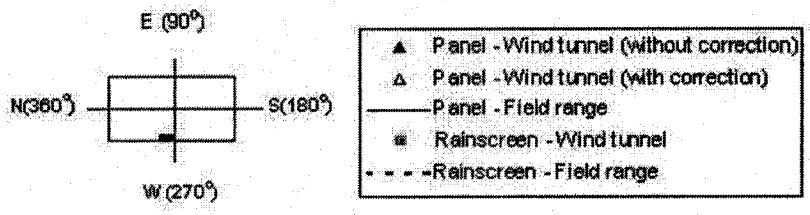

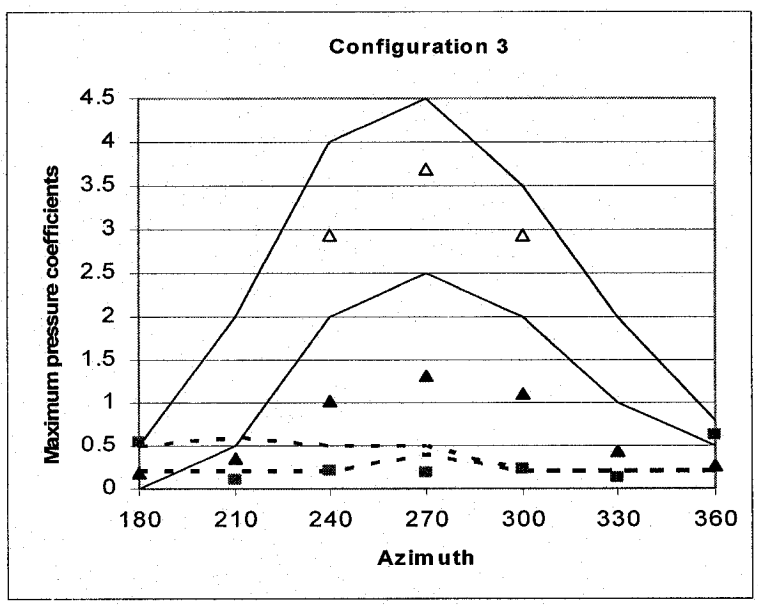

Figure 4.30a: Maximum pressure coefficients for panel and rainscreen: Configurations 3, 4

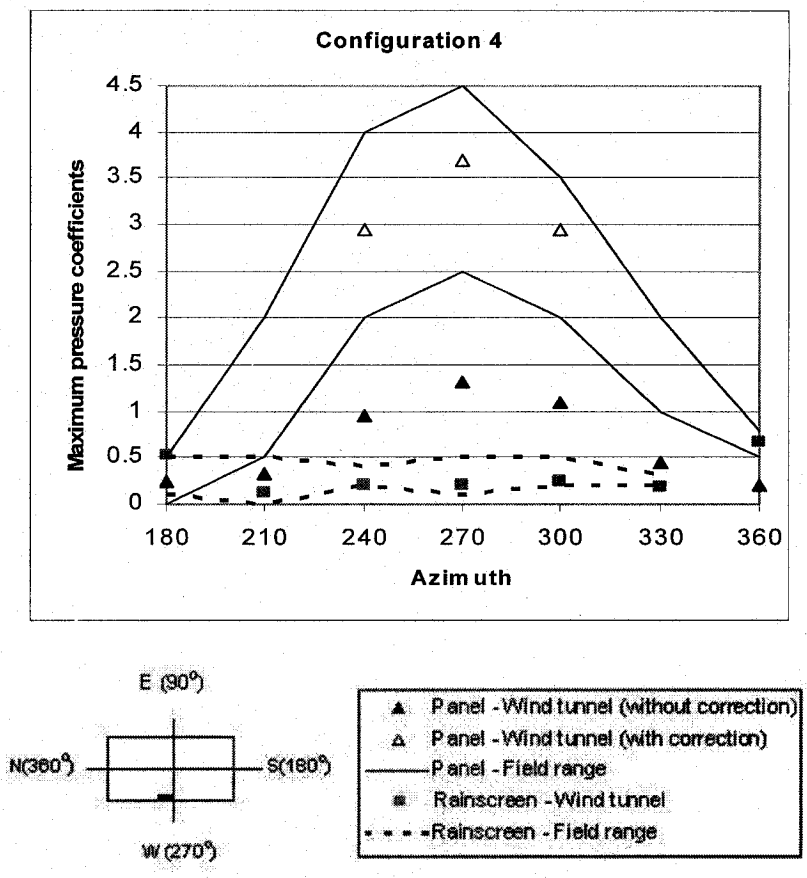

Figure 4.30b: Maximum pressure coefficients for panel and rainscreen: Configurations 3, 4

4.3 *Wind Tunnel Results: Edge Configuration*

The results in this section are presented for wind directions varying from Θ = 30° to 360°, where Θ = 270° represents normal to facade. For future investigations, this would help to draw meaningful comparisons with the field.

4.3.1 Mean and rms pressure coefficients

- The distribution of mean and rms pressure coefficients of the panel depends on wind direction as is shown in Figures 4.31 and 4.32. It appears that the difference between the rainscreen pressure coefficient and the corresponding

panel pressure coefficient decreases as the wind direction differs from Θ = 180°; minimum difference is noticed at Θ = 300°. The amount of load shared by the rainscreen varies depending on the venting area and the air barrier leakage. The mean and rms rainscreen pressure coefficients of configurations 1, 3 and 4 are almost the same while configuration 2 shows somewhat higher values. This increased mean and rms rainscreen load of configuration 2 as compared to configuration 1 could be attributed to the significant reduction of its venting area, as the venting area of configuration 1 is five times that of configuration 2. Thus, in order to have lower rainscreen loads sufficient venting has to be provided in comparison to its leakage.

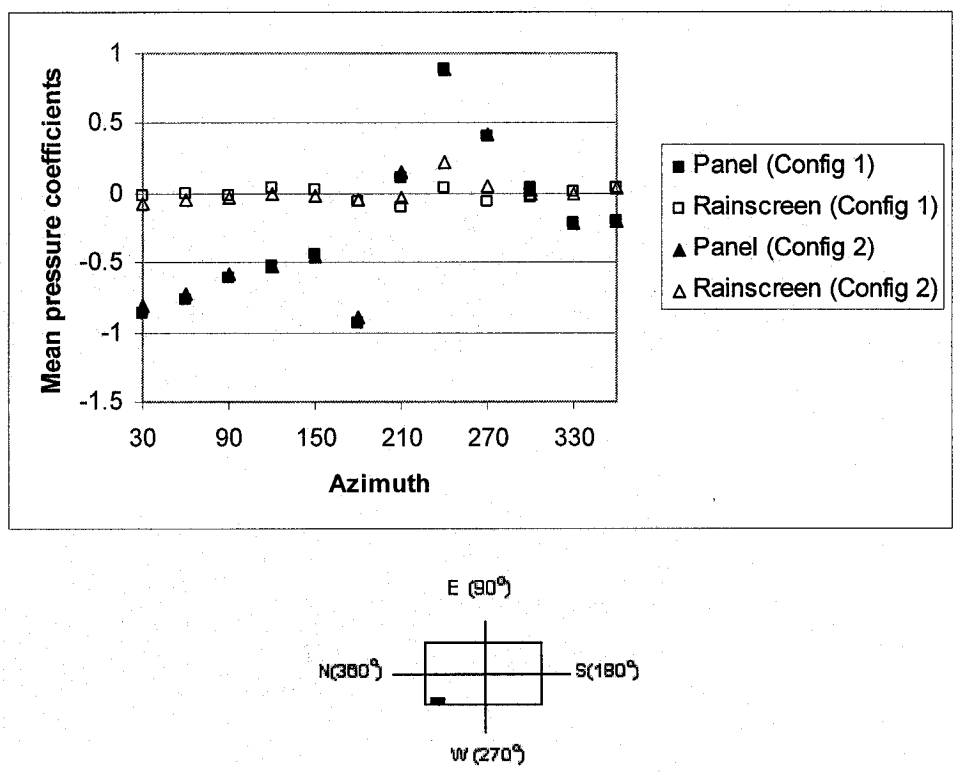

Figure 4.31a: Mean pressure coefficients acting on panel and rainscreen

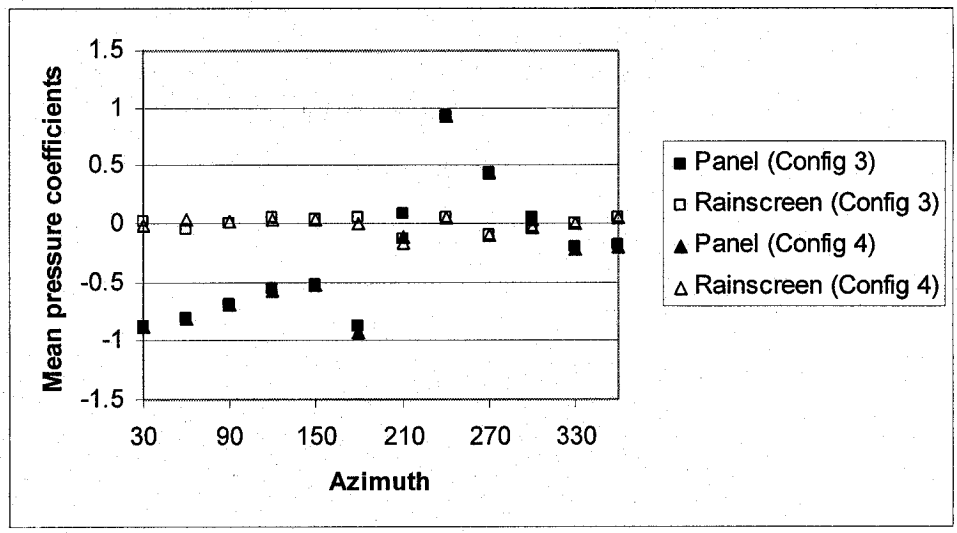

Figure 4.31b: Mean pressure coefficients acting on panel and rainscreen

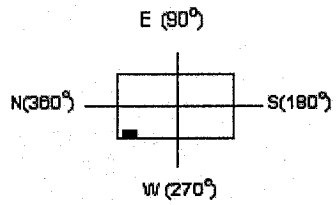

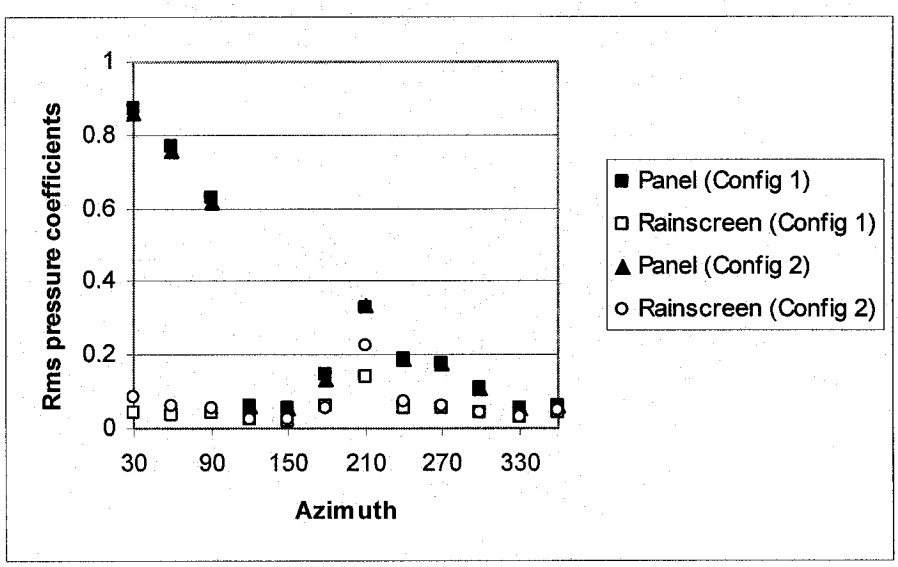

Figures 4.32a: Rms pressure coefficients acting on panel and rainscreen

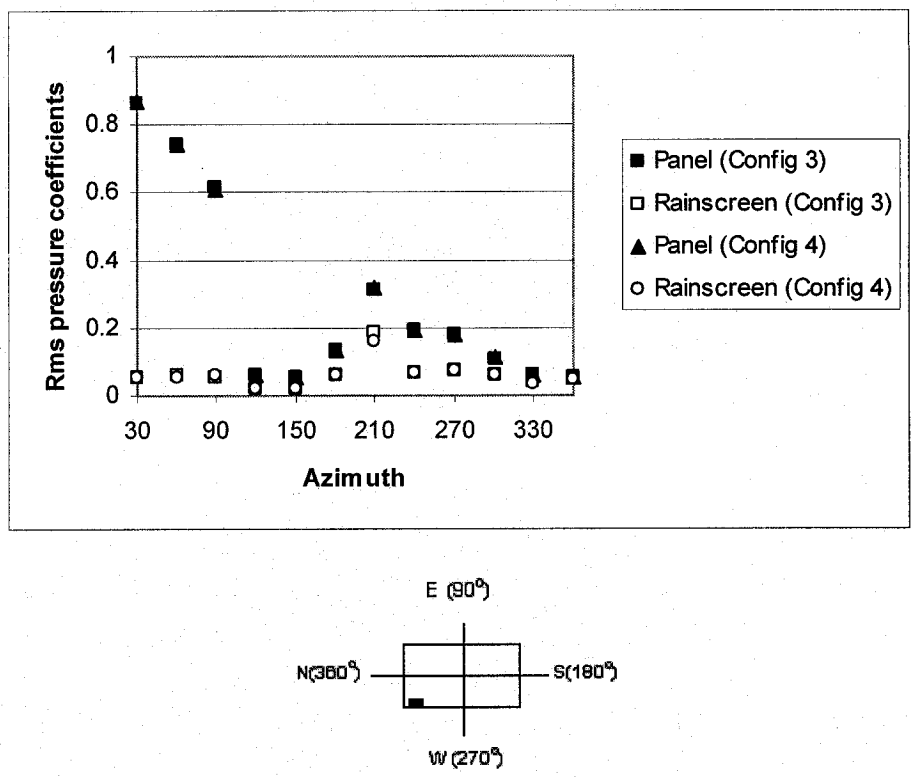

Figures 4.32b: Rms pressure coefficients acting on panel and rainscreen

- Figures 4.33 and 4.34 show the mean as well as rms rainscreen pressure coefficients compared with the corresponding mean as well as rms pressure coefficients acting on the panel. The mean rainscreen pressure coefficients of all configurations seem to be dependent on the mean pressure coefficients acting on the panel. In general, an increase in the mean panel pressure coefficient sees a corresponding increase in the mean rainscreen pressure coefficient, but the magnitude depends on the wind azimuth. In the case of rms rainscreen pressure coefficients, the same behaviour as that of mean is noticed; however it is highly dependent on the wind azimuth. For wind azimuth 210°, poor pressure equalization performance is noticed. This generates high rms rainscreen pressure coefficients slightly lower than the respective panel values.

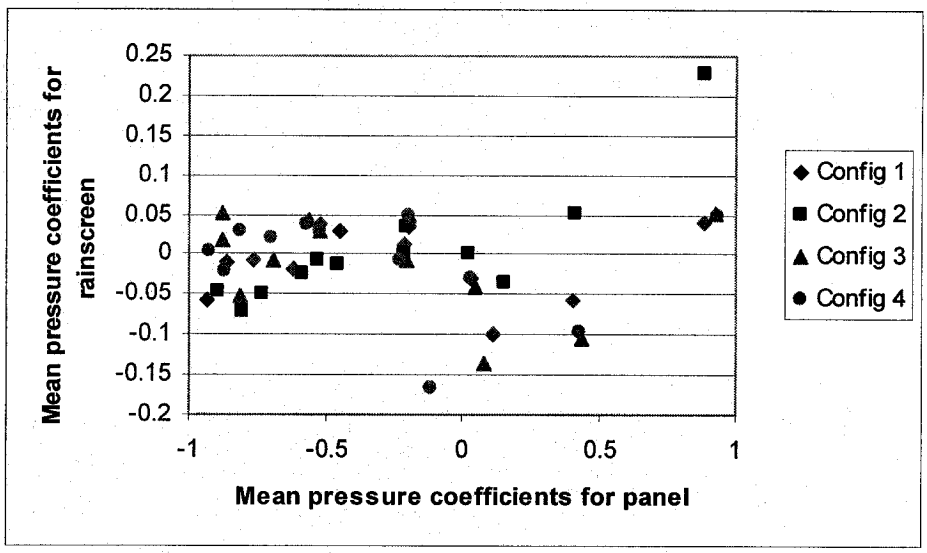

Figure 4.33: Comparison of mean pressure coefficients acting on rainscreen with mean pressure coefficients acting on panel

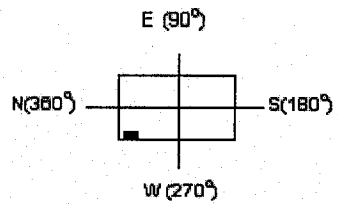

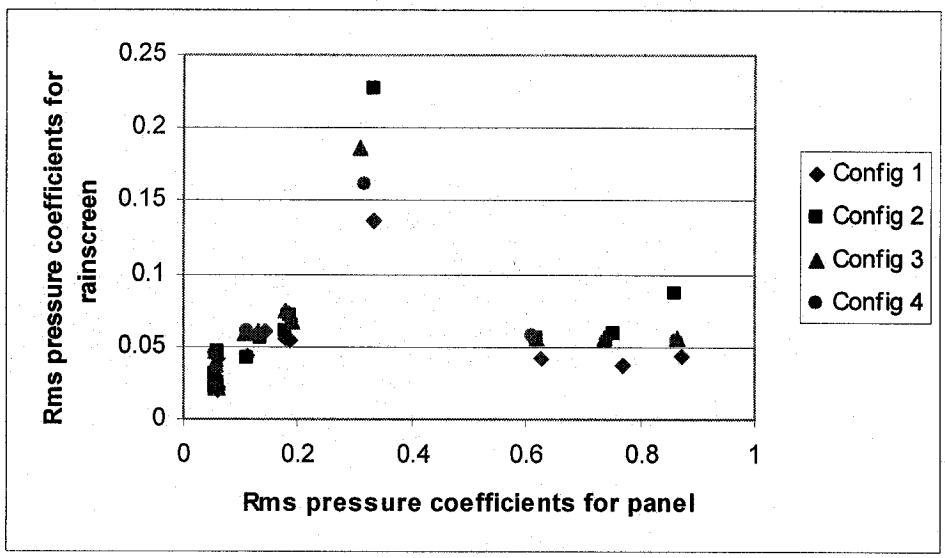

Figure 4.34: Comparison of rms pressure coefficients acting on rainscreen with rms pressure coefficients acting on panel

4.3.2 *MPEC and SPEC values*

- The variation of MPEC values with respect to wind direction and mean pressure coefficients for the panel as well as rainscreen are shown in Figures 4.35 to 4.37. It is interesting to note the dependency of MPEC on wind direction. MPEC values are seen to be maximum at $\Theta = 210^{o}$ and 300^{o}. Though this trend is observed in all configurations, MPEC values of configuration 2 at these azimuths are significantly lower than those of other configurations. This is opposite to that noticed in central configuration – see Figure 4.5. Unlike the central panel configuration, there occurs good pressure equalization for configuration 2 at the edge and poor pressure equalization for other configurations at these azimuths. This is due to the low rainscreen pressures taken by configuration 2 at the edge in comparison to other configurations. Further, it is noticed that in case of configurations 3 and 4, the MPEC values exceed one, indicating the rainscreen to carry more load than the panel. This is caused by the insensitivity of the rainscreen pressures at very low panel pressures. Interestingly, the mean rainscreen pressure coefficients at these azimuths ($\Theta = 210^{o}$ and 300^{o}) are low, making the MPEC values unimportant for design. The dependency of MPEC values on mean pressure coefficients of the panel and rainscreen are also noted. In case of configuration 2, there is not much of variation in the MPEC values as the mean pressure coefficient for the panel decreases from its maximum. For other configurations, a significant increase in MPEC values is noted when the panel takes in no load. This is caused by the minor fluctuations of the rainscreen pressures around zero when the panel pressure is about zero. For all

configurations, the MPEC values are insensitive to the variation of mean rainscreen pressure coefficients.

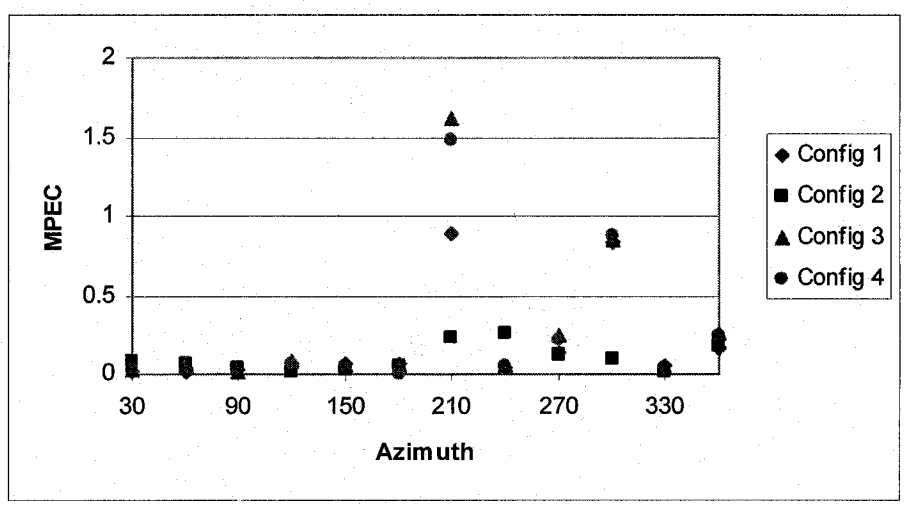

Figure 4.35: Variation of MPEC with respect to wind direction

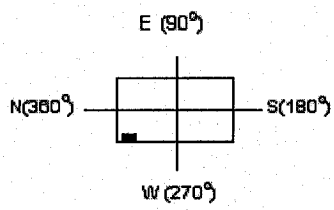

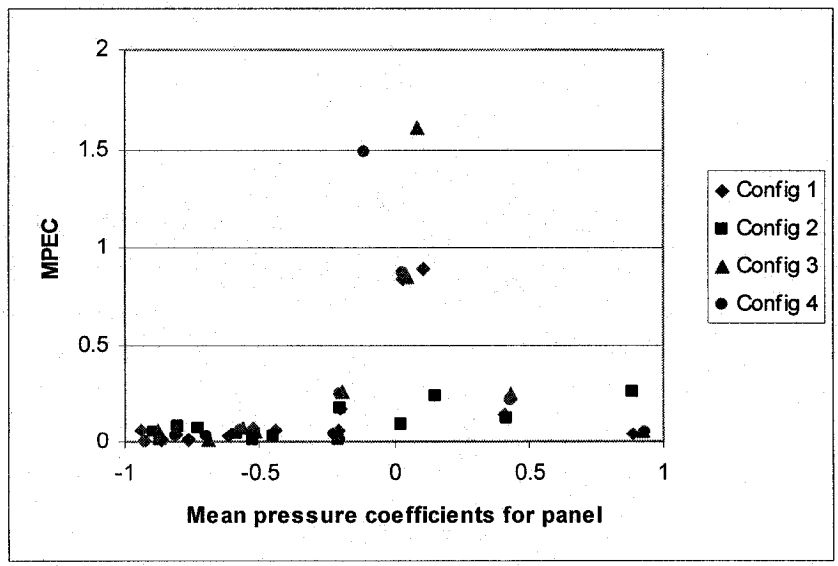

Figure 4.36: Variation of MPEC with respect mean panel pressure coefficients

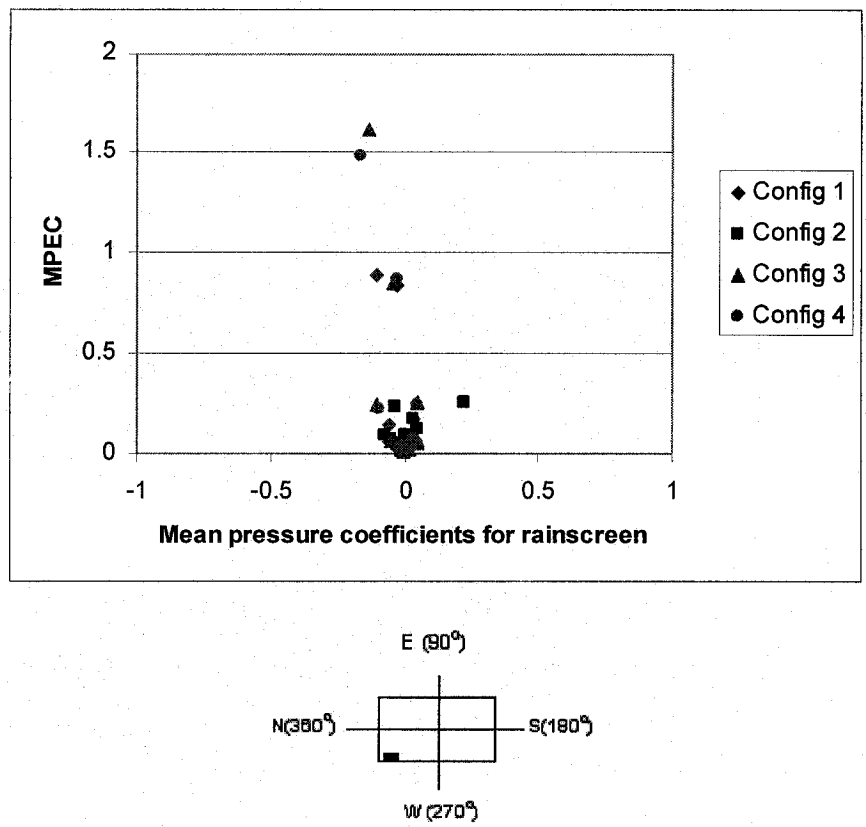

Figure 4.37: Variation of MPEC with respect mean rainscreen pressure coefficients

- The variation of SPEC values with respect to wind direction and rms pressure coefficients for the panel as well as rainscreen are shown in Figures 4.38 to 4.40. SPEC values are clearly dependent on wind directions for all configurations. Further, maximum SPEC values are noted at $\Theta = 330^{\circ}$ and 360° in all configurations. This indicates poor pressure equalization for wind directions normal and near normal to façade. As shown in Figures 4.39 and 4.40, SPEC values are high for low rms panel and rainscreen pressures.

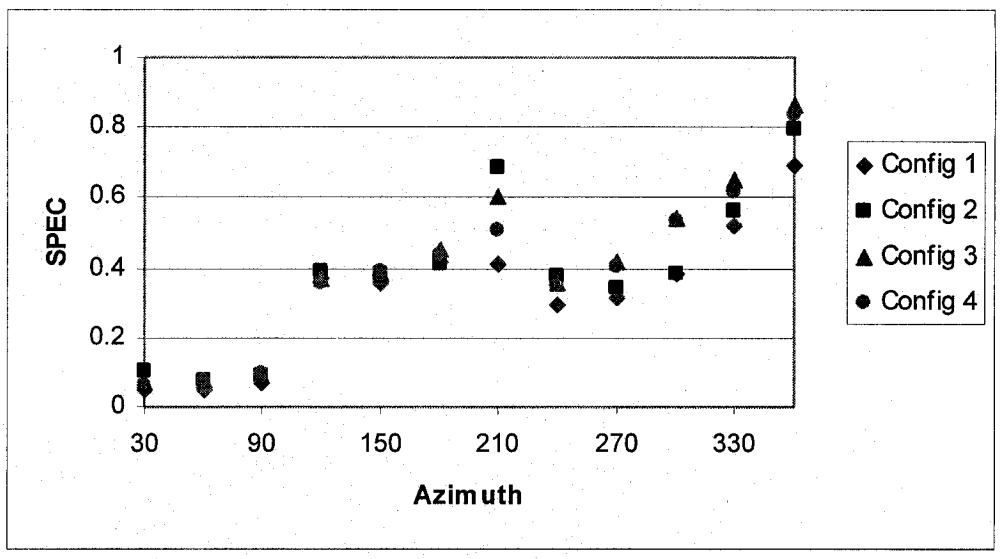

Figure 4.38: Variation of SPEC with respect to wind direction

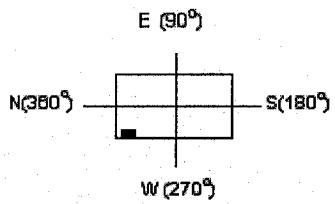

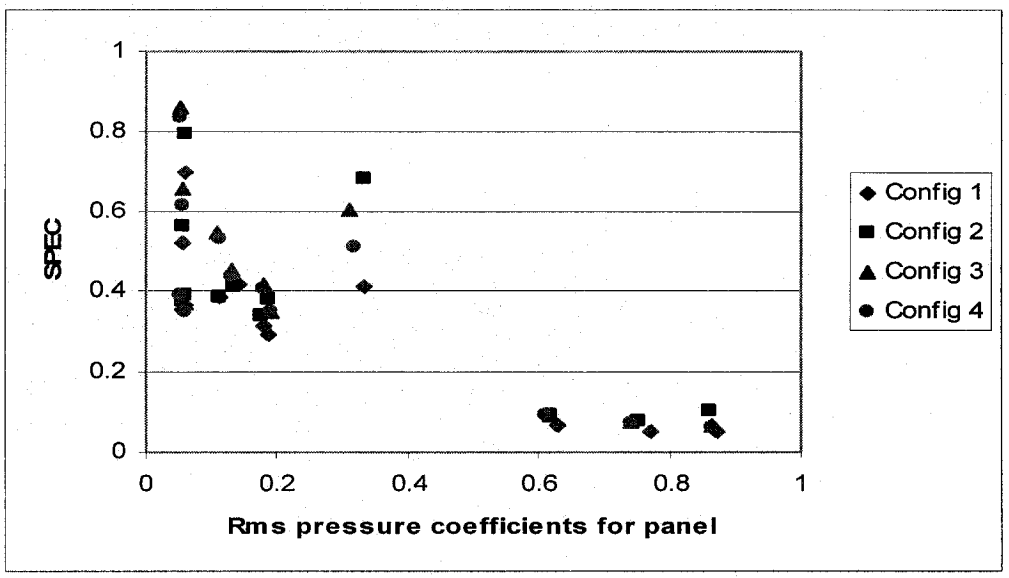

Figure 4.39: Variation of SPEC with respect to rms panel pressure coefficients

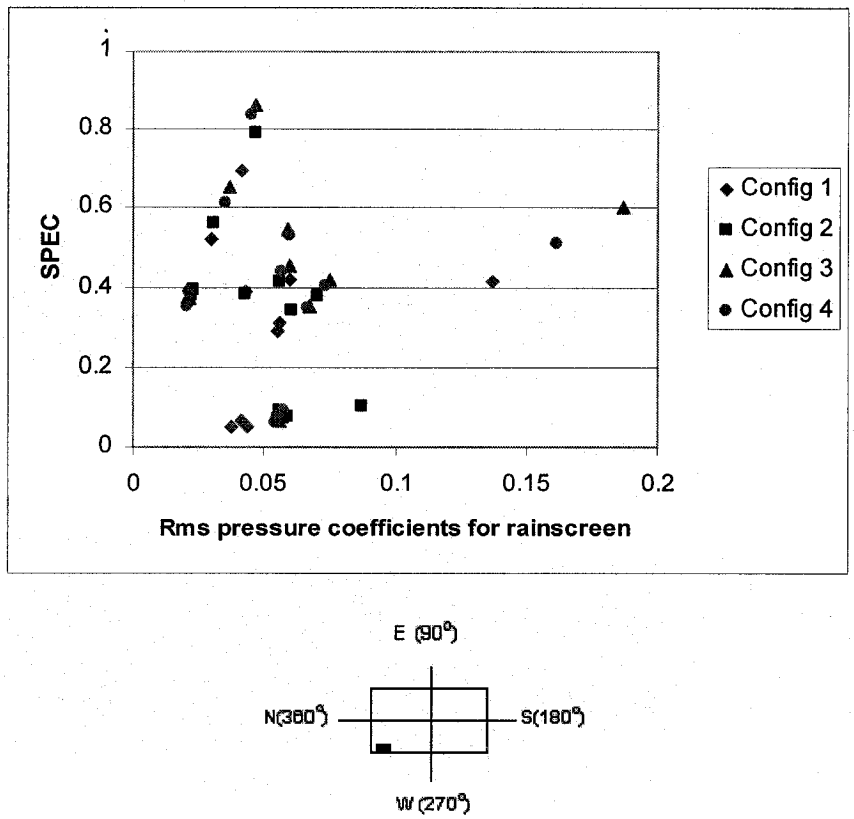

Figure 4.40: Variation of SPEC with respect to rms rainscreen pressure coefficients

4.3.3 *Extreme pressure coefficients and peak factors*

- Maximum and minimum pressure coefficients as well as peak factors acting on the panel are shown in Figures 4.41 to 4.46. Note that in all cases, the maximum and minimum panel pressure coefficients decrease as the wind deviates away from $\Theta = 240^{\circ}$. Close to this wind direction, positive mean pressure coefficients are obtained; the corresponding maximum and absolute minimum pressure coefficients are high and low respectively. Maximum and minimum peak factors are plotted against wind directions in Figures 4.43 and 4.44. The highest maximum and minimum peak factors obtained are close to 4.8 and -6.8 respectively. The variation of peak panel factors against rms

pressure coefficients are shown in Figures 4.45 and 4.46. Apart from being sensitive to variations in rms panel pressure coefficients, it is seen that high maximum and minimum peak factors occur at low rms panel coefficients.

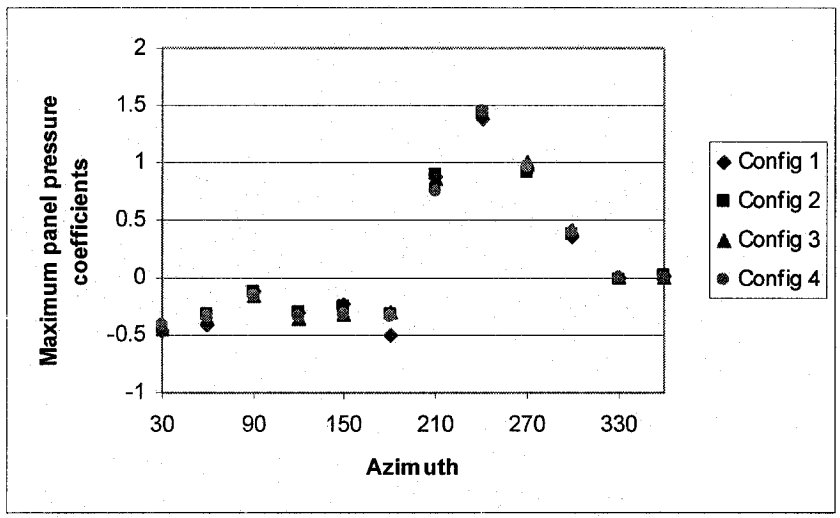

Figure 4.41: Maximum pressure coefficients acting on panel as a function of azimuth

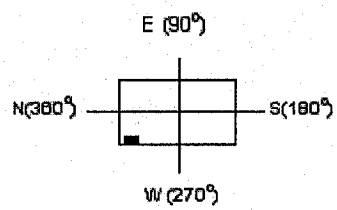

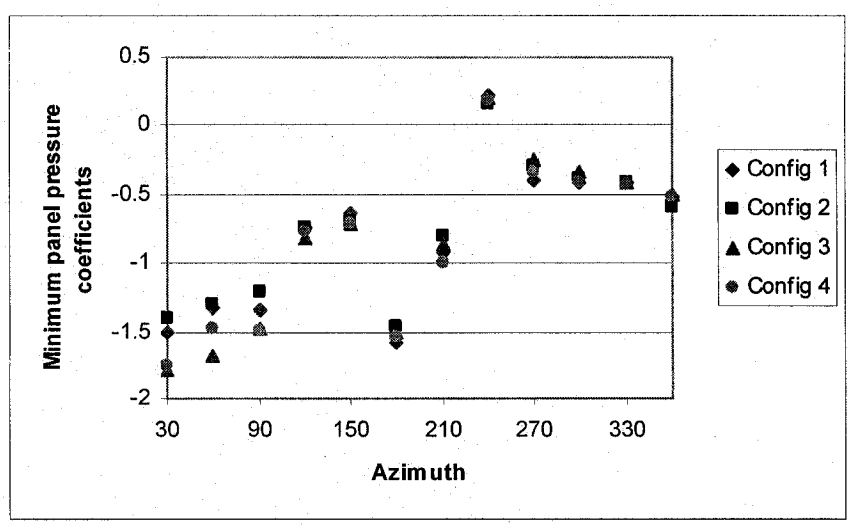

Figure 4.42: Minimum pressure coefficients acting on panel as a function of azimuth

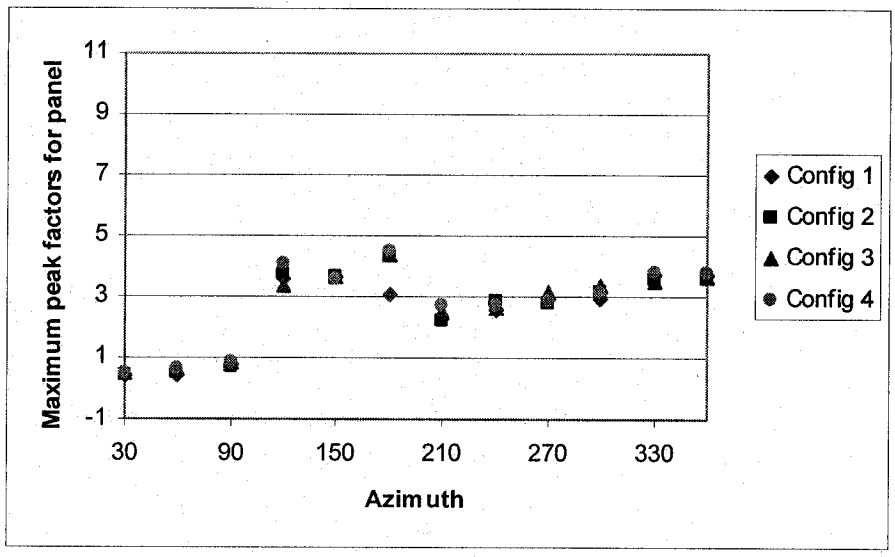

Figure 4.43: Maximum peak factors acting on panel as a function of azimuth

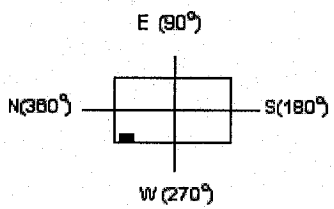

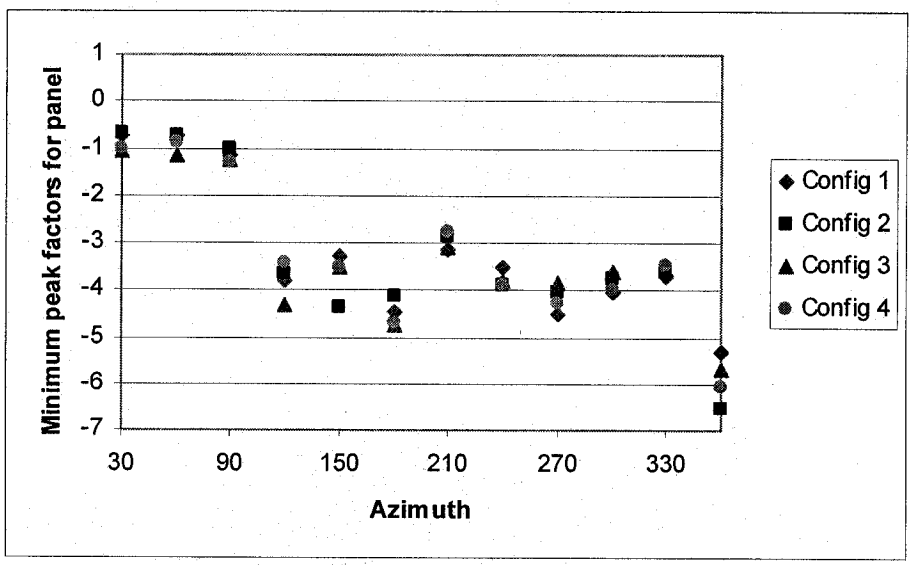

Figure 4.44: Minimum peak factors acting on panel as a function of azimuth

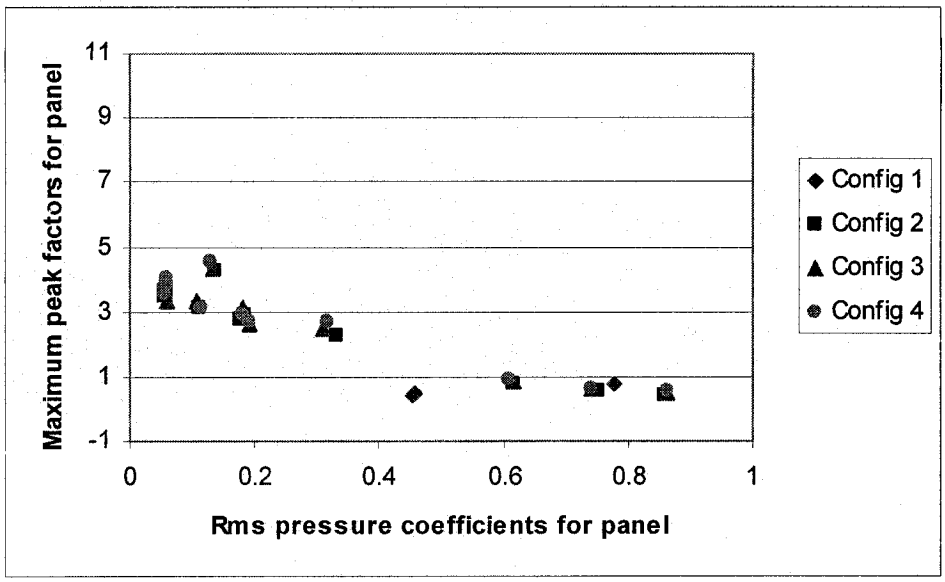

Figure 4.45: Maximum peak factors acting on panel as a function of rms panel pressure coefficients

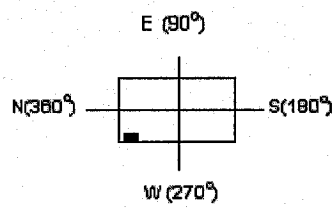

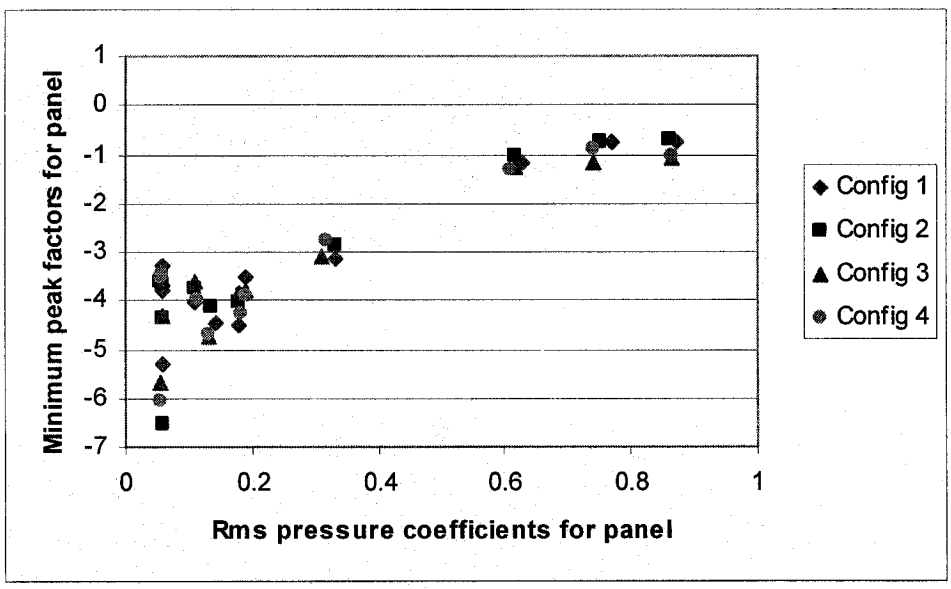

Figure 4.46: Minimum peak factors acting on panel as a function of rms panel pressure coefficients

- Figures 4.47 and 4.48 illustrate the variation of maximum and minimum rainscreen pressure coefficients against wind direction. It is noted that the maximum rainscreen pressure coefficients depend on wind directions with configuration 2 taking in more rainscreen load at normal conditions. The minimum rainscreen pressure also depend on wind directions with the lowest values recorded at $\Theta = 210^{o}$. The magnitudes of maximum and minimum rainscreen pressure coefficients depend on the venting and leakage characteristics of the configuration.

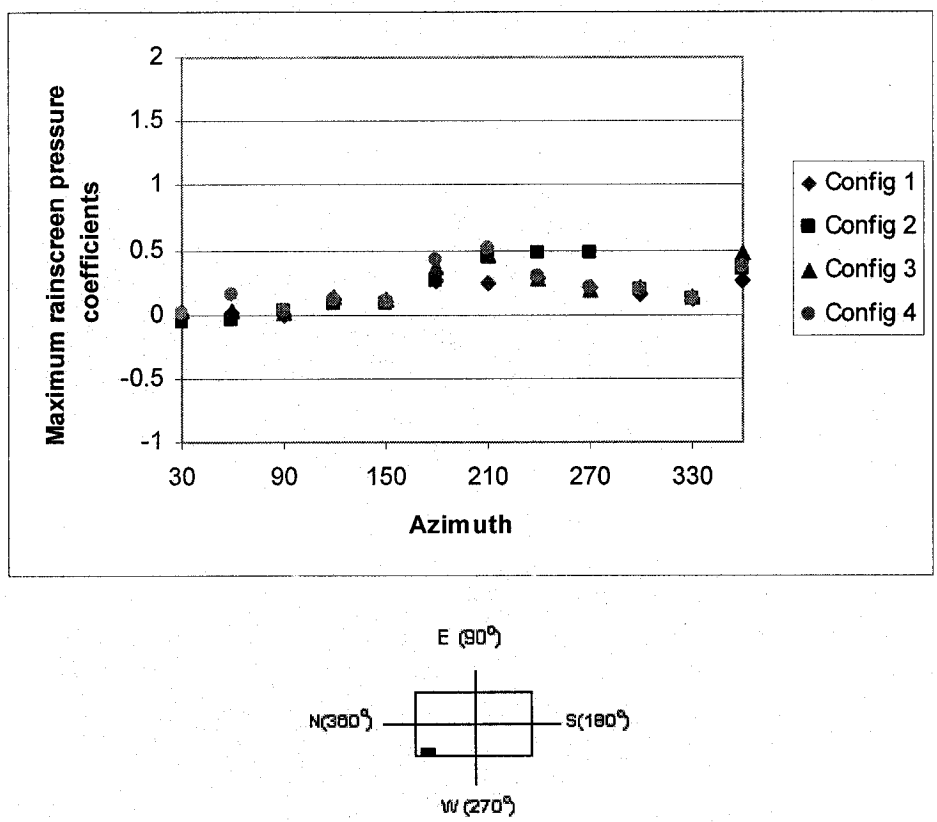

Figures 4.47: Maximum rainscreen pressure coefficients as a function of azimuth

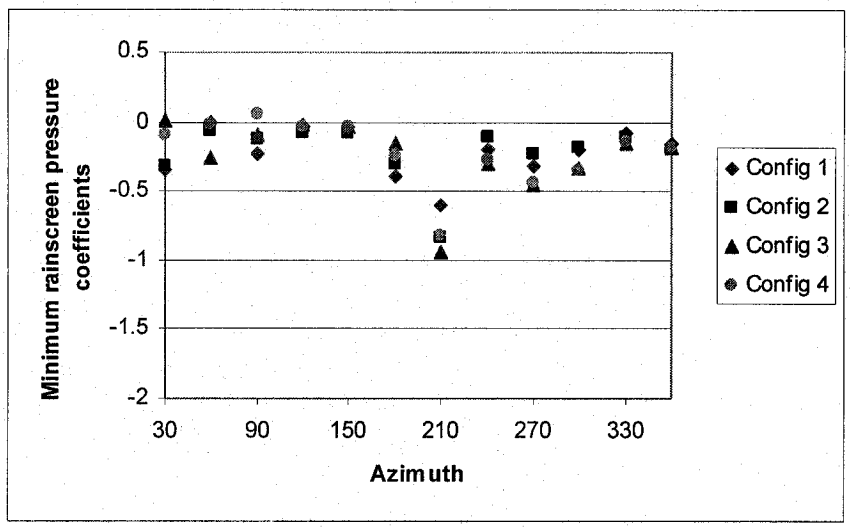

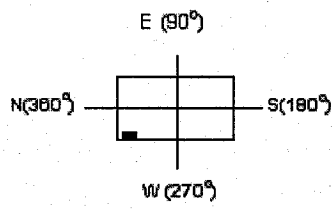

Figures 4.48 Minimum rainscreen pressure coefficients as a function of azimuth

- Variation of maximum and minimum rainscreen peak factors against wind direction and also against the rms rainscreen pressure coefficients are shown Figures 4.49 to 4.52. Note that all configurations except 2 have two large maximum values at $\Theta = 180^{o}$ and $\Theta = 360^{o}$. In the case of minimum rainscreen peak factors, minimum values are obtained when the wind blows normal and parallel to the facade. This is true for all configurations. It's interesting to note from the maximum and minimum plots that where there are high maximum rainscreen peak factors, the corresponding absolute minimum rainscreen peak factors are low and vice-versa. The corresponding maximum and minimum rainscreen pressure coefficients are low as compared to these values. Looking at the variation of maximum and minimum rainscreen peak factors against rms pressure coefficients, it is clear that very high values of maximum as well as

minimum rainscreen peak factors are associated with low rms rainscreen pressure coefficients. This wide scattering of the maximum and minimum peak factors across low rms rainscreen pressure coefficients has little physical significance.

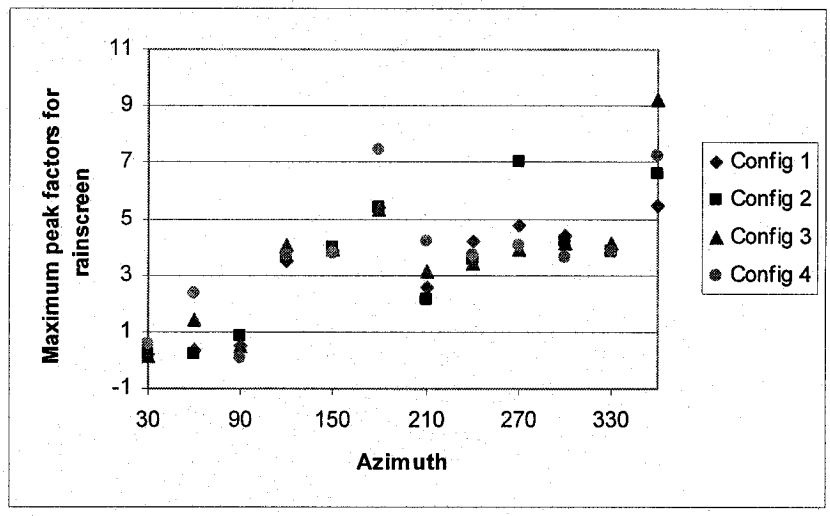

Figure 4.49: Maximum rainscreen peak factors as a function of azimuth

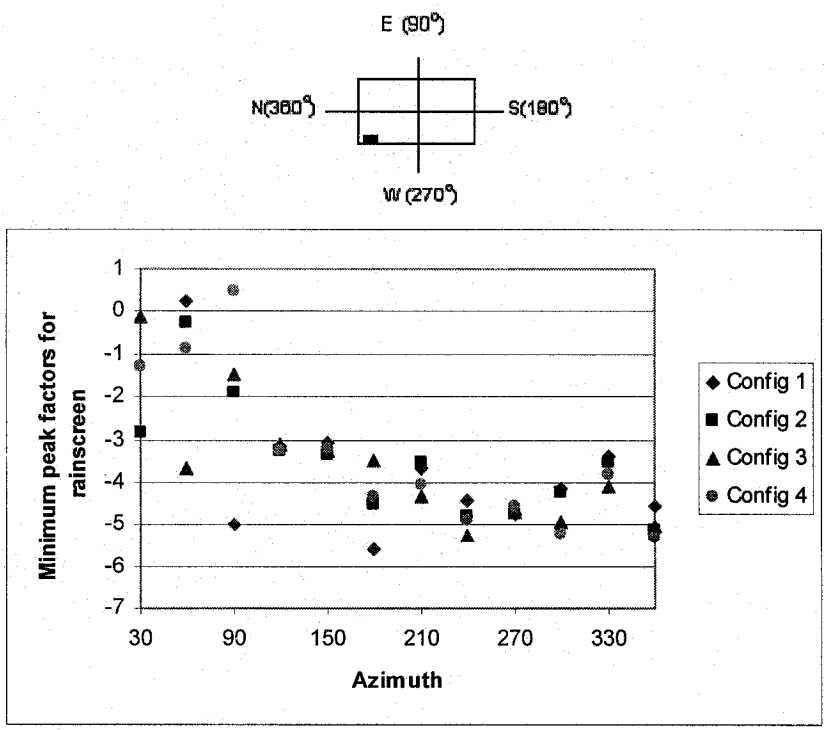

Figures 4.50: Minimum rainscreen peak factors as a function of azimuth

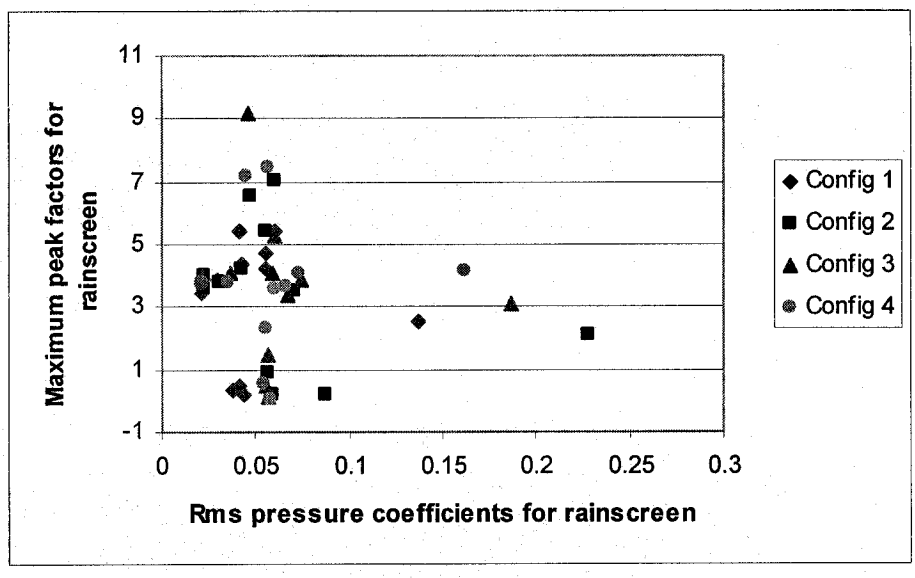

Figure 4.51: Maximum rainscreen peak factors as a function of rms rainscreen pressure coefficients

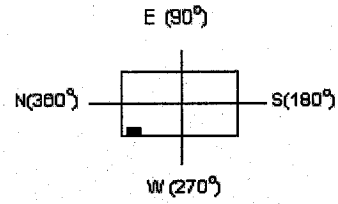

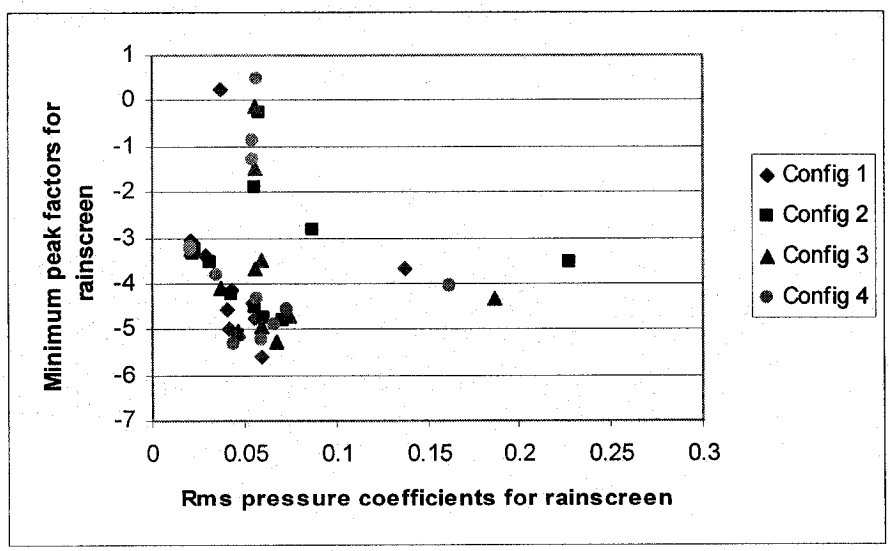

Figures 4.52: Minimum rainscreen peak factors as a function of rms rainscreen pressure coefficients

CHAPTER 5

DESIGN ISSUES

The focus of this study is on developing design guidelines for wind loading on rainscreen walls. For this purpose two expressions to determine the extent of pressure equalization have been used: MPEC = Ratio of the absolute value of the mean pressure acting on the rainscreen to the absolute value of the mean pressure acting on the panel; MaxPEC = Ratio of the absolute value of the maximum pressure acting on the rainscreen to the absolute value of the maximum pressure acting on the panel. A value of MPEC = 0 indicates good pressure equalization with complete load reduction for rainscreen and a value of MPEC = 1 indicates poor pressure equalization with the rainscreen carrying the entire wind load.

For each configuration, the MPEC values are tabulated against the field data in Table 5.1. The field results correspond to the data obtained for wind azimuths ranging from 240° to 300°. Higher reductions of rainscreen loads are found in the wind tunnel in comparison with the field results. The difference is more pronounced for Configuration 2, for which the wind tunnel simulation is more questionable. The higher the load reduction, the better is the pressure equalization. This reduction is higher when the air barrier is impermeable and it is generally higher at the center than at the edge of the wall.

Table 5.2 shows MaxPEC values in similar format. Such reductions are pertinent to the establishment of design provisions for rainscreen walls. Therefore, the relevant provisions of the European Code ENV 1991-2-4 [50] have also been included in Table 5.2. As in the case of mean load reductions, the field data correspond to

measurements for winds coming from 240° to 300°. Wind tunnel values are shown separately for each azimuth tested in order to provide a more complete picture of the results. For example, in configuration 3 at 240°, the maximum rainscreen and panel coefficients are 0.21 and 2.9 respectively – see Figure 4.30a. Accordingly, the peak load ratio is 0.21/2.9 = 0.07 and hence, the load reduction for rainscreen is (1-0.07)*100 = 93% - see Table 5.2. In general, as the venting area increases, the pressure equalization performance improves and correspondingly, the load taken by rainscreen decreases. However, note that the percentage of venting area required for producing good pressure equalization or load reduction depends on the air barrier leakage. For instance, in the case of no air barrier leakage, the panel requires only small venting area to have good pressure equalization. For the venting area with the inclusion of air barrier leakage, the pressure equalization performance worsens. It is noted that for configurations with sufficient leakage and poor venting, there is lowest reduction in rainscreen load both for center and edge panel. Table 5.2 also provides an idea about the required percentage of venting area with respect to the desired reduction in load both for center and edge panel conditions. Effective porosity of the air barrier is estimated based on the traditional orifice plate - meter equation. As per the European Code, configurations 1, 3 and 4 fall in the impermeable category and code proposes no load reduction to the rainscreen though significant load reductions have been noted both in field and wind tunnel. On the other hand, for configuration 2, the Code proposes 72% load reduction. Wind tunnel predicts higher reduction for center panel-configuration 2, about 90%, while the field data shows only 55% [2]; the edge panel for the same configuration predicts a somewhat lower value of 85%. However, it can be noted that the simulation of configuration 2 is rather difficult, as previously discussed in this study.

In order to establish an appropriate wind design guideline for rainscreens, the field measurements of panels located in corners, edges and separation zones along with their pressure equalization performance are needed to compare with wind tunnel results.

Configuration	% Load reduction – Mean (Field – Center)	% Load reduction – Mean (Wind tunnel) Center			% Load reduction – Mean (Wind tunnel) Edge		
		240°	270°	300°	240°	270°	300°
1. μe = 0.75% μi = 0.13%	83	90	92	89	95	86	17
2. μe = 0.15% μi = 0.13%	40	94	80	77	74	88	91
3. μe = 0.15% μi = 0.0%	62	97	98	98	94	76	15
4. μe = 0.45% μi = 0.0%	82	95	96	93	95	78	13

Table 5.1: Comparison of mean pressure load reductions: field and wind tunnel data

Configuration	ENV 1991-2-4	% Load reduction	% Load reduction – Peak (Field - Center)	% Load reduction – Peak (Wind tunnel) Center			% Load reduction – Peak (Wind tunnel) Edge		
				240°	270°	300°	240°	270°	300°
1. μe = 0.75% μi = 0.13%	$\mu e > 3\ \mu i$, μe <1% Outside overpressure	0	95	91	93	93	93	94	91
2. μe = 0.15% μi = 0.13%	$(\mu i/3) < \mu e < 3\ \mu i$	72	55	93	90	90	87	85	89
3. μe = 0.15% μi = 0.0%	$\mu e > 3\ \mu i$, μe <1% Outside overpressure	0	75	93	95	92	93	94	88
4. μe = 0.45% μi = 0.0%	$\mu e > 3\ \mu i$, μe <1% Outside overpressure	0	90	93	95	92	92	94	89

Table 5.2: Comparison of peak pressure load reductions: ENV 1991-2-4 provisions, field and wind tunnel data

CHAPTER 6

CONCLUSION

The emphasis of this thesis is to compare the wind tunnel results of the model scale TUE building with the available limited field data and also to quantify the parameters involved in the design of Pressure-Equalized Rainscreen (PER) Walls in order to establish specific design guidelines for standards and codes of practice.

The results of this study can be summarized as follows:

1. A comprehensive literature review clearly shows the lack of ready to use design guidelines available for PER walls in codes and standards.

2. Further studies involving the quantification of unknown parameters that are involved in PER design needs to be done as a step towards codification.

3. Researchers are often solely in discretion on wind tunnel results for design due to the availability of only limited field data on PER walls.

4. Model scale building is chosen by comparing three building models and it is noted that the large building model is seen as a good approximation over the small building model for both center and edge mean pressure coefficients. However, this model under-predicts the maximum Cp values due to the reduced oncoming turbulence intensity and hence could be used as a good approximation of the TUE building, only with appropriate turbulence correction.

5. Static tests are performed on two rainscreen and three air barrier sections to choose the panel that has close to field leakage characteristics. The rainscreen with 1mm diameter vents and the air barrier with 3.5 mm thickness match the field data and, hence, are chosen as panel designs for further experiments.

6. Wind tunnel experimentation is carried out on four different panel configurations for seven different azimuths for both center and edge panel locations.

7. Results for center panel show that the corrected maximum and rms panel pressure coefficients matched the field data generally well. Rainscreen loads are also simulated adequately, with the exception of a particular configuration with similar venting and air barrier leakage, for which the simulation appears problematic.

8. Results for edge panel show that good pressure equalization occurs in general when the wind blows at $\Theta = 180^{o}$.

9. Pressure equalization of mean and peak pressures can be achieved by providing adequate venting area with respect to the panel area and air barrier leakage. Configurations with sufficient leakage and poor venting carry maximum rainscreen load, which is unfavorable for design.

10. There exist significant differences between the limited code and standard provisions and the respective field and wind tunnel design data for rainscreen walls.

The major contributions of the present research can be summarized as follows:

1. Wind tunnel tests have been carried out to replicate the field measurements of a PER wall at TUE, Eindhoven. Thereafter, wind tunnel experiments are undertaken to build a pool of data, which is required for quantifying the unknown parameters involved in the PER wall design.

2. Edge panel measurements available to aid researchers in carrying out field measurements at edges for comparison purposes.

3. Weakness in existing limited code and standard provisions has demonstrated significant differences between the code, field and wind tunnel design data.

Possible extensions of the present study are:

1. Extensive field investigation of the panel at the edge of the present TUE building, in order to compare with the existing wind tunnel results.

2. Extensive wind tunnel and field investigation on compartmentalization of the panel at center and edge locations on the present building.

REFERENCES

[1] Kumar KS. A Study on Pressure Equalization of Rainscreen Facades: Full-scale Experiments and Computer Simulations, Technical Report: FAGO 99.40.K, Faculteit Bouwkunde, Technical University of Eindhoven, Eindhoven, The Netherlands, 1999

[2] Kumar KS, Stathopoulos T and Wisse JA. Field measurement data of wind loads on rainscreen walls. Journal of Wind Engineering and Industrial Aerodynamics, 91 (2003), pp 1401-1417.

[3] Anderson JM and Gill JR. Rainscreen Cladding: A guide to design principles and practise, Construction Industry Research and Information Assosciation, ISBN 0-408-03093-3.

[4] Birkeland. Curtain walls. Handbook 11B, Oslo, Norway: Norwegian Building Research Institute, 1962.

[5] Garden GK. Rain penetration and its control. In: Canadian Building Digest No. 40 (CBD 40), NRCC, Ottawa, Canada: Division of Building Research, 1963.

[6] Architetural Aluminum Manufacturer's Association, A Brief History of the Aluminum Curtain Wall, AAMA, Chicago, 1972.

[7] Latta JK. Walls, windows and roofs for the Canadian climate – a summary of the current basis for selection and design. Special Technical Publication, NRCC 13487, 1(1973).

[8] Yamaguchi A. Non-Steady Characteristics of Orifices, Bulletin of the JSME, 19 (1976), pp 505-512.

[9] Inculet DR and Davenport AG. Pressure-Equalized Rainscreens: A Study in the Frequency Domain, Journal of Wind Engineering and Industrial Aerodynamics, 53 (1994), pp 63-87.

[10] Kumar KS. Pressure equalization of rainscreen walls: a critical review. Building and Environment, 35(2000), pp 161 – 179.

[11] Irwin PA, Schuyler GD and Wawzonek MA. A wind tunnel investigation of rainscreen wall systems. Morrison Hershfield Limited, Prepared for CMHC, 1984.

[12] Ganguli U and Dalgliesh WA. Wind pressures on open rainscreen walls: Place Air Canada, Journal of Structural Engineering, 114 (1988), pp 642-656.

[13] Morrison Hershfield Limited. A study of the rainscreen concept applied to cladding systems on wood-framed walls. Prepared for CMHC, Ottawa, Canada, 1990.

[14] Inculet DR. Pressure-equalization of rainscreen cladding. M.E.Sc. Thesis, Faculty of Engineering Science, The University of Western Ontario, Canada, 1990.

[15] Gerhardt HJ and Janser F. Wind loads on wind permeable facades, Journal of Wind Engineering and Industrial Aerodynamics, 53 (1994), pp 37-48.

[16] Lin JK and Inculet DR. A study of statistically representative mean pressure gradients. Interim progress report to CMHC, Boundary Layer Wind Tunnel Laboratory, University of Western Ontario, 1994.

[17] Skerlj PF and Surry D. A study of mean pressure gradients, mean cavity pressures and resulting residual mean pressures across a rainscreen for a representative building. Interim Progress Report to CMHC, Boundary Layer Wind Tunnel Laboratory, University of Western Ontario, 1994.

[18] Surry D, Inculet DR, Skerlj PF, Lin JX and Davenport AG. Wind, Rain and the Building Envelope: A Status Report of Ongoing Research at the University of Western Ontario, Journal of Wind Engineering and Industrial Aerodynamics, 53 (1994), pp 19-36.

[19] Inculet DR and Surry D. Optimum Vent Locations for Partially-Pressurized Rainscreens, Wind Engineering into the 21st Century, Balkema, Rotterdam, (1999), pp 1131-1136.

[20] Inculet DR, Surry D and Davenport AG. An Experimental Study of Pressure Gradients and their Implications for the Design of Pressure-moderated Rainscreens, Proceedings of the International Conference on Building Envelope Systems and Technologies, Ottawa, 1 (2001), pp 101-106.

[21] Killip IR and Cheetham DW. The prevention of rain penetration through external walls and joints by means of pressure equalization through external walls and joints by means of pressure equalization. Building and Environment, 19(1984), pp 81 – 91.

[22] Ganguli U and Quirouette RL. Pressure equalization performance of a metal and glass curtain wall. CSCE Centennial Conference, IRC 1542 (1988), NRCC 29024, Montreal, Quebec, Canada, 1987.

[23] Poirier GF, Brown WC and Baskaran A. Pressure equalization and the control of rain water penetration. Proceedings of the 6th Conference on Building Science and Technology, Toronto 1992.

[24] Baskaran BA and Brown WC. Performance of pressure equalized rainscreen walls under cyclic loading. Journal of Thermal Insulation and Building Envelopes, 16(1992), pp 183 -193.

[25] Xie J, Schuyler GD and Resar HR. Prediction of net pressure on pressure equalized cavities. Journal of Wind Engineering and Industrial Aerodynamics, 41 - 44(1992), pp 2449 -2460.

[26] Choi ECC and Wang Z. Study on pressure-equalization of curtain wall systems, Journal of Wind Engineering and Industrial Aerodynamics, 73 (1998), pp 251-266.

[27] Brown WC, Rousseau MZ and Dalgliesh WA. Field testing of pressure equalized rainscreen walls. ASTM STP 1034, Exterior wall symposium, Precast Concrete, Masonry and Stucco, Chicago, Illinois, 1991.

[28] Straube JF. Moisture Control and Enclosure Wall Systems. Ph.D. Thesis, Civil Engineering Department, University of Waterloo, Canada, 1998.

[29] Straube JF and Burnett EFP. Performance measurement of pressure-moderated screened wall systems. ICBEST Proceedings, Singapore, 1994.

[30] Schols SFC. Afstudeerverslag Drukvereffening In Gevelsystemen. Internal Report, FAGO, Faculteit Bouwkunde, Technical University of Eindhoven, Eindhoven, 1997.

[31] van Schijndel AWM and Schols SFC. Modeling pressure equalization in cavities, Journal of Wind Engineering and Industrial Aerodynamics, 74-76 (1998), pp 641-649.

[32] Kumar KS. Pressure equalization performance of rainscreen walls: Experimental investigations. Proceedings of the 2nd East European Conference on Wind Engineering , Prague, Czech Republic, 1998.

[33] Holmes JD. Mean and fluctuating internal pressures induced by wind. Proceedings of the 5th International Conference on Wind Engineering, Boulder, Colorado, 1979.

[34] Vickery BJ and Bloxham C. Internal Pressure Dynamics with a Dominant Opening, Journal of Wind Engineering and Industrial Aerodynamics, 41-44 (1992), pp 193-204.

[35] Kumar KS and Van Schijndel AVM. Cacity pressure dynamics of rainscreen walls. Proceedings of the 4th UK Conference on Wind Engineering, Bristol, UK, 1998.

[36] Kumar KS and van Schijndel AWM. Prediction of pressure equalization performance of rainscreen walls, Wind and Structures, 2(4) (1999), pp 325-345.

[37] Kimura RI. Scientific basis of air conditioning. Applied Science, (1997), pp 175 -186.

[38] Fazio P and Kontopidis T. Cavity pressure in rainscreen walls, Building and Environment, 23(1988), pp 137 – 143.

[39] Tamura GT and Shaw CY. Studies on exterior wall air tightness and air infiltration of tall buildings. ASHRAE Transactions, 82(1976), pp 122 – 134.

[40] Kontopoidis T, Srinivasa Reddy M and Fazio P. Potential of rainscreen walls to prevent rain penetration.: pressurized cavity principle. Building Research and Information, 21(1993), pp 176 – 186.

[41] Burgress JC. Pressure equalized rainscreen joint modeling with numerical model PERAM. Building and Environment, 30(1995), pp 385 – 389.

[42] Chaplin GC, Randall JR and Baker CJ. The Turbulent Ventilation of a Single Opening Enclosure, Journal of Wind Engineering and Industrial Aerodynamics, 85 (2000), pp 145-161.

[43] Baskaran A. A numerical method to evaluate the performance of pressure equalized rainscreen walls. Building and Environment, 29(1994), pp 159 – 171.

[44] Brown WC and Ullett JM. Performance of Pressure-Equalized Rainscreen Walls: a Collaborative Research and Development Project, Client Report A-3028.3, National Research Council of Canada, 1995.

[45] van Mook F. Full-scale measurements and numeric simulations of driving rain on a building, 10th International Conference on Wind Engineering, Kobenhavn, 21-24 (1999).

[46] British Standards Institution, Standard code of practice 8200. Design of non-load bearing external and vertical enclosures of buildings, BSI, London, UK 1985.

[47] NEN 6702, Loadings and deformations TGB 1990. Technische grondslagen voor bouwconstrucies, Nederlands, Normalisatie-instituut, The Netherlands, 1991.

[48] NEN 6707, Fixing of roof coverings – Requirements and determination methods. Technische grondslagen voor bouwconstrucies, Nederlands, Normalisatie-instituut, The Netherlands, 1991.

[49] AS 1170.2, Minimum Design loads on Structures, Part 2: Wind Loads. Standards Association of Australia, North Sydney, Australia, 1989.

[50] ENV 1991-2-3, Eurocode 1: Basis of Design and Actions on Structures, Part 2.3: Wind Actions, CEN/TC250/SC1/1993/N118, 1995.

[51] ASHRAE Handbook of fundamentals. Ventilation and Infiltration, American Society of Heating, Refrigeration and Air-conditioning Engineers, 26(2001).

[52] Karava P. Investigation of the performance of triple ventilators, MASc Thesis, Concordia University, Montreal, Canada, 2002.

[53] Simiu E and Scanlan RH. Wind Effects on Structures: Fundamentals and Applications to Design, Third Edition, ISBN 0-471-12157-6, John Wiley and Sons, Inc., 1996